Thesis for the Degree of Doctor of Philosophy

Some non-linear geometric and kinetic evolutions and their approximations

Ricards Grzibovskis

CHALMERS | GÖTEBORG UNIVERSITY

Department of Mathematics
Chalmers University of Technology and Göteborg University
Göteborg, Sweden 2004

Some non-linear geometric and kinetic evolutions
and their approximations
Ricards Grzibovskis
ISBN **91-7291-467-X**

Doktorsavhandlingar vid Chalmers tekniska högskola
Ny serie nr **2149**
ISSN 0346–718X

Department of Mathematics
Chalmers University of Technology and Göteborg University
SE-412 96 Göteborg
Sweden
Telephone +46 (0)31–772 1000

Printed in Göteborg, Sweden 2004

SOME NON-LINEAR GEOMETRIC AND KINETIC EVOLUTIONS AND THEIR APPROXIMATIONS

RICARDS GRZIBOVSKIS

Abstract

This thesis deals with three non-linear evolution problems: mean curvature flow, Willmore flow, and the evolution of solutions to the space homogeneous Boltzmann equation. Generalized mean curvature flows are also considered. A major part of the study focuses on the construction of approximations to these evolutions. The thesis consists of four papers.

A unified convolution-thresholding approach to the generalized mean curvature flow and to the Willmore flow is suggested in the first and the second paper. The convergence of the approximations to viscosity solutions of the corresponding PDE is shown for the generalized mean curvature flow. For the Willmore flow the convergence of the convolution-thresholding scheme is shown in the case when the evolution is smooth and embedded.

The third paper concentrates on an analytical and numerical study of self-similar (homothetic) mean curvature and Willmore flows. Two qualitatively different families of such evolutions for each type of the flows are found. Representatives from the first family become singular in finite time, while representatives from the second family come from singular initial data. In particular considerably new examples of smooth surfaces that develop a singularity in finite time during the Willmore evolution are obtained numerically. Another new result of this study is the construction of the mean curvature and Willmore evolutions starting from certain surfaces with singularities.

In the fourth paper a new deterministic numerical method for solution of the Boltzmann equation is constructed. The suggested method is the only known deterministic scheme that effectively handles discontinuous solutions. It is based on a combination of two qualitatively different approaches: the approximation of discontinuous solutions on a non-uniform adaptive grid, and the approximation of smooth terms in the Boltzmann equation by a Fourier based spectral method.

Keywords: curvature flow, Willmore flow, convolution-thresholding, homothetic geometric flows, Boltzmann equation, deterministic methods, non-uniform grids.

This thesis consists of an introduction and the following four articles:

[GH1] Ricards Grzibovskis and Alexei Heintz.
A convolution-thresholding approximation of generalized curvature flows.
Chalmers Univ. of Tech., Preprint 39 (revised version), 2002.
Recommended for publication in SIAM J. of Num. Anal.

[GH2] Ricards Grzibovskis and Alexei Heintz.
A convolution-thresholding scheme for the Willmore flow.
Chalmers Univ. of Tech., Preprint 34 (revised version), 2003.

[G1] Ricards Grzibovskis.
On self-similar Willmore and curvature evolutions of surfaces.
Chalmers Univ. of Tech., Preprint 29, 2004.

[HKG] Alexei Heintz, Piotr Kowalczyk, and Ricards Grzibovskis.
Fast numerical method for the Boltzmann equation on non-uniform grids.
Chalmers Univ. of Tech., Preprint 22, 2004.

Acknowledgment

I would like to thank Alexei Heintz, who was my advisor in the areas of this thesis. His support and encouragement as well as many innovative ideas were of great value during my work. I would also like to express my gratitude to all members of the kinetic research group at Chalmers University of Technology for providing me a great working environment and informative seminars. I am thankful to Peter Kumlin for careful reading of paper [GH1] and important critics. I am grateful to my fellows Ph.D. students Anton Evgrafov and Yosief Wondmagegne for helping me to expand my views on mathematics. Finally, I would like to thank my wife Asja for her love, enthusiasm and support.

Göteborg, April 2004 Ricards Grzibovskis

1 Introduction

This thesis is devoted to the study of three evolution processes: mean curvature flow, Willmore flow, and the evolution of solutions to the space homogeneous Boltzmann equation.

The mean curvature flow and the Willmore flow are special types of surface evolutions. They can be characterized by the surface velocity V along the normal at each its point. In the case of the mean curvature evolution this velocity is equal to the mean curvature of the surface $V = H$. We also consider so called generalized mean curvature evolution. In this case $V = G(H)$, where G is some monotonic, continuous function.

In the case of the Willmore flow the velocity V can be written as

$$V = -\left(\Delta H + 2H\left(H^2 - K\right)\right),$$

where K is the Gauss curvature and Δ denotes the Laplace-Beltrami operator on the surface.

In the paper [GH1] we construct convolution-thresholding approximations to the generalized mean curvature flow of $n-1$ dimensional surfaces in $\mathbb{R}^n$. We consider solutions to this flow in the viscosity sense, and the scheme converges to the correct solution even if the evolution develops singularities. Ways to implement this scheme for $n = 2$ and 3 are also demonstrated, and several numerical examples are presented.

A convolution-thresholding scheme to track the Willmore evolution of two dimensional surfaces in $\mathbb{R}^3$ is proposed in the second paper [GH2]. The convergence of the scheme is proved provided the surface is smooth. However, the numerical examples suggest the validity of the approach even in the non-smooth case.

In the paper [G1] we look for surfaces in $\mathbb{R}^3$ that have the following property: their self-similar (homothetic) evolution coincides with the mean curvature flow or with the Willmore flow. We find two qualitatively different families of such surfaces for each type of the flows. Representatives from the first family become singular in finite time, while representatives from the second family come from singular initial data. In particular a considerably new family of smooth surfaces that develop a singularity in finite time during the Willmore evolution is obtained numerically. Another new result of this study is the construction of the mean curvature and Willmore evolutions of certain initially singular surfaces.

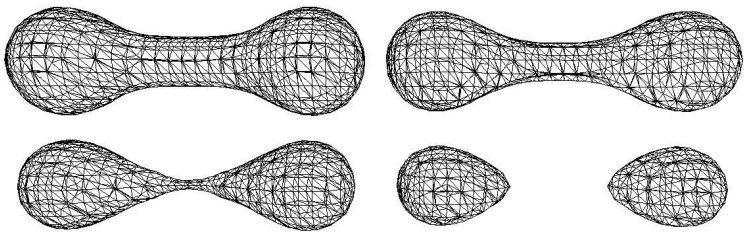

Figure 1: Example: a topological type changes during the mean curvature evolution.

In the paper [HKG] we construct a new deterministic numerical method for solution of the classical Boltzmann equation for dilute gases. Typically the evolution of a solution to the Boltzmann equation starting from discontinuous data preserves this discontinuity during a long time. The goal of our method is to handle effectively discontinuous solutions that are typical for boundary value problems. It is based on a combination of the approximation of discontinuous solutions on a non-uniform adaptive grid and the approximation of smooth terms in the Boltzmann collision operator by a Fourier based spectral method.

An adaptive grid refinement procedure together with an uneqally spaced fast Fourier transform are the main tools in the implementation of numerical methods in papers [GH1], [GH2], [HKG].

In the following sections we give an overview of the underlying theory of the above evolutions and numerical methods for them. We also formulate our results more precisely.

2 Approximation of the generalized curvature flow

It is widely known, that an initially smooth surface in $\mathbb{R}^3$ can develop singularities in finite time during the mean curvature evolution. The classical example is illustrated on Figure 1. There have been three successful attempts to continue the surface evolution past singularities: the varifold approach ([13]), the level-set approach ([49], [51]) and the phase field method ([25], [14], [7],[3]).

Denote the surface under consideration at the time moment t by Γ_t. The main idea of the level-set approach is to evolve some continuous function $g : \mathbb{R}^n \mapsto \mathbb{R}$ in such way that $\Gamma_t \subset \mathbb{R}^n$ would always be a level-set of $u(x,t)$ i.e.

$$\Gamma_t = \{x \in \mathbb{R}^n : u(x,t) = 0\} \ \forall t \geq 0.$$

Being the level set of a continuous function the surface Γ_t may develop singularities and change its topological type.

In this framework the problem of the generalized mean curvature evolution of Γ_0 can be stated as a Cauchy problem

$$\begin{cases} u_t = |Du| \, G\left(\operatorname{div}\left(\frac{Du}{|Du|}\right)\right) & \text{in } \mathbb{R}^n \times (0,T) \\ u = g(x) \in BUC(\mathbb{R}^n) & \text{on } \mathbb{R}^n \times \{0\}, \end{cases} \tag{1}$$

where Γ_0 is some level-set of $g(x)$ and $BUC(\mathbb{R}^n)$ denotes the set of all bounded and uniformly continuous functions on $\mathbb{R}^n$.

The equation in (1) is of degenerate parabolic type. The existence and uniqueness of generalized viscosity solutions (see [23]) to the Cauchy problem was investigated in [29], [19], [37]. The result of [37] in application to the problem (1) states (see [56]):

Theorem 1. *The initial value problem (1) has an unique viscosity solution provided that G is continuous and nondecreasing.*

Various kinds of generalized curvature flows arise naturally in investigations of fast reaction-slow diffusion processes [7], image processing [2], minimal surfaces [20]. Partially because of that, the problem of finding an approximation to the viscosity solution of (1) attracted a lot of interest. Various methods of approximation appeared recently. Among them morphological filters [17], [32], [16], finite difference approximations (fast marching methods) [51], [24] and convolution-thresholding methods [45], [34], [35], [36].

The convolution-thresholding methods are robust, suit well to the problems involving surface evolutions and allow efficient implementation. Consider first a convolution generated motion of a hypersurface in $\mathbb{R}^n$. By this we mean the following. Assume, that initially the surface under consideration is a boundary of a compact set $C \in \mathbb{R}^n$. Take a compactly supported function $\tilde{\rho} : \mathbb{R}_+ \to \mathbb{R}_+$. Define $\rho : \mathbb{R}^n \mapsto \mathbb{R}_+$,

$$\rho(x) = \frac{1}{h^{n/2}} \tilde{\rho}\left(|x| / \sqrt{h}\right)$$

and a convolution

$$M(C)(x,h) = \int_{\mathbb{R}^n} \chi_C(y)\,\rho(x-y)\,dy. \tag{2}$$

Now $M(C)(x,h)$ is a function of x, and we define a new position of the surface by

$$\mathcal{H}(h)\,C = \{x \in \mathbb{R}^n : F(M(C)(x,h)) \geq 0\}, \tag{3}$$

where F is some (thresholding) function.

This approach originates from the so called "Bence-Merriman-Osher" method see [45] where the authors suggested to take $M(C)(x,h)$ as a solution to the diffusion equation with the initial data χ_C after the time h and $F(\xi) = \xi - 1/2$. In this case ρ is the fundamental solution of the diffusion equation. Our method is motivated originally by a kind of Lattice-Boltzmann equation, where the convolution is viewed as a transport of particles and the thresholding as a result of some collision-reaction process.

Since we intend to prove the convergence to a viscosity solution, the construction of an operator acting on bounded functions is necessary: $\mathbb{H}(h) : \mathbb{B}(\mathbb{R}^n) \mapsto \mathbb{B}(\mathbb{R}^n)$.

$$[\mathbb{H}(h)\,u](x) = \sup\{\lambda \in \mathbb{R} : x \in \mathcal{H}(h)\,[u \geq \lambda]\}. \tag{4}$$

The following connection between $\mathbb{H}(h)$ and the system (1) has been established in [28] and [5].

Theorem 2. *Take $M(C)(x,h)$ and $F(\xi)$ as in the "Bence-Merriman-Osher" method, then*

$$\lim_{m \mapsto \infty} \left[\mathbb{H}^m\left(\frac{t}{m}\right) u_0\right](x) = u(x,t),$$

where $u(x,t)$ is the unique viscosity solution of (1) with $G(x) = x$ and the convergence is locally uniform.

The cornerstone of this connection is the following expansion of the convolution (2) at $x \in \partial C$:

$$M(C)(x,h) = \frac{1}{2} + L_1 H(x)\sqrt{h} + O\left(h^{3/2}\right), \tag{5}$$

where L_1 is some constant and $H(x)$ is the mean curvature of ∂C at the point x.

In [34] Ishii extended the Theorem 2 to the case of arbitrary radially symmetric convolution kernel ρ. He shows that in this case the the convolution-thresholding procedure converges to the viscosity solution of (1) where $G(k) = \alpha k$ and the constant α is positive and depends on the kernel. Further generalization of this result considering surface evolutions with boundary conditions can be found in [35].

Suppose, that G is non-linear. We show in [GH1] that in this case one has to use two convolutions M_1 and M_2 and a thresholding function of two variables $F(M_1, M_2)$. This is necessary to ensure that the operator $\mathbb{H}$ is consistent with the PDE in (1). We also show, how to choose convolution kernels in order to get a monotone $\mathbb{H}$. These two conditions - monotonicity and consistency - are crucial for the convergence. For a given function G in (1), we find a corresponding thresholding function F in (3), so that $\mathbb{H}(t/m)^m g(x)$ would converge to the unique viscosity solution of (1). We prove the the following

Theorem 3. *Let $\mathbb{H}(h)$ be defined by (4) with*

$$\mathcal{H}_h C = \{x \in \mathbb{R}^n : F(M_1(C)(x,h), M_2(C)(x,h)) \geq 0\},$$

where

$$\begin{aligned} F(M_1, M_2) &= \frac{1}{\sqrt{h}} \frac{N_1 B_2 - N_2 B_1}{D} - G\left(\frac{1}{\sqrt{h}} \frac{N_2 C_1 - N_1 C_2}{D}\right), \\ N_i &= M_i - A_i. \end{aligned}$$

Here the kernel dependent constants are given by

$$A_i = \int_{\mathbb{R}^{n-1}} \int_{-\infty}^{0} \rho_i(|y|)\, dy_n d\acute{y} \tag{6}$$

$$B_i = \frac{1}{2} \int_{\mathbb{R}^{n-1}} y_k^2 \rho_i(\acute{y}, 0)\, d\acute{y}, \tag{7}$$

$$C_i = \int_{\mathbb{R}^{n-1}} \rho_i(\acute{y}, 0)\, d\acute{y}, \tag{8}$$

and kernels $\tilde{\rho}_1, \tilde{\rho}_2$ have compact support and chosen so that

$$D = C_1 B_2 - C_2 B_1 > 0.$$

Then

$$\mathbb{H}^m_{\frac{t}{m}} g(x) \to u(x,t)$$

locally uniformly when $m \to \infty$. Here $u(x,t)$ is the unique viscosity solution of (1) provided G is continuous nondecreasing and satisfying

$$\frac{B_1}{C_1} \leq G' \leq \frac{B_2}{C_2}. \tag{9}$$

We base our proof on a result by Barles and Souganidis in [6]. They have found criteria for an abstract approximation scheme to converge to the viscosity solution of a degenerate elliptic equation.

The paper [GH1] also discusses ways to overcome the restriction (9). First of all, by comparing (8) with (7) one sees that it is possible to make the lower bound in (9) small by choosing ρ_1 with mass concentration close to the origin. The upper bound will be large if the mass of ρ_2 is concentrated relatively far from the origin. Then we prove that to approximate the evolution defined by (1) one can use G_e instead of G in the thresholding function, where G_e is close to G in the uniform norm.

The rest of the paper focuses on some aspects of efficient implementation of the method. A new convolution-thresholding scheme of higher order is introduced and tested. The construction of this scheme is based on the elimination of the higher order terms in the expansion (5). Several numerical examples are also presented.

3 Approximation of the Willmore flow

The Willmore flow is defined as an evolution of a surface when each point moves with velocity V along the normal equal to

$$V = -\left(\Delta H + 2H\left(H^2 - K\right)\right). \tag{10}$$

Mathematical theory of the Willmore flow has recently become a very popular subject of research. The existence of the flow near a sphere and its convergence to a sphere has been proved by Simonett in [59]. A lower bound on the existence time for smooth solutions in terms of initial concentration of H has been obtained by Kuwert and Schatlze in [39]. They have recently extended this result in [40]. The occurrence of self intersections during the evolution has been studied numerically in [43]. A kind of weak definition of the flow and its extension past singularities has been constructed by Moser in [47] for smooth initial data.

The challenging problem to construct a numerical scheme to approximate the Willmore flow has attracted a lot of attention as well. Since the evolution equation (10) is a quasi-linear with the leading fourth order term ΔH, one might focus on the evolution with

$$V = -\Delta H$$

as an intermediate step. A surface evolution with such normal velocity is of interest on its own and is referred to as the 'surface diffusion flow'. Chopp and Sethian developed a numerical scheme to approximate this flow in [21]. Their approach is based on the level set formulation of the problem. An extension of this results and an applications to the surface smoothing can be found in [61]. A straightforward geometric approach has been proposed by Mayer in [42]. Mayer and Simonett considered surface evolution in the axially symmetric case. In [44] they suggested a numerical scheme for the approximation of several types of surface evolutions assuming the above symmetry. In particular, approximations of the mean curvature, surface diffusion and Willmore flows were constructed. Moreover, some numerical examples in this work suggest that the Willmore flow can develop a singularity in finite time. A numerical algorithm based on finite elements for the Willmore flow in connection with the surface restoration was proposed in [22]. Another recent result about the level-set formulation of the Willmore flow and the finite element approach to the evolution can be found in [27].

In the paper [GH2] we propose a convolution-thresholding scheme to approximate the Willmore flow. This technique is a popular tool when the need to track a surface evolution arises. We refer to [34], [36], [58] and [GH1], where the convolution-thresholding approximation to the evolutions governed by the second order PDEs were constructed. Our idea to use this procedure in the case of the Willmore flow is completely new.

Consider a compact subset C of $\mathbb{R}^3$ with a smooth boundary ∂C and a convolution

$$M(t,x) = (\chi_C \star \rho_{t^{1/4}})(x), x \in \mathbb{R}^3, \tag{11}$$

where χ_C is the characteristic function of C, $\rho_{t^{1/4}}(x) = \rho\left(|x|^2/\sqrt{t}\right)/t^{3/4}$ and $\rho : [0,\infty) \mapsto [0,\infty)$ is smooth with a compact support normalized by $\int_{R^3} \rho dx = 1$.

Pick a point $\mathbf{p} \in \partial C$ and calculate the value of M in this point. Taking $t \to 0$ expand M into a power series in t. Since ∂C is smooth and ρ is normalized,

it is easy to see that $M(0,\mathbf{p}) = 1/2$ and

$$M(t,\mathbf{p}) - \frac{1}{2} = o(1) \text{ as } t \to 0.$$

The next term in this expansion is of order $t^{1/4}$ and is proportional to the mean curvature H of ∂C at $\mathbf{p}$. This fact was used to construct convolution - thresholding approximations of the mean curvature flow [34], [28], [GH1]. The key observation that made it possible to construct such type of scheme for the Willmore flow is that the third term in this expansion is proportional to the expression (10). This leads to the following

Theorem 4. *Suppose ∂C is smooth, $\mathbf{p} \in \partial C$ and $v \in \mathbb{R}$, then the convolution (11) has the following asymptotic expansion with respect to t at the point $O = \mathbf{p} + \mathbf{N}vt$*

$$\begin{aligned} M(O) &= \frac{1}{2} + t^{1/4}\frac{\pi N_3}{2}H + \\ &+ t^{3/4}\frac{\pi}{16}\left[32N_1 v + N_5\left(\Delta H + 2H\left(H^2 - K\right)\right)\right] + O\left(t^{5/4}\right). \end{aligned} \quad (12)$$

where H, K and ΔH are values of the mean curvature, the Gauss curvature and the Laplace-Beltrami operator of the mean curvature of ∂C at $\mathbf{p}$ and $N_i = \int_0^\infty r^i \rho(r^2)\, dr$.

Consider now a kernel with a scaled support $\rho_{at^{1/4}}$ $(0 < a \leq 1)$ and the corresponding convolution $M_a = \chi_C \star \rho_{at^{1/4}}$. The main idea of our method is to combine M_a $(a < 1)$ and M_1 so that only the third and the higher order terms would be present. Suppose C is given, calculate M_1 and M_a at each point and set

$$C_1 = T(t)\, C \equiv \left\{\mathbf{x} \in \mathbb{R}^3 : 2aM_1 - 2M_a + 1 - a \geq 0\right\}.$$

Using Theorem 4 we have, $\partial C_1 = \{\mathbf{p} + vt\mathbf{N} : \mathbf{p} \in \partial C\}$, where

$$v = \frac{a^2 N_5}{32N_1}\left(\Delta H + 2H\left(H^2 - K\right)\right) + O\left(t^{1/2}\right). \quad (13)$$

This leads to the local in time and uniform in space convergence

$$\partial\left(T^m\left(\frac{t}{m}\right)C\right) \to W(t)(\partial C) \text{ as } m \to \infty,$$

where by $W(t)(\partial C)$ we denote the Willmore evolution of the surface ∂C. This convergence takes place as long as the surface $W(t)(\partial C)$ stays smooth and embedded.

The implementation of the scheme is exactly the same as in the case of the generalized mean curvature evolution. The only exception is that in this case values of the convolutions M_1 and M_a have to be computed with higher accuracy.

The results of numerical experiments with this scheme have motivated us to consider the possibility for a Willmore evolution to be self-similar (homothetic). The investigation of this possibility is the subject of the paper [G1].

4 Self-similar curvature and Willmore flows

Consider a round two dimensional sphere in $\mathbb{R}^3$. If we let it evolve by the mean curvature, it would self-similarly shrink to a single point. A straight cylinder $\{(x, y, z) : x^2 + y^2 = 1\}$ would collapse into the z-axis under the same circumstances. The same cylinder expands homothetically during the Willmore evolution. These are simple examples of self-similar (homothetic) evolutions that coincide with the mean curvature flow or with the Willmore flow.

In the case of the curvature flow in the plane, self-similar solutions have been considered in [1]. The authors obtained a class of closed curves that collapse homothetically during the evolution by mean curvature. These curves play certain role in the partial classification of singularities that appear during the curvature flow in $\mathbb{R}^3$ presented in [33].

In the paper [G1] we show, that one can construct a plenty of two dimensional surfaces in $\mathbb{R}^3$ that would evolve homothetically during the mean curvature or the Willmore flows. In the examples mentioned above the evolution either encounters a singularity (sphere collapses to a single point) or originates from a singular shape (expanding cylinder originates from a straight line). We show, that this feature takes place for all self-similar curvature or Willmore evolutions.

Consider an evolving surface Σ and its immersion $\mathbf{s} : \Sigma \to \mathbb{R}^3$ into $\mathbb{R}^3$. We let this surface to evolve homothetically, i.e. at a time moment t the immersion of this surface into $\mathbb{R}^3$ will be

$$\mathbf{s}(t) = T(t)\,\mathbf{x} \tag{14}$$

where $T(t)$ is some smooth scalar function describing scaling in time and

$\mathbf{x} : \Sigma \to \mathbb{R}^3$ describes the preserved shape of the surface. In this case the velocity of the surface along its normal is

$$V(\mathbf{s}) = \dot{T}(t)\,\mathbf{x} \cdot \mathbb{N}(\mathbf{s}), \tag{15}$$

where $\dot{T}(t) = \frac{d}{dt}T(t)$ and $(\cdot)$ denotes the inner product in $\mathbb{R}^3$.

We seek for homothetic evolutions, therefore

$$\dot{T}(t)\,\mathbf{x} \cdot \mathbb{N}(\mathbf{s}) = V(\mathbf{s}), \tag{16}$$

where $V(\mathbf{s})$ is given by $V = W = -(\Delta H + 2H(H^2 - K))$ in the case of the Willmore flow and by $V = H$ in the case of the mean curvature flow. In both cases after the separation of time and space variables we get equations for the time function $T(t)$ and for the shape $\mathbf{x}(u_1, u_2)$

$$\begin{cases} \dot{T}(t)\,T(t) &= A \\ A\mathbf{x} \cdot \mathbb{N}(\mathbf{x}) &= H(\mathbf{x}) \end{cases} \tag{17}$$

for the mean curvature flow and

$$\begin{cases} \dot{T}(t)\,T^3(t) &= A \\ A\mathbf{x} \cdot \mathbb{N}(\mathbf{x}) &= -W(\mathbf{x}) \end{cases} \tag{18}$$

for the Willmore flow, where the constant A is arbitrary. Moreover, the equation for the time function can be solved explicitly in both cases yielding

$$T(t) = (1 + mAt)^{1/m},$$

where $m = 2$ in the case of the mean curvature flow and $m = 4$ in the case of the Willmore flow and we imposed a natural condition $T(0) = 1$. For negative A, the parameterization $\mathbf{s}(t)$ develops a singularity at the time moment $t_* = |mA|^{-1}$. In the case of Willmore flow, this choice of the constant A leads to a new result: an embedded surface develops a singularity in finite time. For a positive value of A the time multiplier vanishes at a time moment $t_* = -|mA|^{-1}$. In this case the corresponding evolution is initially singular.

The equations for the shape function $\mathbf{x}$ in (17) and (18) are treated in the cases of rotational and translational symmetries. By doing so, we reduce the corresponding PDE to a system of ODEs. The shapes of the surfaces are obtained by numerical solution of these systems of ODEs.

We classify shrinking ($A < 0$) homothetic curvature flows in $\mathbb{R}^2$ and give numerical examples of such flows. They correspond evidently to flows with

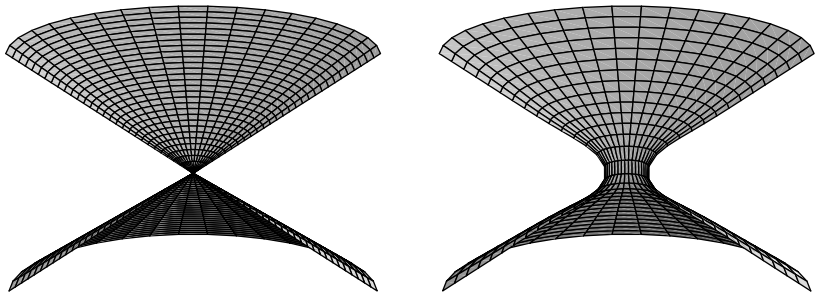

Figure 2: Willmore evolution of a double cone.

translational symmetry in $\mathbb{R}^3$. In this part of the paper we reproduce and provide an alternative elementary prove to one of the results in [1]. We also give numerical examples of axisymmetrical shrinking homothetic curvature flows in $\mathbb{R}^3$ that has not been considered before.

Our consideration of expanding ($A > 0$) homothetic curvature flows is new. In the case of translational symmetry we obtain the curvature evolution of the arbitrary angle of two half-planes. By solving the equation (17) in the case of axial symmetry we get the curvature evolution of non-symmetrical double cones.

Our study of homothetic Willmore flows is completely new. In the case of the shrinking ($A < 0$) Willmore flow we find a family of translationally symmetrical surfaces that tend to an angle of two half-planes in finite time. In the case of axial symmetry we get non-trivial surfaces that shrink to a point via a homothetic Willmore evolution.

Studying the expanding self-similar Willmore evolutions ($A > 0$) we find two qualitatively different types of shapes $\mathbf{x}$: bounded and unbounded ones. The unbounded $\mathbf{x}$ come from the Willmore evolution starting from an angle of two half-planes or from a double cone (see Figure 2). Bounded $\mathbf{x}$ constructed here are homeomorphic to cylinder in the case of translational symmetry and are homeomorphic to sphere in the case of axial symmetry but are quite complicated.

5 Approximation of the Boltzmann equation

The classical *Boltzmann equation* [18] for a dilute gas of particles reads as

$$\frac{\partial f}{\partial t} + \mathbf{v} \cdot \nabla_x f = Q(f, f), \tag{19}$$

where $f = f(t, \mathbf{x}, \mathbf{v})$, $f : \mathbb{R}_+ \times \Omega \times \mathbb{R}^3 \to \mathbb{R}_+$, $\Omega \subset \mathbb{R}^3$, and the function f describes the time evolution of particles which move with velocity $\mathbf{v}$ in the position $\mathbf{x}$ at time t. We consider the case of potentials with cut off when the collision operator $Q(f, f)$ can be decomposed into the *gain* and the *loss* terms

$$Q(f, f)(\mathbf{v}) = Q^+(f, f)(\mathbf{v}) - Q^-(f, f)(\mathbf{v}), \tag{20}$$

where the *gain* term is

$$Q^+(f, f)(\mathbf{v}) = \int_{\mathbb{R}^3} \int_{S^2} B(|\mathbf{u}|, \theta) f(\mathbf{v} - \frac{1}{2}(\mathbf{u} - |\mathbf{u}|\,\omega)) f(\mathbf{v} - \frac{1}{2}(\mathbf{u} + |\mathbf{u}|\,\omega)\, d\omega\, d\mathbf{u} \tag{21}$$

and the *loss* term is

$$Q^-(f, f)(\mathbf{v}) = f(\mathbf{v}) q^-(f)(\mathbf{v}) \tag{22}$$

with q^- denoting the *collision frequency*

$$q^-(f)(\mathbf{v}) = \int_{\mathbb{R}^3} f(\mathbf{v} - \mathbf{u}) \int_{S^2} B(|\mathbf{u}|, \theta)\, d\omega\, d\mathbf{u}.$$

The kernel $B(|\mathbf{u}|, \theta)$ contains the information about the binary interactions between particles and reflects the physical properties of the model. Moreover θ is the angle between $\mathbf{u}$ and ω.

The main problem for the efficient numerical computations with the Boltzmann equation is a proper approximation of the collision operator $Q(f, f)$.

Space dependent problems have an additional complication, that the process of collisions described by the operator $Q(f, f)$ and the collisionless transport of particles are weakly coupled in the Boltzmann equations. This fact leads to bad compactness and regularity properties of solutions and to certain problems for both theoretical and numerical treatment of the Boltzmann equation [26].

The numerical solution of the Boltzmann equation is difficult due to the nonlinearity of the collision integral, the large number of independent variables

and the complicated integration over the sphere S^2 in the operator $Q(f, f)$. Particular symmetries of the collision operator imply the conservation laws of mass, momentum and energy that in turn cause important connections between the Boltzmann equation and the equations of classical gas dynamics.

The analytical structure of $Q(f, f)$ implies that a straightforward computation of the collision integral by a standard quadrature has the computational cost N_v^3 for N_v points representing states of a gas in the velocity space. We point out that this is the cost of computations just in for point x in physical space for a space inhomogeneous problem.

Consequently the major part of practical applied computations concerning the Boltzmann equation is based on different variants of the probabilistic Monte Carlo methods. Monte Carlo methods are advantageous for many high dimensional problems in physics, giving realistic and meaningful results with low computational cost proportional to the number of particles (points) representing the system. On the other hand getting high precision results by Monte Carlo methods requires a longer computational time and for the number N_{tr} of stochastic trajectories the convergence order is $\frac{1}{\sqrt{N_{tr}}}$. We refer to the direct simulation method (DSMC) by Bird [9] and to variants of Monte Carlo method for the Boltzmann equation by Nanbu [48] and Babovsky [4].

Development of deterministic methods for the Boltzmann equation is usually motivated, see [55], [50] by the desire of higher precision results, and by the presence of situations (low Knudsen numbers, slow convection flows) when probabilistic methods are not effective enough. Also not at the last place in the motivation of studies in this direction one finds the mathematical challenge of the problem itself.

Historically so called discrete velocity models (DVM) with uniform cubic grid of velocities were the first example of a deterministic numerical approach designed specially for the Boltzmann equation, starting from [31]. Later several different ideas led to other types of models all satisfying exact conservation laws in the discrete form [57], [15], [53]. Also rigorous consistency and convergence results for such models were proved [52], [46], [53].

Let n denote the number of points along one coordinate direction in this uniform velocity grid. All these DVM methods have high n^7 computational cost and have also a disadvantage that the integration over the sphere S^2 of the possible outputs of collisions in $Q(f, f)$ is approximated with low precision of order $1/\sqrt{n}$ [52]. In the case of the alternative so called Carleman

formulation for $Q(f, f)$ this integration is substituted by the integration over some arbitrarily oriented planes with the same approximation problems [53]. It happens because only a small number of points from the uniform cubic grid meets spheres and arbitrarily oriented planes and these points are distributed not uniformly.

The Kyoto group in kinetic theory developed a family of finite difference methods for the Boltzmann equation, linearized Boltzmann equation, and BGK equation and investigated numerically many mostly stationary problems [50],[38]. These computations demonstrate precise results but they are very time and memory consuming.

The simpler structure of the Boltzmann collision operator in the case of Maxwell pseudo-molecules, by applying Fourier transform lets to reduce the collision operator to an expression with smaller dimension of the integration [11]. Using this reduction and Fast Fourier Transform (FFT) led authors in [30] and [10] to a fast deterministic method restricted to so called Maxwell pseudo-molecules and having low computational cost N^4 but still low accuracy $1/\sqrt{N}$. Here N is the number of Fourier modes along one coordinate direction. Another method designed for the model of hard spheres and also using FFT was suggested in [12] and has computational cost $N^6 \log N$ and a higher accuracy of order $1/N^2$.

A general spectral method based on the restriction of the solution to the Boltzmann equation to a finite domain and on the representation of solutions by Fourier series was suggested in [54], and developed further in [55]. This method has an advantage of high spectral accuracy for smooth solutions to the Boltzmann equation and complexity N^6.

Any effort to develop a deterministic scheme for the boundary value problems for the Boltzmann equation, includes as a necessary step computation of the collision operator for distribution functions typical for flows with boundaries. A distribution function for a gas close to the boundary with a different temperature has a discontinuity along a plane. One observes easily that in a collisionless flow around a body the distribution function has a discontinuity in velocity space along a cone like surface that is built of the contour of the body seen from the point of observation. Computations done by the Kyoto kinetic group show that typical distribution functions for flows around a body have actually a similar discontinuity for a wide spectrum of Knudsen numbers [60]. It means that solutions to a boundary value problem are typically not smooth and Fourier based spectral approximations for them loose accuracy. The Gibbs phenomenon makes an alternative way of approximation

necessary for such solutions.

The main purpose of the paper [HKG] is to overcome the above mentioned difficulties with deterministic numerical methods for the Boltzmann equation and to develop a fast numerical method effective for problems with discontinuous solutions.

One of the main ideas of the paper is based on the classical result that the gain term $Q^+(f,f)$ in the collision operator has certain smoothing properties [41], [62]. One can illustrate this fact by the graph of $Q^+(f,f)$ for a discontinuous function, see Figure 3. Collision frequency $q^-(f)$ is also a smooth function.

The main difficulty for computation of $Q(f,f)$ is the gain term $Q^+(f,f)$. It can be represented as a kind of bilinear pseudodifferential operator

$$Q^+(f,f)(\mathbf{v}) = F_l^{-1}(\mathbf{v})F_m^{-1}(\mathbf{v})\left[\hat{f}_l\hat{f}_m\hat{B}(\mathbf{l},\mathbf{m})\right], \tag{23}$$

with symbol $\hat{B}(\mathbf{l},\mathbf{m})$:

$$\hat{B}(\mathbf{l},\mathbf{m}) = \int_{\mathbb{R}^3}\int_{S^2} B(|\mathbf{u}|,\theta)e^{2\pi\imath(\frac{\mathbf{l}+\mathbf{m}}{2},\mathbf{u})}e^{2\pi\imath|\mathbf{u}|(\frac{\mathbf{m}-\mathbf{l}}{2},\omega)}\,d\omega d\mathbf{u}. \tag{24}$$

Here $\hat{f}_m$ is the Fourier transform of the distribution function $f(\mathbf{v})$ and $F_m^{-1}(\mathbf{v})$ is the inverse Fourier transform. Using this fact and the above mentioned regularity of $Q^+(f,f)$, one can compute $Q^+(f,f)$ effectively in the case one can compute $\hat{f}_m$ fast for some not very large domain of frequencies m.

The last task is nontrivial because the solutions f we are looking for are non-regular and using the standard FFT is prohibitively inefficient.

We introduce in an approximation scheme that can efficiently handle solutions to the Boltzmann equations discontinuous in velocity space. It is based on a new method for approximation of the Boltzmann collision operator and solutions using non-uniform grids in velocity space. We illustrate the method by examples of space homogenious evolution solutions to the Boltzmann equation for different discontinuous initial distribution functions typical for boundary value problems.

The combination of the following techniques make input to its computational efficiency:

i) Fourier based spectral representation of the gain part of collision operator as a bilinear pseudodifferential operator excluding effectively the integration over the sphere S^2 from the computations of $Q(f,f)$.

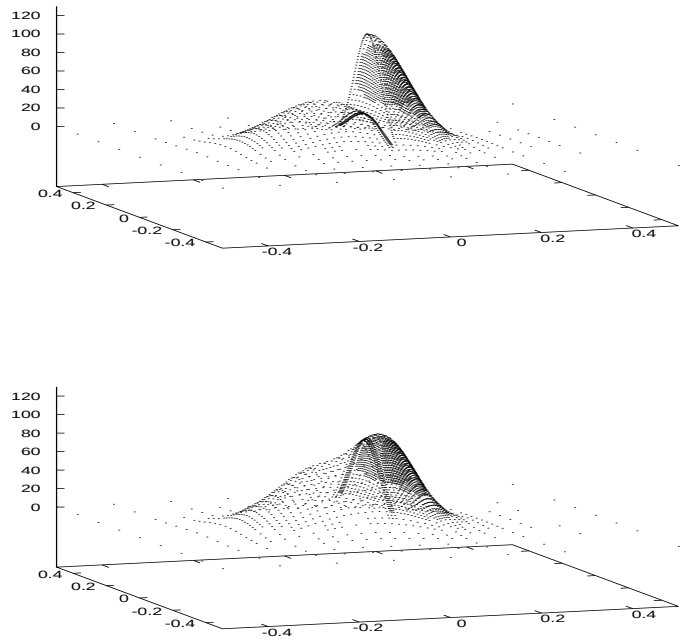

Figure 3: A distribution function f with discontinuity and the corresponding gain term $Q^+(f, f)$

ii) effective resolution of discontinuities of solutions using an adaptive grid

iii) high precision spectral representation for the smooth terms $Q^+(f,f)$ and $q^-(f)$ in the Boltzmann equation

iv) application of an approximate Fast Fourier Transform on non-uniform grid by Beylkin [8] for fast computation of the gain term $Q^+(f,f)$ and collision frequency $q^-(f)$ for f defined on an adaptive non-uniform grid.

v) an approximate algebraic decomposition of the symbol $\hat{B}(\mathbf{l},\mathbf{m})$ in the bilinear pseudodifferential expression for the gain term $Q^+(f,f)$.

The novelty of [HKG] consists in creating a robust deterministic numerical method that in a flexible way uses specific convolution structure of Boltzmanns collision operator and at the same time recovers singularities of solutions typical for the boundary value problems. These two points contradict each other to some extend and it is a key technical point in the paper.

• The general idea to combine a spectral representation for smooth terms in the Boltzmann equation with approximation of the discontinuous solution f on and adaptive grid is completely new.

• Among mentioned above key points in the method i) and ii) were known before, iii), iv), v) vi) are new for the Boltzmann equation.

• The computational cost of the numerical approximation of the collision operator is $\mathrm{O}(p^3 N_v) + \mathrm{O}(\sigma N^6 \log N)$. Here N_v is the number of collocation points in velocity space, σ is a small number and $3 < p < 7$, depending on the required accuracy.

We point out that the computational cost consists of two parts. The first one depends on the approximation of the discontinuous solution and increases linearly with the number N_v of points in the adaptive velocity grid. Another part depends on the approximation of the smooth terms in the equation. Here N is the number of Fourier modes along one coordinate direction necessary for approximating smooth terms in the Boltzmann equation that is moderate, It implies that the suggested deterministic method for computing the Boltzmann collision operator seems to be considerably more effective than previous ones.

• The suggested method is the only one known that within a "fast Fourier framework" works for discontinuous solutions to the Boltzmann equation.

References

[1] U. Abresch and J. Langer, *The normalized curve shortening flow and homothetic solutions*, J. Differential Geom., 23 (1986), pp. 175–196.

[2] L. Alvarez, F. Guichard, P.-L. Lions, and J.-M. Morel, *Axioms and fundamental equations of image processing*, Arch. Rational Mech. Anal., 123 (1993), pp. 199–257.

[3] F. Andreu-Vaillo, V. Caselles, and J. M. Mazón, *Existence and uniqueness of a solution for a parabolic quasilinear problem for linear growth functionals with L^1 data*, Math. Ann., 322 (2002), pp. 139–206.

[4] H. Babovsky, *On a simulation scheme for the Boltzmann equation*, Math. Methods Appl. Sci., 8 (1986), pp. 223–233.

[5] G. Barles and C. Georgelin, *A simple proof of convergence for an approximation scheme for computing motions by mean curvature*, SIAM J. Numer. Anal., 32 (1995), pp. 484–500.

[6] G. Barles and P. E. Souganidis, *Convergence of approximation schemes for fully nonlinear second order equations*, Asymptotic Anal., 4 (1991), pp. 271–283.

[7] G. Bellettini, M. Paolini, and C. Verdi, *Front-tracking and variational methods to approximate interfaces with prescribed mean curvature*, in Numerical methods for free boundary problems (Jyväskylä, 1990), vol. 99 of Internat. Schriftenreihe Numer. Math., Birkhäuser, Basel, 1991, pp. 83–92.

[8] G. Beylkin, *On the fast Fourier transform of functions with singularities*, Appl. Comput. Harmon. Anal., 2 (1995), pp. 363–381.

[9] G. A. Bird, *Recent advances and current challenges for DSMC*, Comput. Math. Appl., 35 (1998), pp. 1–14. Simulation methods in kinetic theory.

[10] A. Bobylev and S. Rjasanow, *Difference scheme for the Boltzmann equation based on the fast Fourier transform*, European J. Mech. B Fluids, 16 (1997), pp. 293–306.

[11] A. V. Bobylev, *The method of the Fourier transform in the theory of the Boltzmann equation for Maxwell molecules*, Dokl. Akad. Nauk SSSR, 225 (1975), pp. 1041–1044.

[12] A. V. Bobylev and S. Rjasanow, *Fast deterministic method of solving the Boltzmann equation for hard spheres*, Eur. J. Mech. B Fluids, 18 (1999), pp. 869–887.

[13] K. A. Brakke, *The motion of a surface by its mean curvature*, Princeton University Press, Princeton, N.J., 1978.

[14] L. Bronsard and R. V. Kohn, *Motion by mean curvature as the singular limit of Ginzburg-Landau dynamics*, J. Differential Equations, 90 (1991), pp. 211–237.

[15] C. Buet, *A discrete-velocity scheme for the Boltzmann operator of rarefied gas dynamics*, Transport Theory Statist. Phys., 25 (1996), pp. 33–60.

[16] F. Cao, *Partial differential equations and mathematical morphology*, J. Math. Pures Appl. (9), 77 (1998), pp. 909–941.

[17] F. Catté, F. Dibos, and G. Koepfler, *A morphological scheme for mean curvature motion and applications to anisotropic diffusion and motion of level sets*, SIAM J. Numer. Anal., 32 (1995), pp. 1895–1909.

[18] C. Cercignani, *The Boltzmann equation and its applications*, vol. 67 of Applied Mathematical Sciences, Springer-Verlag, New York, 1988.

[19] Y. G. Chen, Y. Giga, and S. Goto, *Uniqueness and existence of viscosity solutions of generalized mean curvature flow equations*, J. Differential Geom., 33 (1991), pp. 749–786.

[20] D. L. Chopp, *Computing minimal surfaces via level set curvature flow*, J. Comput. Phys., 106 (1993), pp. 77–91.

[21] D. L. Chopp and J. A. Sethian, *Motion by intrinsic Laplacian of curvature*, Interfaces Free Bound., 1 (1999), pp. 107–123.

[22] U. Clarenz, U. Diewald, G. Dziuk, M. Rumpf, and R. Rusu, *A finite element method for surface restoration with smooth boundary conditions*, CAGD, (2004). to appear.

[23] M. G. Crandall, H. Ishii, and P.-L. Lions, *User's guide to viscosity solutions of second order partial differential equations*, Bull. Amer. Math. Soc. (N.S.), 27 (1992), pp. 1–67.

[24] M. G. Crandall and P.-L. Lions, *Convergent difference schemes for nonlinear parabolic equations and mean curvature motion*, Numer. Math., 75 (1996), pp. 17–41.

[25] E. De Giorgi, *Conjectures on limits of some quasilinear parabolic equations and flow by mean curvature*, in Partial differential equations and related subjects (Trento, 1990), Longman Sci. Tech., Harlow, 1992, pp. 85–95.

[26] R. J. DiPerna and P.-L. Lions, *On the Cauchy problem for Boltzmann equations: global existence and weak stability*, Ann. of Math. (2), 130 (1989), pp. 321–366.

[27] M. Droske and M. Rumpf, *A level set formulation for willmore flow*, Interfaces and Free Boundaries, (2004). accepted.

[28] L. C. Evans, *Convergence of an algorithm for mean curvature motion*, Indiana Univ. Math. J., 42 (1993), pp. 533–557.

[29] L. C. Evans and J. Spruck, *Motion of level sets by mean curvature. I*, J. Differential Geom., 33 (1991), pp. 635–681.

[30] E. Gabetta and L. Pareschi, *The Maxwell gas and its Fourier transform towards a numerical approximation*, in Waves and stability in continuous media (Bologna, 1993), vol. 23 of Ser. Adv. Math. Appl. Sci., World Sci. Publishing, River Edge, NJ, 1994, pp. 197–201.

[31] D. Goldstein, B. Sturtevant, and J. Broadwell, *Investigation of the motion of discrete-velicity gases*, in Proceedings of the 16-th Int. Symp. on RGD, in: Ser. Progress in Astronautics and Aeronautics. Vol. 118, ed. E.P. Muntz et al., pp. 100-117, 1989, vol. 118, 1989, pp. 100–117.

[32] F. Guichard and J.-M. Morel, *Partial differential equations and image iterative filtering*, in The state of the art in numerical analysis (York, 1996), Oxford Univ. Press, New York, 1997, pp. 525–562.

[33] G. Huisken, *Local and global behaviour of hypersurfaces moving by mean curvature*, in Differential geometry: partial differential equations on manifolds (Los Angeles, CA, 1990), vol. 54 of Proc. Sympos. Pure Math., Amer. Math. Soc., Providence, RI, 1993, pp. 175–191.

[34] H. Ishii, *A generalization of the Bence, Merriman and Osher algorithm for motion by mean curvature*, in Curvature flows and related topics (Levico, 1994), Gakkōtosho, Tokyo, 1995, pp. 111–127.

[35] H. Ishii and K. Ishii, *An approximation scheme for motion by mean curvature with right-angle boundary condition*, SIAM J. Math. Anal., 33 (2001), pp. 369–389 (electronic).

[36] H. Ishii, G. E. Pires, and P. E. Souganidis, *Threshold dynamics type approximation schemes for propagating fronts*, J. Math. Soc. Japan, 51 (1999), pp. 267–308.

[37] H. Ishii and P. Souganidis, *Generalized motion of noncompact hypersurfaces with velocity having arbitrary growth on the curvature tensor*, Tohoku Math. J. (2), 47 (1995), pp. 227–250.

[38] S. Kosuge, K. Aoki, and S. Takata, *Shock-wave structure for a binary gas mixture: Finite-difference analysis of the boltzmann equation for hard-sphere molecules*, European J. Mech. B Fluids, 20 (2001), pp. 87–101.

[39] E. Kuwert and R. Schätzle, *Gradient flow for the Willmore functional*, Comm. Anal. Geom., 10 (2002), pp. 307–339.

[40] ——, *Removability of isolated singularities of Willmore surfaces*, Ann. of Math., (to appear).

[41] P.-L. Lions, *Compactness in Boltzmann's equation via Fourier integral operators and applications. I, II*, J. Math. Kyoto Univ., 34 (1994), pp. 391–427, 429–461.

[42] U. F. Mayer, *Numerical solutions for the surface diffusion flow in three space dimensions*, Comput. Appl. Math., 20 (2001), pp. 361–379.

[43] U. F. Mayer and G. Simonett, *Self-intersections for the Willmore flow*, Proceedings of the Seventh International Conference on Evolution Equations: Applications to Physics,Industry, Life Sciences and Economics, (2000), p. 9.

[44] ——, *A numerical scheme for axisymmetric solutions of curvature-driven free boundary problems, with applications to the Willmore flow*, Interfaces Free Bound., 4 (2002), pp. 89–109.

[45] B. Merriman, J. K. Bence, and S. J. Osher, *Motion of multiple functions: a level set approach*, J. Comput. Phys., 112 (1994), pp. 334–363.

[46] S. Mischler, *Convergence of discrete-velocity schemes for the Boltzmann equation*, Arch. Rational Mech. Anal., 140 (1997), pp. 53–77.

[47] R. Moser, *Weak solutions of the Willmore flow*, Max Planck Institute for Mathematics in the Sciences, Preprint Nr. 97, (2001).

[48] K. Nanbu, *Stochastic solution method of the master equation and the model Boltzmann equation*, J. Phys. Soc. Japan, 52 (1983), pp. 2654–2658.

[49] T. Ohta, D. Jasnow, and K. Kawasaki, *Unioversal scaling in the motion of random interfaces*, Phys. Rev. Lett., 47 (1982), pp. 1223–1226.

[50] T. Ohwada, *Structure of normal shock waves: direct numerical analysis of the Boltzmann equation for hard-sphere molecules*, Phys. Fluids A, 5 (1993), pp. 217–234.

[51] S. Osher and J. A. Sethian, *Fronts propagating with curvature-dependent speed: algorithms based on Hamilton-Jacobi formulations*, J. Comput. Phys., 79 (1988), pp. 12–49.

[52] A. Palczewski, J. Schneider, and A. V. Bobylev, *A consistency result for a discrete-velocity model of the Boltzmann equation*, SIAM J. Numer. Anal., 34 (1997), pp. 1865–1883.

[53] V. A. Panferov and A. G. Heintz, *A new consistent discrete-velocity model for the Boltzmann equation*, Math. Methods Appl. Sci., 25 (2002), pp. 571–593.

[54] L. Pareschi and B. Perthame, *A Fourier spectral method for homogeneous Boltzmann equations*, in Proceedings of the Second International Workshop on Nonlinear Kinetic Theories and Mathematical Aspects of Hyperbolic Systems (Sanremo, 1994), vol. 25, 1996, pp. 369–382.

[55] L. Pareschi and G. Russo, *Numerical solution of the Boltzmann equation. I. Spectrally accurate approximation of the collision operator*, SIAM J. Numer. Anal., 37 (2000), pp. 1217–1245 (electronic).

[56] D. Pasquignon, *Approximation of viscosity solution by morphological filters*, ESAIM Control Optim. Calc. Var., 4 (1999), pp. 335–359 (electronic).

[57] F. Rogier and J. Schneider, *A direct method for solving the Boltzmann equation*, Transport Theory Statist. Phys., 23 (1994), pp. 313–338.

[58] S. J. Ruuth and B. Merriman, *Convolution-thresholding methods for interface motion*, J. Comput. Phys., 169 (2001), pp. 678–707.

[59] G. Simonett, *The Willmore flow near spheres*, Differential Integral Equations, 14 (2001), pp. 1005–1014.

[60] S. Takata, Y. Sone, and K. Aoki, *Numerical analysis of a uniform flow of a rarefied gas past a sphere on the basis of the Boltzmann equation for hard-sphere molecules*, Phys. Fluids A, 5 (1993), pp. 716–737.

[61] T. Tasdizen, R. Whitaker, P. Burchard, and S. Osher, *Geometric surface smoothing via anisotropic diffusion of normals*, Proceedings of the conference on Visualization, 1 (2002), pp. 125–132.

[62] B. Wennberg, *The geometry of binary collisions and generalized Radon transforms*, Arch. Rational Mech. Anal., 139 (1997), pp. 291–302.

Paper [GH1]

A convolution-thresholding approximation of generalized curvature flows

Ricards Grzibovskis * Alexei Heintz†

Abstract

We construct a convolution-thresholding approximation scheme for the geometric surface evolution in the case when the velocity of the surface at each point is a given function of the mean curvature. Conditions for the monotonicity of the scheme are found and the convergence of the approximations to the corresponding viscosity solution is proved. We also discuss some aspects of the numerical implementation of such schemes and present several numerical results.

Keywords: generalized curvature flow, convolution-thresholding scheme, viscosity solution, level-set equation

AMS Subject classification: 65M12, 53C44, (49L25, 35K55)

1 Introduction

Curvature flows of different types were during last 20 years and still are a popular topic both in pure and applied mathematics. By curvature flow we mean a family $\{\Gamma_t\}_{t\geq 0}$ of hyper-surfaces in $\mathbb{R}^n$ depending on time t with local normal velocity equal to the mean curvature or a function of it for generalized curvature flows. The mean curvature in turn denotes here the sum of principal curvatures.

*Department of Mathematics, Chalmers University of Technology, 41296 Göteborg, Sweden (richards@math.chalmers.se).

†Department of Mathematics, Chalmers University of Technology, 41296 Göteborg, Sweden (heintz@math.chalmers.se).

In the three dimensional case a smooth initial surface can develop singularities after some finite time. There have been several successful attempts to deal with singularities and topological complications: the varifold approach ([7], [2]), the phase field method ([14], [8]) and the level-set method. This approach was suggested in the physical literature [26] and was extensively developed for numerical purposes by Osher and Sethian [27]. The main idea of this method is to evolve some continuous function $u : [0,\infty) \times \mathbb{R}^n \mapsto \mathbb{R}$ in such way that $\Gamma_t \subset \mathbb{R}^n$ would always be a level-set of $u(x,t)$ i.e. $\Gamma_t = \{x \in \mathbb{R}^n : u(x,t) = 0\} \ \forall t \geq 0$. In the case of the mean curvature flow the evolution equation for u turns out to be

$$u_t = |Du| \operatorname{div}\left(\frac{Du}{|Du|}\right). \tag{1}$$

The evolution equation for a function u with each point of a level-set moving along the normal with velocity equal to some function G of the mean curvature is, so called generalized mean curvature evolution PDE

$$u_t = |Du| G\left(\operatorname{div}\left(\frac{Du}{|Du|}\right)\right). \tag{2}$$

These equation are degenerate parabolic. The existence and uniqueness of generalized viscosity solutions (see [12]) to the initial value problem

$$\begin{cases} u_t = |Du| G\left(\operatorname{div}\left(\frac{Du}{|Du|}\right)\right) & \text{in } \mathbb{R}^n \times (0,T) \\ u = g(x) \in BUC(\mathbb{R}^n) & \text{on } \mathbb{R}^n \times \{0\}. \end{cases} \tag{3}$$

was investigated in [17], [11], [22].

Curvature flows arise naturally in various problems. Among these are fast reaction-slow diffusion problem ([29], [4], [16], [19]) and image processing [1].

In the present work we construct a class of approximations of a convolution - thresholding type to the generalized curvature flows. By this we mean the following. Assume, that initially the surface under consideration is a boundary of a compact set $C \in \mathbb{R}^n$. Take compactly supported functions $\tilde{\rho}_i : \mathbb{R}_+ \longmapsto \mathbb{R}_+ \ i = 1,2$ (in fact, one can also take $\tilde{\rho}_i$ with unbounded support decreasing fast for large x). We define $\rho_i : \mathbb{R}^n \mapsto \mathbb{R}_+$,

$$\rho_i(x) = \frac{1}{h^{n/2}} \tilde{\rho}_i\left(|x| / \sqrt{h}\right)$$

and introduce a convolution

$$M_i(C)(x,h) = \int_{\mathbb{R}^n} \chi_C(y) \rho_i(x-y)\, dy.$$

Now $M_i(C)(x,h)$ are functions of x, and we define a new position of the surface as a boundary of the set

$$\mathcal{H}_h C = \{x \in \mathbb{R}^n : F(M_1(C)(x,h), M_2(C)(x,h)) \geq 0\}, \tag{4}$$

where F is some (thresholding) function. Next we follow Evans [15] and introduce an operator on the space of bounded functions $\mathbb{B}(\mathbb{R}^n)$: $H(h) : \mathbb{B}(\mathbb{R}^n) \mapsto \mathbb{B}(\mathbb{R}^n)$ by

$$[H(h)u](x) = \sup\{\lambda \in \mathbb{R} : x \in \mathcal{H}_h[u \geq \lambda]\}. \tag{5}$$

The purpose of the present study is for a given function G in (3), to find a corresponding thresholding function F in (4), so that $H(t/m)^m g(x)$ would converge to the unique viscosity solution of (3) as $m \to \infty$.

Such function in case when G is linear was proposed by Merriman, Bence and Osher in [25]. This result is often referred to as the "Bence-Merriman-Osher method". Rigorous proofs of the convergence of such approximations can be found in [15], [20] and [3]. In this case it is enough to take a thresholding function depending only on one convolution.

Suppose, that G is non-linear. As we show in Section 3, in this case one has to use two convolutions M_1 and M_2 and a thresholding function depending on two variables $F(M_1, M_2)$. This is necessary to ensure that the operator H is consistent with the PDE in (3). We also show, how to choose convolution kernels in order to get a monotone H. These two conditions - monotonicity and consistency - are crucial for the convergence.

Using our approach we also suggest a new construction of higher order schemes for the classical curvature flows. The numerical experiments with these schemes show a considerable improvement in the accuracy.

Finite difference approximations for (3) have been studied in [27], [31], [13].

Another class of approximation operators, so called Matheron filters, comes from the image processing. The connection between such operators and the mean curvature evolution PDE (2) was established in [10]. This result was then extended in [18] and [9].

Threshold dynamics models, introduced earlier in [21], lead to approximations of the solution of the Cauchy problem to a nonlinear parabolic equation, where the right hand side can be interpreted as a general elliptic operator on a level set of the solution. This is a generalization of the curvature flow, but it does not entirely include (3) as a special case.

Another generalization of the Bence-Merriman-Osher method can be found in [23]. The author suggests an approximation procedure that allows tracking the surface evolution when the velocity of the surface depends also on the coordinates. The convergence of this approximations is also proved.

Kinetic motivation. The following kinetic approximation scheme can serve as a useful physical interpretation of the more general convolution - thresholding approximation methods for generalised curvature flows that we suggest in the present paper. This kinetic approximation is similar to the phase field approach but is more flexible.

Let $f(t,x,\xi)$ with $\xi \in \mathbb{R}^n$ be the distribution function having the sense of the amount of particles in the volume $dxdv$. The function $u(t,x) = \int f(t,x,\xi)\, d\xi$ has the sense of the mean density of the gas with distribution function f at position x at time t. General mean values like $M(t,x) = \int f(t,x,\xi)\,\lambda(\xi)\, d\xi$ with a weight function $\lambda(\xi) \geq 0$ are traditionally interpreted as macro parameters for a gas with the distribution function f.

We consider the following BGK type model kinetic equation for $f(t,x,\xi)$ with collision term consisting of two qualitatively different terms

$$\frac{\partial f}{\partial t} + \xi \nabla_x f = \frac{1}{Kn}\left(u\rho(\xi) - f\right) + \frac{1}{\gamma} f(\xi)\, G(u,M). \tag{6}$$

The first one is a usual relaxation term with normalised "Maxwellian" distribution $\rho(\xi)$, $\int \rho(\xi)\, d\xi = 1$. The second term describes a kind of chemical reaction that generates particles or eliminate them depending on the values of the density $u(t,x)$ and possibly of some other macroparameter $M(t,x)$. The relaxation term makes f tend to a local equilibrium $u(t,x)\,\rho(\xi)$.

The choice of the function $G(\rho, M,)$ determines qualitative properties of solutions.

A standard method for solving an equation of kinetic type is the splitting method. Instead of solving equation (6) one can sequentially solve on small time steps Δt the following simpler equations having a clear physical meaning:

$$\begin{aligned} \frac{\partial f_1}{\partial t} + \nabla_x \xi f_1 = 0, &\qquad - \text{ collisionless flow,} \\ f_1|_{t=0} &= F_0; \\ \frac{\partial f_2}{\partial t} = \frac{1}{\gamma} f_2(\xi)\cdot G(u,M), &\qquad - \text{ chemical reaction} \end{aligned} \tag{7}$$

$$
\begin{aligned}
f_2|_{t=\Delta t} &= f_1(\Delta t); \\
\frac{\partial f_3}{\partial t} = \frac{1}{Kn}(u\rho(\xi) - f_3), & \quad - \text{ relaxation} \\
f_3|_{t=2\Delta t} &= f_2(2\Delta t);
\end{aligned}
$$

where the macro parameters u, M ingoing in the equations are calculated for the actual approximation, correspondingly f_1, f_2 , f_3.

The first step means that the initial data $F_0(x,\xi)$ are transported from each point $x_0 \in R^n$ along the collisionless paths $x = x_0 + t\xi$ to the points $x = x_0 + \Delta t\xi$. The resulting distribution function $f_1(\Delta t, x, \xi)$ differs much from the locally equilibrium $u(\Delta t, x)\rho(\xi)$ function.

We choose parameters γ and Kn small in comparison with Δt. The solutions of the second and the third equations of the splitting scheme will be after the time Δt close to stationary solutions corresponding to zeroes of operators in the right hand sides of these equations. These zeroes determine geometrical properties and the character of the whole process.

Zeroes of the linear operator $(u\rho(\xi) - f)$ are evidently all functions of the form $u(x)\rho(\xi)$. We still do not concretize the function $\rho(\xi)$. The only requirement is the existence of moments of high enough order. Depending on what kind of surface dynamics we want to model we will impose more concrete conditions.

The integration of (7) with respect to ξ with weights 1 and $\lambda(\xi)$ gives the equations

$$
\begin{aligned}
\frac{\partial u}{\partial t} &= \frac{1}{\gamma} uG(u, M) \\
\frac{\partial M}{\partial t} &= \frac{1}{\gamma} MG(u, M)
\end{aligned}
$$

We choose the chemical reaction term $G(u, M)$ such that this system of differential equations has two stable stationary points (u_1, M_1) and $(u_2\ , M_2)$ in the plane of macro parameters and one unstable stationary manifold determined by the equation $F(u, M) = 0$.

For $\gamma << 1$ the $u(t,x)$ and $M(t,x)$ reach after the finite time Δt one of the stationary states depending on the initial data at the point x . This process leads to the formation of two sets with constant density values u_1 and u_2, and an interface set Γ that we shell use for the approximation of generalised

curvature flows. One can observe from here that only the thresholding function $F(u, M)$ is important for our approximations. Details of the chemical reaction term do not play any role for our scheme.

At the third step of the splitting method the distribution function evolves independently at all space points x tending to a locally equilibrium stage of the form $u(x) M(\xi)$ depending on x only via the density $u(x)$. If the parameter $Kn << 1$ this convergence to equilibrium is fast and the equilibrium is achieved after the time Δt . Now we apply this procedure to particular initial data for modeling surface dynamics.

Consider the family $\Gamma(t)$ of surfaces with initial state $\Gamma(0)$ such that $\Gamma(0) = \partial C_0$ is a boundary for a compact set C_0 . We use here the notation $t = \Delta t$.

Take the initial distribution function $f_1(0, x, \xi) = F_0(x, \xi)$ in the form

$$F_0(x, \xi) = u_0 \cdot \rho(\xi),$$

where u_0 is the characteristic function of the set C_0 times the equilibrium distribution $\rho(\xi)$. Moments of different orders of the function $f_1(t, x, \xi)$ play a crucial role in the construction of our approximations to the differential characteristics of the surface $\Gamma(t)$.

We require here that the function $\rho(\xi)$ is non negative, dependent only on $|\xi|$ and has enough many moments.

We consider the function $f_1(\Delta t, x, \xi)$ and corresponding values of mean values u , M.

$$u_1(t, x) = \int_{R^n} u_0(x - t\xi) \rho(\xi) d\xi$$

The change of variables $y = x - t\xi$ gives

$$u_1(t, x) = \int_{R^n} u_0(y) \frac{1}{t^n} \rho((x - y)/t) dy = u_0 * m_t(x) \tag{8}$$

namely that the function $u_1(x)$ is a convolution of the initial density u_0 with the function $m_t(y) = \frac{1}{t^n} \rho(y/t)$.

The same proof shows similar convolution formulas for any weight $\lambda(\xi)$ with $m_\lambda(y) = \frac{1}{t^n} \lambda(y/t) \rho(y/t)$:

$$M_\lambda(t, x) = \int_{R^n} \rho_0(x - t\xi) \lambda(\xi) \rho(\xi) d\xi =$$

$$
\begin{aligned}
&= \int_{R^n} \rho_0(y)\,\lambda\left((x-y)/t\right)\frac{1}{t^n}\rho\left((x-y)/t\right)dy = \\
&= \left(\rho_0 * m_{\lambda,t}\right)(x)
\end{aligned}
$$

with $m_{\lambda,t} = \lambda(y/t)\cdot\dfrac{1}{t^n}\rho(y/t)$.

The result $f_3(3\Delta t, x, \xi)$ after the chemical reactions step and the relaxation step has the form $f_3(3\Delta t, x, \xi) = u_3(x)\,\rho(\xi)$ where u_3 is a characteristic function of a compact domain bounded by the surface where the thresholding function $F(u, M) = 0$.

We see that the kinetic splitting scheme generates a kind of convolution thresholding dynamics of surfaces with thresholding depending on two (or more) convolutions. The simpler example given at the beginning of the section is reproduced if we choose chemical reactions $G = G(u)$ depending only on the density u of the gas and take the time scaling $t = \sqrt{h}$.

Outline This paper is organized as follows. After introducing the basic notions and stating some results for viscosity solutions in Section 2, we turn to our method of approximation for such solutions. In Section 3, where we construct F in order to get the convergence of the convolution-thresholding approximation to the viscosity solution of (3) with a monotone continuous function G. This is the main result of the paper. More precisely, the following local uniform convergence is proved

$$
\left(\left(H(t/m)\right)^m g\right)(x) \to u(x,t), m \to \infty,
$$

where H defined by (5) and $u(x,t)$ is the viscosity solution of (3).

We use this construction for numerical calculation for some cases of the generalized curvature flows in $\mathbb{R}^2$ and $\mathbb{R}^3$. Numerical results and two approaches to the implementation are described in Section 4.

2 The viscosity solution framework

Consider the non-linear equation (2) on an open set $\Omega \times (0,T)$ with function G continuous and nondecreasing. This is the second order equation with right hand side that is monotonic and degenerate elliptic (see [12]) provided that G is nondecreasing and $Du \neq 0$.Viscosity solution to (2) was defined

by Evans and Spruck in [17] and by Chen, Giga and Goto in [11]. In our presentation we will use a somewhat more general definition of viscosity solutions introduced by Ishii and Souganidis in [22] to allow a wider class of functions G in (2). For general degenerate elliptic equation

$$u_t + \mathcal{G}\left(Du, D^2u\right) = 0 \tag{9}$$

they introduce a special class of test functions and adapt the definition of viscosity solution for possible singularities of the right hand side. Representation of (3) in the form of (9) gives

$$\mathcal{G}(p, X) = -|p| G\left(\frac{1}{|p|}\mathrm{tr}\left(\left(I - \frac{p \otimes p}{|p|^2}\right) X\right)\right).$$

Let us begin by introducing an auxiliary subclass of $C^2([0,\infty))$. We say that $f : [0,\infty) \mapsto \mathbb{R}$ lies in $\mathcal{F} \subset C^2$ if $f(0) = f'(0) = f''(0) = 0$, $f''(r) > 0$ for $r > 0$ and the following limits hold

$$\lim \frac{f'(|p|)}{|p|}\mathcal{G}(p, I) = \lim \frac{f'(|p|)}{|p|}\mathcal{G}(p, -I) = 0.$$

As was shown in [22], this set of functions is a non-empty cone, provided that the right hand side lies in $C((\mathbb{R}^n \setminus \{0\}) \times \mathbb{S}(n))$. The class of test functions $\mathcal{A}(\mathcal{G})$ depends on $\mathcal{G}$ and is defined as follows.

Definition 1. *A function ϕ is admissible if it is in $C^2(\mathbb{R}^n \times (0,T))$ and for each $\acute{z} = \left(\acute{x}, \acute{t}\right)$ where $D\phi(\acute{z}) = 0$, there is $\delta > 0$, $f \in \mathcal{F}$ and $\omega \in C([0,\infty))$ such that $\omega = o(r)$ and for all $(x,t) \in B(\acute{z}, \delta)$*

$$\left|\phi(x,t) - \phi(\acute{z}) - \phi_t(\acute{z})\left(t - \acute{t}\right)\right| \leq f(|x - \acute{x}|) + \omega\left(\left|t - \acute{t}\right|\right).$$

Let us also denote by u^* and u_* the upper and lower semi-continuous envelopes of u:

$$u^*(x,t) = \limsup_{(y,s)\to(x,t)} u(y,s), \quad u_*(x,t) = \liminf_{(y,s)\to(x,t)} u(y,s)$$

The definition of viscosity solution becomes

Definition 2. *Take an open set $\tilde{\mathcal{O}} \subset \mathbb{R}^n$ and $\mathcal{O} = \tilde{\mathcal{O}} \times (0,T)$. $u : \mathcal{O} \subset \mathbb{R}^n \times (0,T) \mapsto \mathbb{R} \cup \{-\infty\}$ is a viscosity subsolution (supersolution) of (2)*

in an open $\mathcal{O}$ if $u^* < \infty$ ($u_* > -\infty$) and for all $\phi \in \mathcal{A}(G)$ and all local maximum (minimum) points (z_0, t_0) of $u^* - \phi$ ($u_* - \phi$),

$$\begin{cases} \phi_t(z_0,t_0) \leq (\geq) \left|D\phi(z_0,t_0)\right| G\left(div \dfrac{D\phi(z_0,t_0)}{\left|D\phi(z_0,t_0)\right|}\right) & \text{if } D\phi(z) \neq 0 \\ \phi_t(z_0,t_0) \leq (\geq) 0 & \text{otherwise.} \end{cases}$$

Consequently, a viscosity solution is a function that is sub- and supersolution simultaneously.

The result by Ishii and Souganidis presented in [22] can be restated in terms of the level-set equation (see [28]) as follows:

Theorem 1. *Assume, that G is continuous and nondecreasing. Then the initial value problem (3) has a unique viscosity solution $u \in BUC(\mathbb{R}^n \times (0,T))$.*

In what follows, we also use another result by Ishii and Souganidis [22] concerning locally uniform perturbations of the right hand side of the equation. One can restate this result in the case of (2) as follows (see [28]):

Theorem 2. *Assume, that G is continuous and nondecreasing. Suppose also, that $\{G_m\}_1^\infty$ is a sequence of continuous, nondecreasing functions on $\mathbb{R}$ and $G_m \to G$ locally uniformly. Let for any m, $\mathcal{F}(G) \subset \mathcal{F}(G_m)$ and for any $f \in \mathcal{F}(G)$,*

$$\begin{aligned} \liminf_{p\to,\, m\to\infty} f'(|p|)\, G_m(1/p) &\geq 0 \\ (resp.\ \limsup_{p\mapsto 0,\, m\to\infty} f'(|p|)\, G_m(-1/p) &\leq 0) \end{aligned}$$

Let u_m be a subsolution (resp. supersolution) of

$$\frac{\partial u_m}{\partial t} = |Du_m|\, G_m\left(div \frac{Du_m}{|Du_m|}\right) \text{ in } \mathcal{O}.$$

Then

$$u^+(z) = \limsup_{r\mapsto 0} \{u_m(y), |y-z| \leq r,\ m > 1/m\} \tag{10}$$

$$(resp. u_+(z) = \liminf_{r\to 0} \{u_m(y), |y-z| \leq r,\ m > 1/m\}) \tag{11}$$

is a subsolution (resp. supersolution) of (2) in $\mathcal{O}$ provided that $u^+ < \infty$ (resp. $u_+ > -\infty$).

3 A convolution-thresholding method for a generalized curvature flow

3.1 Convergence of approximation schemes

Here we make use of a theorem by Barles and Souganidis proved in [5]. In order to base the proof of our main result on this theorem, we follow Pasquignon [28] and restate it in terms of the equation (2).

Let $H(h)$ be the approximation operator i.e.

$$\begin{aligned} u_h(x,(n+1)h) &= H(h)\,u_h(x,nh) = H(h)^{n+1}\,u_0(x), \\ u_h(x,0) &= u_0(x). \end{aligned}$$

Definition 3.

1. *Consistency*
   An approximation operator $H(h)$, $h>0$ is consistent with (2) if for any $\phi \in C^\infty\left(\bar{\Omega}\right)$ and for any $x \in \bar{\Omega}$, the following holds,

$$\frac{(H(h)\,\phi)(x)-\phi(x)}{h} = |D\phi|\,G\left(div\frac{Du}{|Du|}\right)+o_x(1) \text{ for } D\phi \neq 0. \quad (12)$$

   If the convergence of $o_x(1)$ is locally uniform on sets, where $Du \neq 0$, then $H(h)$ is said to be uniformly consistent with the PDE.

2. *Monotonicity*
   An operator $H(h)$, $h>0$ is locally monotone if there exists $r>0$ such that for any functions $u(y), v(y) \in \mathbb{B}\left(\bar{\Omega}\right)$ with $u \geq v$ on $B(x,r)\setminus\{x\}$, the following holds

$$H(h)\,u(y) \geq H(h)\,v(y)+o(h),$$

   where the convergence of $o(h)$ is uniform on $B(x,r)\setminus\{x\}$

3. *Stability*
   An approximation scheme $H(h)$ is stable if $H(h)^n\,u \in \mathbb{B}\left(\bar{\Omega}\right)$ for every $u \in B\left(\bar{\Omega}\right), n \in \mathbb{N}, h>0$, with bound independent of h and n.

In this setting the result of Barles and Souganidis reads:

Theorem 3. *Consider a monotone, stable approximation operator $H(h)$ that commutes with additions of constants (i.e $H(h)(u+C) = H(h)u + C$, $\forall C \in \mathbb{R}$) and is uniformly consistent with (2). Suppose also, that*

$$\lim_{h\to 0} \frac{H(h)(f(|x-x_0|))(x_0)}{h} = 0 \tag{13}$$

for any $f \in \mathcal{F}(G)$. Then $u_h(x, nh)$ converges locally uniformly to the unique viscosity solution $u(x,t)$ of (2) as $nh \mapsto t$.

3.2 Properties of $\mathcal{H}$

We consider a convolution generated motion of a hypersurface in $\mathbb{R}^n$ defined by (4) and the corresponding evolution of an initially bounded function $g : \mathbb{R}^n \mapsto \mathbb{R}$ defined by (5). Consider also the initial value problem (3) with given G and g. We are looking for such a thresholding function F in (4), that $H^m_{t/m} g(x)$ would converge (in some sense) to the unique viscosity solution of (3).

For example, set $F(M_1, M_2) = M_1 - 1/2$ and $\tilde{\rho}_1(x) = \frac{1}{(4\pi)^{n/2}} e^{-x^2/4}$ to get corresponding operators $\mathcal{H}_h$ and $H(h)$ by (4) and (5). Then we get the Bence-Merriman-Osher procedure to which the main result of [15] applies, and $H(h)^n u_0$ converges locally uniformly to the unique viscosity solution of (3) with $G(k) = k$.

We will see that, in fact, one has to use two convolutions M_1 and M_2 with different kernels and construct a thresholding function depending on two variables respectively to resolve this problem when G is not linear.

Let us now consider an operator $H(h)$ defined by (5) with the help of an operator $\mathcal{H}_h$ with an arbitrary thresholding function (4). We look for requirements on F sufficient to fulfill the conditions of Theorem 3.

Stability
Suppose $u(x) \in \mathbb{B}(\mathbb{R}^n)$. We shell show, that $H(h)u \in \mathbb{B}(\mathbb{R}^n)$. Intuitively, we require

$$\mathcal{H}_h \mathbb{R}^n = \mathbb{R}^n, \tag{14}$$

$$\mathcal{H}_h \emptyset = \emptyset, \tag{15}$$

and denote $A = \max|u|$. With these settings $[u \le A] = \mathbb{R}^n$ and

$$-A \le H(h)u(x) = \inf\{\lambda \in \mathbb{R} : x \in \mathcal{H}_h[u \le \lambda]\} \le A.$$

It remains to find out for which F the conditions (14) and (15) are satisfied. To do this, we substitute the corresponding sets into the definition of $\mathcal{H}$

$$\begin{aligned}
\mathcal{H}_h\mathbb{R}^n &= \left\{x \in \mathbb{R}^n : F\left(M_1\mathbb{R}^n(x,h), M_2\mathbb{R}^n(x,h)\right) \geq 0\right\} = \\
&= \left\{x \in \mathbb{R}^n : F\left(\int_{\mathbb{R}^n} \rho_1 dx, \int_{\mathbb{R}^n} \rho_2 dx\right) \geq 0\right\} = \mathbb{R}^n \\
\mathcal{H}_h\emptyset &= \left\{x \in \mathbb{R}^n : F\left(M_1\emptyset(x,h), M_2\emptyset(x,h)\right) \geq 0\right\} = \\
&= \left\{x \in \mathbb{R}^n : F(0,0) \geq 0\right\} = \emptyset.
\end{aligned}$$

Thus, the requirements on F become

$$\begin{aligned}
F\left(\int_{\mathbb{R}^n} \rho_1 dx, \int_{\mathbb{R}^n} \rho_2 dx\right) &\geq 0, \\
F(0,0) &< 0.
\end{aligned}$$

Monotonicity
Let us now show, that if $\mathcal{H}_h$ satisfies the so called inclusion principle, then H_h is monotonous.

Lemma 1. *Assume, that $\mathcal{H}_h$ satisfies the inclusion principle i.e.*

$$\forall C_1, C_2 \subseteq \mathbb{R}^n : C_1 \subseteq C_2 \text{ we have } \mathcal{H}_h C_1 \subseteq \mathcal{H}_h C_2, \tag{16}$$

then H_h is monotone, that is

$$\forall u, v \in \mathbb{C}(\mathbb{R}^n) : v \leq u \text{ we have } H_h(v) \leq H_h(u).$$

Proof. Suppose, there exists x_0 s.t. $H(h)u(x_0) < H(h)v(x_0)$. We denote $\lambda_1 = H(h)u(x_0)$, $\lambda_2 = H(h)v(x_0)$ and $\epsilon = \frac{\lambda_2 - \lambda_1}{2} > 0$. Since

$$\lambda_1 + \epsilon < \inf\left\{\lambda \in \mathbb{R} : x_0 \in \mathcal{H}_h[v \leq \lambda]\right\},$$

$x_0 \notin \mathcal{H}_h[v \leq \lambda_1 + \epsilon]$, but

$$\mathcal{H}_h[v \leq \lambda_1 + \epsilon] \supseteq \mathcal{H}_h[u \leq \lambda_1 + \epsilon].$$

Therefore $x_0 \notin \mathcal{H}_h[u \leq \lambda_1 + \epsilon]$, which is in contradiction with the definition of λ_1. □

Consistency
We sum up some calculations in the following

Lemma 2. *Let $\phi \in C^{\infty}(\mathbb{R}^n)$ $\phi(0) = 0$ and $D\phi(0) = (0, 0, \ldots, \beta)$. Then the consistency of an operator $H(h)$ with (3) is equivalent to*

$$\gamma(h, 0) = hG(-\Delta\gamma(h, 0)) + o(h), \tag{17}$$

where $\Delta\gamma(h, 0) = \sum_{i=1}^{n-1} \partial^2\gamma/\partial x_i^2(0)$ and $x_n = \gamma(h, \acute{x})$ is a parameterization of the surface

$$\{x \in \mathbb{R}^n : \phi(x) = H(h)\phi(0)\}$$

near $\acute{x} = 0$.

We observe that in these settings $-\Delta\gamma(h, 0) \equiv k$ is the mean curvature of the graph of γ at the point $(0, \gamma(h, 0))$.

Proof. Without loss of generality, one can consider the consistency condition (12) only for ϕ as in the statement. We rewrite (12) in a more convenient form

$$(H(h)\phi)(0) = h|D\phi(0)| G\left(\operatorname{div}\frac{D\phi}{|D\phi|}(0)\right) + o(h). \tag{18}$$

We use the equality

$$\operatorname{div}\left(\frac{D\phi}{|D\phi|}\right) = \frac{1}{|D\phi|}\sum_{i,j=1}^{n}\left(\delta_{i,j} - \frac{\phi_{x_i}\phi_{x_j}}{|D\phi|^2}\right)\phi_{x_i x_j}.$$

Since $\phi(0) = 0$ and $\phi_{x_i}(0) = \delta_{ni}\beta$,

$$\begin{aligned}\operatorname{div}\frac{D\phi}{|D\phi|}\Big|_{x=0} &= \frac{1}{\beta}\left[\sum_{i=1}^{n}\phi_{x_i x_i}(0) - \frac{\phi_{x_n}(0)\phi_{x_n}(0)}{\beta^2}\phi_{x_n x_n}(0)\right] = \\ &= \frac{1}{\beta}\Delta'\phi(0). \end{aligned}\tag{19}$$

Here $\Delta'\phi = \sum_{i=1}^{n-1}\phi_{x_i x_i}$. Our next step is to take small $\acute{x}$, namely $|\acute{x}| < Rh$. For such $\acute{x}$ we apply the inverse function theorem to ϕ,

$$H(h)\phi(0) = \phi(\acute{x}, \gamma(h, \acute{x})) = \phi(0) + \beta\gamma(h, 0) + O\left(h^2\right). \tag{20}$$

Putting (20) and (19) into (18) we get

$$\gamma(h, 0) = hG\left(\frac{1}{\beta}\Delta'\phi(0)\right) + o(h). \tag{21}$$

Furthermore, differentiating both sides of $H(h)\phi(0) = \phi(\acute{x}, \gamma(h, \acute{x}))$ gives

$$\begin{aligned} \phi_{x_i} + \phi_{x_n}\gamma_{x_i} &= 0 \\ \phi_{x_ix_j} + \phi_{x_ix_n}\gamma_{x_j} + \phi_{x_nx_j}\gamma_{x_i} + \phi_{x_nx_n}\gamma_{x_j}\gamma_{x_i} + \phi_{x_n}\gamma_{x_ix_j} &= 0 \end{aligned}$$

for $j, i = 1, \ldots, n-1$. We deduce $\gamma_{x_i}(h, 0) = 0$ from the first equality and rewrite the second one for $i = j$

$$\phi_{x_jx_j}(0) + \phi_{x_n}(0)\gamma_{x_jx_j}(h, 0) = 0.$$

After a summation over j this becomes

$$\frac{1}{\beta}\Delta'\phi(0) = -\Delta\gamma(h, 0).$$

It remains to put this relation into (21) to get the desired equality (17). □

3.3 The convergence result for general G

In this subsection we construct the thresholding function $F(M_1, M_2)$ and show that the corresponding convolution thresholding scheme (4), (5) converges to the viscosity solution $u(x, t)$ of (3)

$$H^m_{\frac{t}{m}}g(x) \to u(x, t) \text{ as } m \to \infty.$$

We start with $F(M_1C(x, h), M_2C(x, h))$, where

$$M_iC(x, h) = \int_C \rho_i(x - y)\, dy.$$

For each ρ_i we expand this integral into the power series in h (see (30)), i.e.

$$M_i[\phi \le H(h)\phi(0)](0, h) = A_i + \sqrt{h}vC_i + \sqrt{h}\Delta\gamma(h, 0)B_i + O\left(h^{3/2}\right), \quad (22)$$

where

$$A_i = \int_{\mathbb{R}^{n-1}} \int_{-\infty}^{0} \rho_i(|y|)\, dy_n d\acute{y} \quad (23)$$

$$B_i = \frac{1}{2}\int_{\mathbb{R}^{n-1}} y_k^2\rho_i(\acute{y}, 0)\, d\acute{y}, \quad (24)$$

$$C_i = \int_{\mathbb{R}^{n-1}} \rho_i(\acute{y}, 0)\, d\acute{y} \quad (25)$$

and $i = 1, 2$. This is a system of linear algebraic equations for $\Delta\gamma(h, 0)$ and v. We choose the kernels so, that the determinant of this system is positive

$$D = C_1 B_2 - C_2 B_1 > 0,$$

denote $N_i = M_i [\phi \leq H(h)\phi(0)](0, h) - A_i$ and write the solution

$$\begin{aligned} v = \frac{\gamma(h, 0)}{h} &= \frac{1}{\sqrt{h}} \frac{N_1 B_2 - N_2 B_1}{C_1 B_2 - C_2 B_1} + O(h), \\ \Delta\gamma(h, 0) &= \frac{1}{\sqrt{h}} \frac{N_2 C_1 - N_1 C_2}{C_1 B_2 - C_2 B_1} + O(h). \end{aligned}$$

Lemma 2 implies that the operator H is consistent with the PDE in (3) if we take

$$\begin{aligned} F(N_1, N_2) &= v - G(-\Delta\gamma(h, 0)) = \\ &= \frac{1}{\sqrt{h}} \frac{N_1 B_2 - N_2 B_1}{D} - G\left(\frac{1}{\sqrt{h}} \frac{N_1 C_2 - N_2 C_1}{D}\right). \end{aligned} \tag{26}$$

In the case of thresholding function of one variable, the inclusion principle (16) holds for $\mathcal{H}$ when F is nondecreasing. In the case of two variables we require

$$\frac{\partial F}{\partial N_1} = \frac{B_2}{D} - \frac{C_2}{D} G' \geq 0, \tag{27}$$

$$\frac{\partial F}{\partial N_2} = -\frac{B_1}{D} + \frac{C_1}{D} G' \geq 0. \tag{28}$$

This implies

$$\frac{B_1}{C_1} \leq G' \leq \frac{B_2}{C_2}. \tag{29}$$

Therefore, for a while, we restrict ourselves with G having bounded and positive derivative. Comparing (25) with (24) one sees that it is possible to make lower bound in (29) small by choosing ρ_1 with mass concentration close to the origin. The upper bound will be large if the mass of ρ_2 is concentrated relatively far from the origin.

Next, we state some auxiliary results.

Lemma 3. *Suppose (27) and (28) hold and $\mathcal{H}$ is defined by (4), then $\forall h \in \mathbb{R}_+$, then*

1. $\mathcal{H}(h)(\mathbb{R}^n) = \mathbb{R}^n$,
   $\mathcal{H}(h)(\emptyset) = \emptyset$,

2. $\forall a, b \in \mathbb{X} : a \subseteq b \Rightarrow \mathcal{H}(h) a \subseteq \mathcal{H}(h) b.$

Proof.

1. It is enough to show that $F(M_1(\mathbb{R}^n)(x,h), M_2(\mathbb{R}^n)(x,h)) \geq 0$ and $F(M_1(\emptyset)(x,h), M_2(\emptyset)(x,h)) < 0$. First we observe, that $F(A_1, A_2) = 0$, $M_i(\mathbb{R}^n)(x,h) \geq A_i$ and $M_i(\emptyset)(x,h) = 0 < A_i$. This, together with $\frac{\partial F}{\partial N_i} > 0$ gives the desired inequalities.
2. Since $M_i(b) \geq M_i(a)$, $F(M_1(b), M_2(b)) \geq F(M_1(a), M_2(a))$, therefore $[F(M_1(a), M_2(a)) \geq 0] \subseteq [F(M_1(b), M_2(b)) \geq 0]$, which is equivalent to $\mathcal{H}(h) a \subseteq \mathcal{H}(h) b$.

□

Proposition 1. *Define H by (5) and $\mathcal{H}$ by (4), then for each $h > 0$ and $u \in \mathbb{B}(\mathbb{R}^n)$ one has $H(h) u \in \mathbb{B}(\mathbb{R}^n)$.*

Proof. Without loss of generality we assume, that $S_1 \leq u(x) \leq S_2$ for some $S_1, S_2 \in \mathbb{R}$. From $\forall h \in \mathbb{R}_+ \quad \mathcal{H}(h)(\mathbb{R}^n) = \mathbb{R}^n$ and $\mathcal{H}(h)(\emptyset) = \emptyset$ follows $x \in \mathcal{H}(h)[u \leq S_2]$ and
$x \notin \mathcal{H}(h)[u \leq S_1]$. Therefore, we see that:

$$S_1 \leq H(h) u(x) = inf\{\lambda \in \mathbb{R} : x \in \mathcal{H}(h)[u \leq \lambda]\} \leq S_2.$$

□

With the results above, we are ready to state the convergence of the approximations $H(t/m)^m g$ to the unique viscosity solution of (3).

Theorem 4. *Let $H(h)$ be defined by*

$$\begin{aligned} [H(h) u](x) &= \sup\{\lambda \in \mathbb{R} : x \in \mathcal{H}_h[u \geq \lambda]\} \\ \textit{with} \quad \mathcal{H}_h C &= \{x \in \mathbb{R}^n : F(M_1(C)(x,h), M_2(C)(x,h)) \geq 0\}, \\ \textit{where} \quad F(N_1, N_2) &= \frac{1}{\sqrt{h}} \frac{N_1 B_2 - N_2 B_1}{D} - G\left(\frac{1}{\sqrt{h}} \frac{N_2 C_1 - N_1 C_2}{D}\right), \end{aligned}$$

and $\tilde{\rho}_1, \tilde{\rho}_2$ have compact support, G is continuous nondecreasing satisfying (29). Then

$$H_{\frac{t}{m}}^m g(x) \to u(x,t)$$

locally uniformly when $m \to \infty$. Here $u(x,t)$ is the unique viscosity solution of (3) with G satisfying (29).

Proof. Our aim is to show here that the operator $H(h)$ satisfies the conditions of the Theorem 3. The **monotonicity** of H_h is ensured by Lemma 1 and Lemma 3.

The **stability** of H is exactly the result of the Proposition 1: $H(h)u \in \mathbb{B}\left(\bar{\Omega}\right)$

Another requirement in Theorem 3 is that $H(h)$ must commute with addition of constants, i.e:

$$\forall a \in \mathbb{R} \quad H(h)(u(x)+a) = H(h)u(x) + a$$

This follows from the very definition of $H(h)$:

$$\begin{aligned} H(h)(u(x)+a) &= inf\{\lambda \in \mathbb{R} : x \in \mathcal{H}(h)[u(x)+a \leq \lambda]\} = \\ &= inf\{\beta + a \in \mathbb{R} : x \in \mathcal{H}(h)[u(x) \leq \beta]\} = H(h)u(x) + a \end{aligned}$$

The operator $H(h)$ has to fulfill 13 as well. The limit we are interested in is:

$$\lim_{h\to 0} \frac{H(h)u(x_0)}{h} = 0$$

for u of the form $u(x) = f(|x - x_0|)$, where $f \in C^2([0,\infty))$ with $f(0) = f'(0) = f''(0) = 0$ and $f''(r) > 0$ for $r > 0$.

It is enough to show, that this is true for $x_0 = 0$. First, we observe, that $\mathcal{H}_h^{-1}[\{0\}] = \{u \leq \lambda_1\}$, where $\lambda_1 = H(h)u(0)$. Since both ρ_1 and ρ_2 have compact support, we can be sure, that there exists R s. t. $\left\{|x| \leq R\sqrt{h}\right\} \supseteq \mathcal{H}_h^{-1}[\{0\}]$. Now we observe, that $\left\{|x| \leq R\sqrt{h}\right\} = \{u \leq \lambda_2\}$ for some $\lambda_2 > \lambda_1$. From the latter equality we deduce $\lambda_2 = O\left(h^{\frac{3}{2}}\right)$ and conclude by

$$\lim_{h\to 0} \frac{H(h)u(x_0)}{h} \leq \lim_{h\to 0} \frac{O\left(h^{\frac{3}{2}}\right)}{h} = 0.$$

To show that our approximation operator is *consistent* with the PDE, we use Lemma 2. It is enough to prove the following

$$\gamma(h,0) = hG(-\Delta\gamma(h,0)) + o(h),$$

where $x_n = \gamma(h,\acute{x})$ is a parameterization of the surface

$$\{x \in \mathbb{R}^n : u(x) = H(h)u(0)\}$$

near $\acute{x} = 0$. To show this, we use the fact that:

$$F\left(M_1\left[u \leq \mu\right], M_2\left[u \leq \mu\right]\right)|_{x=0} = 0$$

We begin by writing the expressions for M_i in detail:

$$M_i = \left(\chi_{[u\leq\mu]} \star \frac{1}{h^{\frac{n}{2}}}\rho_i\left(\frac{|\cdot|}{\sqrt{h}}\right)\right)(0) = \int_{\mathbb{R}^n} \chi_{[u\leq\mu]}(y)\,\frac{1}{h^{\frac{n}{2}}}\rho_i\left(\frac{|y|}{\sqrt{h}}\right)dy =$$

$$= \int_{\mathbb{R}^{n-1}}\int_{-\infty}^{\gamma(h,\acute{y})} \frac{1}{h^{\frac{n}{2}}}\rho_i\left(\frac{|y|}{\sqrt{h}}\right)dy_n d\acute{y} = A_i + \int_{\mathbb{R}^{n-1}}\int_0^{\frac{1}{\sqrt{h}}\gamma\left(h,\sqrt{h}\acute{y}\right)} \rho_i\left(|y|\right)dy_n d\acute{y}.$$

Here A_i is given by (23). Expanding $\gamma\left(h,\sqrt{h}\acute{y}\right)$ in Taylor series with respect to the spatial variables (keeping h as a parameter) we get:

$$\frac{1}{\sqrt{h}}\gamma\left(h,\sqrt{h}\acute{y}\right) = \sqrt{h}\frac{\gamma(h,0)}{h} + \frac{\sqrt{h}}{2}\sum_{i,j=1}^{n-1}\gamma_{y_iy_j}(h,0)\,y_iy_j +$$
$$+\frac{h}{6}\sum_{i,j,l=1}^{n-1}\gamma_{y_iy_jy_l}(h,0)\,y_iy_jy_l + O\left(h^{3/2}\acute{y}^4\right).$$

Observing that $\gamma(h,0) = O\left(\sqrt{h}\right)$, we denote $\frac{\gamma(h,0)}{h} = v$. The expression for M_i becomes:

$$\begin{aligned} M_i &= A_i + \\ &+ \int_{\mathbb{R}^{n-1}}\rho_i(\acute{y},0)\left[\sqrt{h}v + \frac{\sqrt{h}}{2}\sum_{i,j=1}^{n-1}\gamma_{y_iy_j}(h,0)\,y_iy_j + O\left(h^{3/2}\acute{y}^4\right)\right]dy_n d\acute{y} \\ &= A_i + \sqrt{h}vC_i + \sqrt{h}\Delta\gamma(h,0)\,B_i + O\left(h^{3/2}\right), \end{aligned} \tag{30}$$

where we have used the fact that $\rho_i(\acute{x}, x_n)$ is smooth and radially symmetric in particular

$$\frac{\partial\rho_i}{\partial x_n}(\acute{x},0) = 0.$$

The constants B_i, C_i depend only on ρ_i and are given by (24) and (25).

Remark 1. *At this point it is easy to see, that a scheme with a thresholding depending only on one variable can be consistent with the PDE (2) only in the case of linear G. The thresholding condition becomes*

$$F\left(A + \sqrt{h}vC + \sqrt{h}\Delta\gamma(h,0)\,B + O\left(h^{3/2}\right)\right) = 0.$$

As it was required by the inclusion principle, the function F is non decreasing. This implies

$$A + \sqrt{h}vC + \sqrt{h}\Delta\gamma\left(h,0\right)B + O\left(h^{3/2}\right) = a,$$

where a is the unique solution of $F\left(a\right) = 0$. Thus

$$v = \frac{\gamma\left(h,0\right)}{h} = -\frac{B}{C}\Delta\gamma\left(h,0\right) - \frac{a-A}{\sqrt{h}C} + o\left(\sqrt{h}\right).$$

Comparing this relationship with the one in Lemma 2, we see that the only G's we can resolve by thresholding depending on one variable are the linear ones: $G\left(k\right) = const \cdot k + const$.

Let us denote here $k = \Delta\gamma\left(h,0\right)$.

Now we can express v and k in terms of M_i and constants A_i, B_i and C_i :

$$\begin{aligned} v &= \frac{1}{\sqrt{h}}\frac{N_1B_2 - N_2B_1}{C_1B_2 - C_2B_1} + O\left(h\right), \\ k &= \frac{1}{\sqrt{h}}\frac{N_2C_1 - N_1C_2}{C_1B_2 - C_2B_1} + O\left(h\right). \end{aligned}$$

Since $F\left(M_1, M_2\right) = v - G\left(-k\right) = 0$, we have:

$$\gamma\left(h,0\right) = hG\left(-\Delta\gamma\left(h,0\right)\right) + o\left(h\right).$$

□

Remark 2. *As it was already mentioned above, convolution kernels $\tilde{\rho}_i$ can also be taken with unbounded support. For example, the exponential decay for large arguments is sufficient in order for Theorem 4 to hold.*

The requirement (29) is quite restrictive. Our next result shows, that it is enough to take G_ϵ satisfying (29) and uniformly close to G in order to approximate the solutions of (3).

Proposition 2. *Suppose G_ϵ, G are continuous and $G_\epsilon \to G$ uniformly on $\mathbb{R}$ as $\epsilon \to 0$. Then $\mathcal{F}\left(G\right) = \mathcal{F}\left(G_\epsilon\right)$.*

Proof. Suppose $f \in \mathcal{F}\left(G\right)$. It means, that $f\left(0\right) = f'\left(0\right) = f''\left(0\right)$, $f\left(r\right) > 0$ for $r > 0$ and

$$\lim_{p\to 0} f'\left(p\right) G\left(\frac{1}{p}\right) = \lim_{p\to 0} f'\left(p\right) G\left(\frac{-1}{p}\right) = 0$$

Since $G_\epsilon \to G$ uniformly, $G(k) = G_\epsilon(k) + o_\epsilon(1)\,\alpha(k)$, where $\alpha \in \mathbb{B}(\mathbb{R})$. We write

$$\begin{aligned} 0 &= \lim_{p \mapsto 0} f'(p)\, G\left(\frac{1}{p}\right) = \\ &= \lim_{p \to 0} f'(p) \left(G_\epsilon\left(\frac{1}{p}\right) + o_\epsilon(1)\,\alpha\left(\frac{1}{p}\right)\right) = \lim_{p \to 0} f'(p)\, G_\epsilon\left(\frac{1}{p}\right) \end{aligned}$$

to see, that $f \in \mathcal{F}(G_\epsilon)$.

The proof of the reverse inclusion is analogous. □

Lemma 4. *Suppose G_ϵ, G are nondecreasing continuous and $G_\epsilon \to G$ uniformly on $\mathbb{R}$ as $\epsilon \to 0$. Suppose also, that for each $\epsilon > 0$ the operator H_ϵ is monotone, stable, commuting with additions of constants and consistent with*

$$\frac{\partial u_\epsilon}{\partial t} = |Du_\epsilon|\, G_\epsilon\left(div \frac{Du_\epsilon}{|Du_\epsilon|}\right). \tag{31}$$

Additionally, let the following limit hold

$$\lim_{h \to} \frac{H_h(h)\,(f(|x - x_0|))(x_0)}{h} = 0 \tag{32}$$

for each $f \in \mathcal{F}(G)$. Then

$$H^m_{\frac{t}{m}}\left(\frac{t}{m}\right) u_0(x) \to u(x,t)$$

locally uniformly as $m \to \infty$, where $u(x,t)$ is the unique viscosity solution of (3)

Proof. We show here, that the operator $H_h(h)$ satisfies the conditions of the Theorem 3. This operator commutes with additions of constants and satisfies limit (32) by the assumption. Since the operator H_ϵ is stable for all $\epsilon > 0$, it is in particular stable for $\epsilon = h$ for each $h > 0$.
Since the operator H_ϵ is monotonic for all $\epsilon > 0$, it is in particular monotonic for $\epsilon = h$ for each $h > 0$.
We have to show consistency, i.e. for each $\phi \in C^\infty(\mathbb{R}^n)$ at each point where $|D\phi| \neq 0$

$$H_h(h)\,\phi(x) - \phi(x) = h\,|D\phi(x)|\, G\left(\mathrm{div} \frac{D\phi(x)}{|D\phi(x)|}\right) + o(h). \tag{33}$$

has to hold. Since the operator H_ϵ is consistent with the equation (31) and $G_h(k) = G(k) + o_h(1)\,\alpha(k)$ for some $\alpha \in \mathbb{B}(\mathbb{R})$, we write

$$\begin{aligned} H_h(h)\,\phi(x) - \phi(x) &= h\,|D\phi(x)|\,G_h\left(\operatorname{div}\frac{D\phi(x)}{|D\phi(x)|}\right) + o(h) = \\ = h\,|D\phi(x)|\left(G\left(\operatorname{div}\frac{D\phi(x)}{|D\phi(x)|}\right)\right. &+ \left. o_h(1)\,\alpha\left(\operatorname{div}\frac{D\phi(x)}{|D\phi(x)|}\right)\right) + o(h) = \\ &= h\,|D\phi(x)|\,G\left(\operatorname{div}\frac{D\phi(x)}{|D\phi(x)|}\right) + o(h), \end{aligned}$$

here $o_h(1) \to 0$ as $h \to 0$. □

Theorem 5. *Consider a convolution-thresholding scheme*

$$\begin{aligned} H_\epsilon(h)\,u(x) &= \inf\{\lambda \in \mathbb{R} : x \in \mathcal{H}_\epsilon(h)\,[u \le \lambda]\} \\ \mathcal{H}_\epsilon(h)\,C &= \{x \in \mathbb{R}^n : F_\epsilon(M_1(C)(x,h), M_2(C)(x,h)) \ge 0\}, \end{aligned}$$

where the thresholding function $F_\epsilon(M_1, M_2)$ is chosen so, that the scheme is monotone and consistent with the equation (31) and the convolution kernels have compact support. If $G_\epsilon \to G$ uniformly then

$$H^m_{\frac{t}{m}}\left(\frac{t}{m}\right)u_0(x) \to u(x,t)$$

locally uniformly as $m \to \infty$, where $u(x,t)$ is the unique viscosity solution of (3).

Proof. The convergence follows form Lemma 4 if we show that the limit (32) holds. Let us set $x_0 = 0$, then the set $[f(|x|) \le \lambda]$ is a ball centered at the origin with radius $O\left(\lambda^{1/3}\right)$. We denote $H_h(h)\,f(0) = \lambda_1$. Observe, that λ_1 can be characterized as a number for which $\mathcal{H}_h(h)\,[f \le \lambda_1] = \{0\}$. Since we know, that $F_h(A_1, A_2) > 0$, the radius of $[f \le \lambda_1]$ must be less or equal to the radius of the greatest support of the kernel: $O\left(\lambda_1^{1/3}\right) \le R\sqrt{h}$. From this inequality we deduce $H_h(h)\,f(0) = \lambda_1 \le O\left(h^{3/2}\right)$. This establishes the desired limit (32). □

Let us now consider the particular interesting case with $G(k) = k\,|k|^{\alpha-1}$ with $\alpha > 1$. We set

$$G_m(k) = \begin{cases} (1-\alpha)\,m^\alpha + \alpha m^{\alpha-1}k & \text{for } k < -n \\ m^{1-\alpha}k & \text{for } |k| < 1/n \\ -(1-\alpha)\,m^\alpha + \alpha m^{\alpha-1}k & \text{for } k > n \\ k\,|k|^{\alpha-1} & \text{elsewhere.} \end{cases}$$

G_m is continuous, increasing and its derivative is bounded from below and above: $m^{1-\alpha} \leq G_m' \leq \alpha m^{\alpha-1}$. Moreover, $G_m \to k\,|k|^{\alpha-1}$ locally uniformly as $m \to \infty$. Using Theorem 2 it is easy to show the following

Theorem 6. *Let u_m be the viscosity solution of*

$$\frac{\partial u_m}{\partial t} = |Du_m|\, G_m\left(div\frac{Du_m}{|Du_m|}\right) \text{ in } \mathcal{O},$$

where G_m is defined above. Then $u_m \to u$ locally uniformly as $m \to \infty$, where u is the viscosity solution of (2) in $\mathcal{O}$, with $G(k) = k\,|k|^{\alpha-1}$, $\alpha > 1$.

Proof. First we establish the inclusion $\mathcal{F}(G) \subset \mathcal{F}(G_m)$. Take $f \in \mathcal{F}(G)$. By the definition of $\mathcal{F}(G)$, $f'(x) = o(x^\alpha)$. This immediately gives

$$\lim_{p\to 0} f'(p)\, G_m(1/p) = \lim_{p\to 0} f'(p)/p = 0,$$

since $\alpha > 1$. We observe also, that the remaining conditions of Theorem 2 are satisfied. Hence a subsolution and a supersolution u^+ and u_+ can be constructed by means of (10) and (11). Since the equation has the strong comparison property (see [12]), $u^+ = u_+$ and the result follows. □

Remark 3. *In a more general case when $G(k) = O(k^\alpha)$, $\alpha > 1$, one can pick a sequence of increasing functions with derivative bounded below and above and apply the Theorem 2 to get a result similar to Theorem 6.*

4 Numerical implementation

This section is devoted to a description of our numerical implementations of the convolution-thresholding scheme developed in Section 3.

Given a compact set $C \subset \mathbb{R}^n$, we fix convolution kernels ρ_1, ρ_2 and the time step h and approximate C_t at a time moment $t = mh$ by $(\mathcal{H}(h))^m C$. The algorithm of computations consists of the following steps:

1. Compute convolutions and the thresholding function

$$M_i C(x,h) = \int_{\mathbb{R}^n} \chi_C(y)\,\rho_i(x-y)\,dy \;\; i = 1,2 \tag{34}$$

$$F(x,h) = F(M_1 C(x,h), M_2 C(x,h)). \tag{35}$$

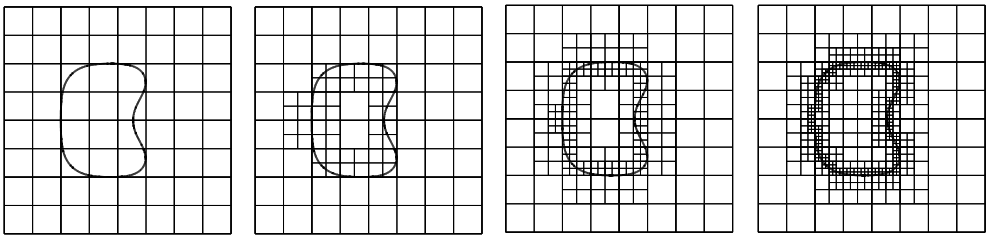

Figure 1: On the spatial discretization.

2. Find the evolved set $\mathcal{H}(h)C = \{x \in \mathbb{R}^n : F(x,h) \geq 0\}$.

3. Repeat the procedure with the evolved set to get $\mathcal{H}^2(h)C$ and so on.

We used two different algorithms for the calculation of the convolution step, which constitutes the main computational part of the algorithm.

4.1 Spatial discretization

We assume that initially the surface is closed and is contained in a unit cube. The surface under consideration is always an isosurface of some function. In our implementation we use a modification of so called Marching Cubes algorithm for extracting an isosurface. The algorithm was originally proposed in [24] and was first applied for the mean curvature flow calculations in [30]. The algorithm creates an adaptive spatial discretization of C (see Fig. 4.1). In doing so, we significantly reduce the number of grid points. Besides that, the accurate piecewise polynomial approximation of the ∂C can be arranged.

4.2 Spectral method

One can use Fourier series to calculate the convolutions (34). Numerical aspects of this approach have been presented by Ruuth in [30].

In order to compute Fourier coefficients of χ_C given on a non uniform grid the unequally spaced approximate fast Fourier transform algorithm [6] is used. The numerical cost of this transform algorithm combined with the Marching Cubes procedure is [30] $O\left(m^n N_p + N_f^n \log(N_f)\right)$, where m is a constant depending on a desired accuracy in the calculation of the Fourier

coefficients (in case $m = 23$ the accuracy is comparable with the machine truncation error), N_f is a number of the Fourier modes along each axis and N_p is the number of nodes in the grid.

4.3 Direct method

If ρ_1 and ρ_2 are simple enough and have compact support, their convolutions with χ_C can be calculated explicitly. Let us choose

$$\begin{aligned} \tilde{\rho}_1(x) &= \begin{cases} \frac{1}{|\mathcal{B}_1|} & \text{if } x < 1 \\ 0 & \text{otherwise} \end{cases} \\ \tilde{\rho}_2(x) &= \frac{1}{\alpha^n}\tilde{\rho}_1\left(\frac{x}{\alpha}\right) \end{aligned}$$

where $|\mathcal{B}_1|$ is the Lebesgue measure of an unit ball in $\mathbb{R}^n$ and $\alpha \in \mathbb{R}_+,\ \alpha < 1$. In this case, the convolutions in (34) are proportional the measure of the intersection of C with a ball of radius proportional to $\sqrt{h}$ placed in the point x.

We present expressions for the thresholding function $F(M_1, M_2))$ in the case $n = 2$:

$$\begin{aligned} F(M_1, M_2) &= v - G(k), \text{ where} \\ v &= \frac{\pi\alpha(2\alpha M_1 - 2M_2 - \alpha + 1)}{4\sqrt{h}(\alpha^2 - 1)} \\ k &= \frac{-3\pi(2M_1 - 2\alpha M_2 + \alpha - 1)}{2\sqrt{h}(\alpha^2 - 1)}. \end{aligned}$$

In this case convolutions M_1 and M_2 can be calculated as follows. We represent C as a disjoint union of squares and triangles (or cubes in tetrahedron in case $n = 3$) using the Marching Cubes method and calculate the area (volume) of intersection of the ball (suppρ) with each square and triangle. The numerical cost of each step of the evolution can be estimated by $O(N_p * N_i + N_p)$, where N_i is the number of points inside the ball of radius $\sqrt{h}$ with the center at some grid point. When h is large, the accuracy of the method is low, therefore one can take less grid points. Thus, N_i is entirely determined by the desired accuracy.

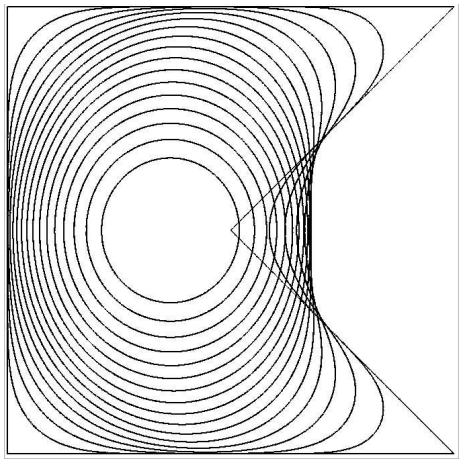

Figure 2: The mean curvature evolution of a non-smooth, non-convex curve

4.4 Computed examples

In the case of the mean curvature curve evolution in $\mathbb{R}^2$ the accuracy of calculations can be monitored with help of the Von Neumann-Mullins parabolic law. It asserts $dS/dt = -2\pi$, where S is the area enclosed by the curve.

Consider a non-convex, non-smooth initial curve depicted on Fig 2. The mean curvature evolution of this curve was calculated using the direct method with timestep values $dt = 1/600$ and $1/6000$. The shape of the curve is plotted on the Fig. 2 for times $t = 1/600, 2/600, \cdots$, when calculated with the fine timestep. The comparison between local relative errors

$$e_i = \frac{|S_i - S_{i+1} - 2\pi dt|}{2\pi dt} \tag{36}$$

for calculations with different timesteps is seen on the Fig. 3. One can observe, that the error indeed depends linearly on the timestep.

The evolution with the velocity $v = k^{1/3}$ is depicted on Figure 4. In this case the flow is affine invariant [1], hence the eccentricity e of the evolving ellipse remains constant. In this particular example, the curvature is bounded from above and below by some positive constants for some evolution time. This means that we never use the parts of $G(k) = k^{1/3}$, where its derivative is too large or too small. This allows to apply the thresholding procedure without any approximation of G.

In figures 5 and 6 computed 3D evolution of a non-convex surface is repre-

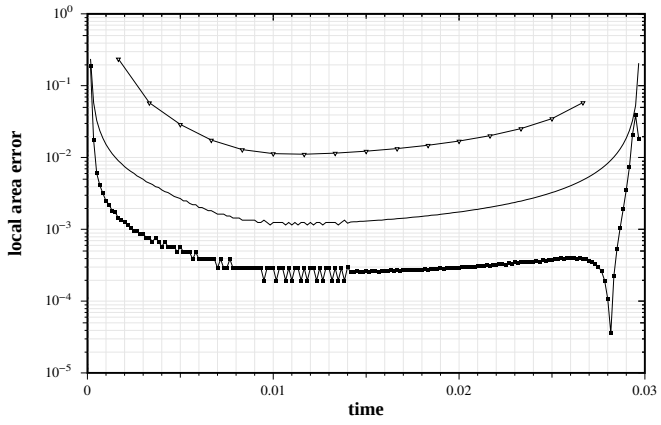

Figure 3: Local area error dependence on time. The first order method with timestep 1/600 – the line with triangle markers; the first order method with timestep 1/6000 – the thin line; the second order method with timestep 1/6000 – the line with square markers.

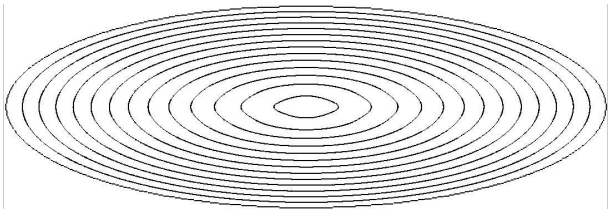

Figure 4: The evolution $v = k^{1/3}$ of an ellipse.

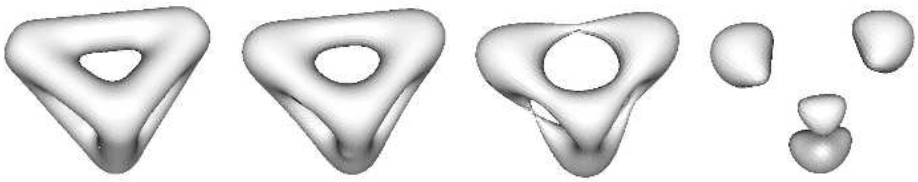

Figure 5: Computed mean curvature evolution

sented for curvature flow and for a flow with velocity $v = G(k)$ as on fig. 7 with ~ 200000 triangles approximating the surface.

4.5 On the higher order schemes for the mean curvature motion

Let us now look at approximations to the mean curvature evolution. It is easy to see, that if the surface is smooth, the Bence-Merriman-Osher method gives the first order approximation in time for a curvature flow. A higher order scheme by an extrapolation argument in time was proposed by Ruuth in [30]. We propose here higher order approximations to the mean curvature evolution using some properties of functions M_i.

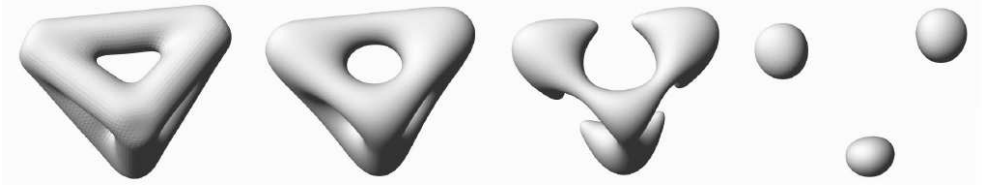

Figure 6: Computed generalized mean curvature evolution

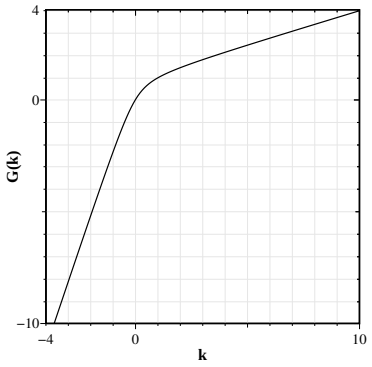

Figure 7: Function $G(k)$ used in the computation

We rewrite the equations (22) and keep an additional term of order $h^{3/2}$ in each equation with a kernel dependent multiplier E_i to get the error term of order $h^{5/2}$. Considering two equations we get the relation

$$\begin{aligned} E_2N_1 - E_1N_2 &= \qquad (37) \\ &= \sqrt{h}[(E_2C_1 - E_1C_2)v + (E_2B_1 - E_1B_2)\gamma''(h,0)] + O\left(h^{5/2}\right). \end{aligned}$$

This relationship motivates to take the thresholding function $F(N_1, N_2) = E_2N_1 - E_1N_2$ to approximate the mean curvature evolution with the second order accuracy for smooth curves. However this thresholding function does not simultaneously satisfy (27) and (28) and, therefore, the stability of the numerical scheme is not guaranteed by the previous argumentation.

The calculations with the above thresholding function were performed. No sign of instability was observed in the numerical experiments and, as one can see on the Fig. 3, the accuracy was increased by approximately one order. This increase agrees with the construction (37).

Acknowledgment

A part of the work was completed during our visit to the University of South Carolina. We are grateful to Prof. Björn Jawerth for the opportunity to work there and for fruitful discussions. We would also like to thank referees for pointing out necessary corrections in the formulation in the Theorem 3.2, for making some key points in the text more clear and for additional references. This research was partially supported by the TFR grant "Kinetic modelling of geometric flows of surfaces" and the TMR contract "Asymptotic methods in kinetic theory" (ERB FMRX CT97 0157).

References

[1] L. Alvarez, F. Guichard, P.-L. Lions, and J.-M. Morel, *Axioms and fundamental equations of image processing*, Arch. Rational Mech. Anal., 123 (1993), pp. 199–257.

[2] S. Angenent, T. Ilmanen, and D. L. Chopp, *A computed example of nonuniqueness of mean curvature flow in* $\mathbf{R}^3$, Comm. Partial Differential Equations, 20 (1995), pp. 1937–1958.

[3] G. Barles and C. Georgelin, *A simple proof of convergence for an approximation scheme for computing motions by mean curvature*, SIAM J. Numer. Anal., 32 (1995), pp. 484–500.

[4] G. Barles, H. M. Soner, and P. E. Souganidis, *Front propagation and phase field theory*, SIAM J. Control Optim., 31 (1993), pp. 439–469.

[5] G. Barles and P. E. Souganidis, *Convergence of approximation schemes for fully nonlinear second order equations*, Asymptotic Anal., 4 (1991), pp. 271–283.

[6] G. Beylkin, *On the fast Fourier transform of functions with singularities*, Appl. Comput. Harmon. Anal., 2 (1995), pp. 363–381.

[7] K. A. Brakke, *The motion of a surface by its mean curvature*, Princeton University Press, Princeton, N.J., 1978.

[8] L. Bronsard and R. V. Kohn, *Motion by mean curvature as the singular limit of Ginzburg-Landau dynamics*, J. Differential Equations, 90 (1991), pp. 211–237.

[9] F. Cao, *Partial differential equations and mathematical morphology*, J. Math. Pures Appl. (9), 77 (1998), pp. 909–941.

[10] F. Catté, F. Dibos, and G. Koepfler, *A morphological scheme for mean curvature motion and applications to anisotropic diffusion and motion of level sets*, SIAM J. Numer. Anal., 32 (1995), pp. 1895–1909.

[11] Y. G. Chen, Y. Giga, and S. Goto, *Uniqueness and existence of viscosity solutions of generalized mean curvature flow equations*, J. Differential Geom., 33 (1991), pp. 749–786.

[12] M. G. Crandall, H. Ishii, and P.-L. Lions, *User's guide to viscosity solutions of second order partial differential equations*, Bull. Amer. Math. Soc. (N.S.), 27 (1992), pp. 1–67.

[13] M. G. Crandall and P.-L. Lions, *Convergent difference schemes for nonlinear parabolic equations and mean curvature motion*, Numer. Math., 75 (1996), pp. 17–41.

[14] E. De Giorgi, *Conjectures on limits of some quasilinear parabolic equations and flow by mean curvature*, in Partial differential equations and related subjects (Trento, 1990), Longman Sci. Tech., Harlow, 1992, pp. 85–95.

[15] L. C. Evans, *Convergence of an algorithm for mean curvature motion*, Indiana Univ. Math. J., 42 (1993), pp. 533–557.

[16] L. C. Evans, H. M. Soner, and P. E. Souganidis, *Phase transitions and generalized motion by mean curvature*, Comm. Pure Appl. Math., 45 (1992), pp. 1097–1123.

[17] L. C. Evans and J. Spruck, *Motion of level sets by mean curvature. I*, J. Differential Geom., 33 (1991), pp. 635–681.

[18] F. Guichard and J.-M. Morel, *Partial differential equations and image iterative filtering*, in The state of the art in numerical analysis (York, 1996), Oxford Univ. Press, New York, 1997, pp. 525–562.

[19] T. Ilmanen, *Convergence of the Allen-Cahn equation to Brakke's motion by mean curvature*, J. Differential Geom., 38 (1993), pp. 417–461.

[20] H. Ishii, *A generalization of the Bence, Merriman and Osher algorithm for motion by mean curvature*, in Curvature flows and related topics (Levico, 1994), Gakkōtosho, Tokyo, 1995, pp. 111–127.

[21] H. Ishii, G. E. Pires, and P. E. Souganidis, *Threshold dynamics type approximation schemes for propagating fronts*, J. Math. Soc. Japan, 51 (1999), pp. 267–308.

[22] H. Ishii and P. Souganidis, *Generalized motion of noncompact hypersurfaces with velocity having arbitrary growth on the curvature tensor*, Tohoku Math. J. (2), 47 (1995), pp. 227–250.

[23] F. Leoni, *Convergence of an approximation scheme for curvature-dependent motions of sets*, SIAM J. Numer. Anal., 39 (2001), pp. 1115–1131 (electronic).

[24] W. Lorensen and H. Cline, *Marching cubes: A high resolution 3d surface construction algorithm*, ACM Computer Graphics (Proceedings of SIGGRAPH' 87), 21 (1987), pp. 163–170.

[25] B. Merriman, J. K. Bence, and S. J. Osher, *Motion of multiple junctions: a level set approach*, J. Comput. Phys., 112 (1994), pp. 334–363.

[26] T. Ohta, D. Jasnow, and K. Kawasaki, *Unioversal scaling in the motion of random interfaces*, Phys. Rev. Lett., 47 (1982), pp. 1223–1226.

[27] S. Osher and J. A. Sethian, *Fronts propagating with curvature-dependent speed: algorithms based on Hamilton-Jacobi formulations*, J. Comput. Phys., 79 (1988), pp. 12–49.

[28] D. Pasquignon, *Approximation of viscosity solution by morphological filters*, ESAIM Control Optim. Calc. Var., 4 (1999), pp. 335–359 (electronic).

[29] J. Rubinstein, P. Sternberg, and J. B. Keller, *Fast reaction, slow diffusion, and curve shortening*, SIAM J. Appl. Math., 49 (1989), pp. 116–133.

[30] S. J. Ruuth, *Efficient algorithms for diffusion-generated motion by mean curvature*, J. Comput. Phys., 144 (1998), pp. 603–625.

[31] J. A. Sethian, *Level set methods and fast marching methods*, Cambridge University Press, Cambridge, second ed., 1999. Evolving interfaces in computational geometry, fluid mechanics, computer vision, and materials science.

Paper [GH2]

A convolution-thresholding scheme for the Willmore flow

Ricards Grzibovskis,
Alexei Heintz
Department of Mathematics,
Chalmers University of Technology,
41296 Göteborg, Sweden

1 Introduction

Let Σ be a smooth compact and orientable surface. The Willmore functional is defined as

$$W(\mathbf{f}) = \int_{\Sigma} H^2 dS \tag{1}$$

for any isometric immersion $\mathbf{f} : \Sigma \mapsto \mathbb{R}^3$. Here H denotes the mean curvature of Σ and dS is the area measure. We refer to [22] for the general discussion of this functional as well as description of some stationary points. The variation of this integral for a perturbation ϕ of the surface along the normal is (see [22])

$$\delta\mathcal{W} = \int_{\Sigma} \phi \left(\Delta H + 2H\left(H^2 - K\right)\right) dA,$$

where K is the Gaussian curvature of Σ. The Willmore flow for Σ is defined as an evolution of the surface when each point of it moves with the normal velocity

$$v = -\Delta H - 2H\left(H^2 - K\right).$$

As an evolution that minimizes the curvature this flow can be used in surface smoothing. We refer to [3] where authors propose numerical scheme to track

the so called surface diffusion flow i.e. the evolution of the surface with the normal velocity $v = -\Delta H$. An extension of this results and an applications to the surface smoothing can be found in [21]. A numerical algorithm based on the finite elements for the Willmore flow in connection with the surface restoration was proposed in [4]. Another recent result about the level-set formulation of the Willmore flow and the finite element approach to the evolution can be found in [6].

Another application of the Willmore flow comes from the biophysics. The functional (1) is a special case of the Helfrich functional that describes the free energy of a bilayer membrane [2], [5]. We comment on this topic in Section 4.

The mathematical properties of this type of surface evolution attracted much attention during the last years. Simonett have studied the Willmore flow near spheres in [20]. An example of occurrence of a self-intersection during the evolution is constructed in [15]. Small initial energy was considered by Kuwert and Schatzle in [11]. In [12] they have obtained a lower bound on the existence time of the flow. This bound is expressed in terms of the initial concentration of the mean curvature. In [13] the existence result was developed further by the same authors. They have proved that the Willmore flow of a smooth embedding of a sphere into $\mathbb{R}^3$ exists, is smooth and converges to a round sphere provided that the initial energy is bounded by 8π. A definition of the weak solutions can be found in [17]. The author defines a continuation of the flow after eventual singularities occur and establishes the existence of the weak solution.

A numerical scheme to track the evolution in $\mathbb{R}^3$ for axisymmetric surfaces was proposed in [16].

The purpose of this study is to develop a simple convolution-thresholding scheme for tracking such evolutions of a two dimensional surfaces in $\mathbb{R}^3$. Convolution-thresholding schemes have proved to be a useful tool for the numerics of the surface evolution [9], [10], [18], [19], [8]. Furthermore, the convolution structure of the method allows a numerically efficient implementation of the method.

This paper is organized as follows. In section 2 we consider the graph of a smooth function and explicitly expressing its geometrical properties (i.e. H, K and ΔH) by the derivatives of the function. We use these elementary relations in the section 3, where the asymptotics for the convolution of an indicator function of a subset of $\mathbb{R}^3$ with a smooth, compactly supported

kernel. We show that the third term of this asymptotics is proportional to $\Delta H + 2H\left(H^2 - K\right)$ and therefore can be efficiently used to construct a convolution-thresholding schemes for the Willmore flow. The convergence of the scheme is established for smooth initial data. Several numerical examples of the flow are presented in the section 4.

2 Geometric properties of a smooth graph

Let us consider the graph Σ of a smooth function $f : \mathbb{R}^2 \mapsto \mathbb{R}$ such that $\partial f/\partial u_i\,(0,0) = f_i = 0$ for $i = 1, 2$. We express the mean curvature H, the Gaussian curvature K, the Laplace-Beltrami operator of the mean curvature ΔH of Σ at the origin in terms of f and its derivatives.

Consider a mapping $\mathbf{x} : \mathbb{R}^2 \mapsto \mathbb{R}^3$ by $\mathbf{x}\,(u_1, u_2) = (u_1, u_2, f\,(u_1, u_2))$. Denote $\mathbf{x}_i = \partial\mathbf{x}/\partial u_i$ for $i = 1..2$. The outer unit normal $\mathbf{N}$ of Σ is given by

$$\mathbf{N} = \frac{\mathbf{x}_1 \times \mathbf{x}_2}{|\mathbf{x}_1 \times \mathbf{x}_2|}. \tag{2}$$

The coefficients of the first fundamental form are $g_{ij} = \langle \mathbf{x}_i, \mathbf{x}_j \rangle$ and the second fundamental form have coefficients $h_{ij} = -\langle \mathbf{N}_i, \mathbf{x}_j \rangle$, where $\mathbf{N}_i = \partial\mathbf{N}/\partial u_i$. The mean curvature is

$$H = \frac{1}{2}\sum_{i,j} g^{ij} h_{ij},$$

where g^{ij} denotes the elements of the matrix inverse to g. Setting $u_1 = u_2 = 0$ we get

$$H = \frac{1}{2}\left(f_{11}\,(0,0) + f_{22}\,(0,0)\right). \tag{3}$$

In order to calculate ΔH we use the Christoffel symbols

$$\Gamma_{ij}^k = \frac{1}{2}\sum_h g^{hk}\left(\partial g_{ih}/\partial u_j + \partial g_{jh}/\partial u_i - \partial g_{ij}/\partial u_h\right).$$

The covariant derivatives of H are

$$\nabla_i H = H_i = \frac{\partial H}{\partial u_i} \tag{4}$$

$$\nabla_i \nabla_j H = H_{ij} - \sum_k \Gamma_{ji}^k H_k \tag{5}$$

The Laplacian of H can be written as

$$\Delta H = \sum_{i,j} g^{ij} \nabla_i \nabla_j H. \tag{6}$$

After substituting (2) - (5) into (6) we get the following equality at the origin

$$\Delta H = \frac{1}{2} \left(\Delta \left(\Delta f \right) - 2H \left(12H^2 - 8K \right) \right), \tag{7}$$

where K is the Gaussian curvature, namely

$$K = \det \left(g^{ij} h_{ij} \right) = f_{11}(0,0) f_{22}(0,0) - f_{12}^2(0,0). \tag{8}$$

3 Asymptotics of the convolution

In this section we consider a compact subset C of $\mathbb{R}^3$ with a smooth boundary ∂C. We study the geometric properties of ∂C by considering the following convolution

$$M(t,x) = \left(\chi_C \star \rho_{t^{1/4}} \right)(x), x \in \mathbb{R}^3, \tag{9}$$

where χ_C is the characteristic function of C , $\rho_{t^\alpha}(x) = \rho\left(|x|^2 / t^{2\alpha} \right) / \left(t^\alpha \right)^3$ and $\rho : (0,\infty) \mapsto [0,\infty)$ is smooth with a compact support (or exponentially decreasing) normalized by $\int_{R^3} \rho dx = 1$.

We pick a point $\mathbf{p} \in \partial C$ associate a unit normal $\mathbf{N}$ to it, and calculate M in the point $\mathbf{p} + \mathbf{N} v t$. Here $v \in \mathbb{R}$. Taking $t \mapsto 0$ we expand M into a power series in t.

Theorem 1. *Suppose ∂C is smooth, $\mathbf{p} \in \partial C$ and $v \in \mathbb{R}$, then the convolution (9) has the following asymptotic expansion with respect to t at the point $O = \mathbf{p} + \mathbf{N} v t$*

$$\begin{aligned} M(O) &= \frac{1}{2} + t^{1/4} \frac{\pi N_3}{2} H + \\ &+ t^{3/4} \frac{\pi}{16} \left[-32 N_1 v + N_5 \left(\Delta H + 2H \left(H^2 - K \right) \right) \right] + O\left(t^{5/4} \right) \end{aligned} \tag{10}$$

where H, K and ΔH are values of the mean curvature, the Gauss curvature and the Laplace-Beltrami of the mean curvature of ∂C at $\mathbf{p}$ and $N_i = \int_0^\infty r^i \rho\left(r^2 \right) dr$.

Proof. In order to get the power series for (9) at $O = \mathbf{p}+\mathbf{N}vt$ it is convenient to choose O as the origin and Oz-axis parallel to $\mathbf{N}$. Then $\mathbf{p} = (0, 0, vt)$ and the boundary ∂C can be represented as a graph of a smooth function $\gamma : \mathbb{R}^{n-1} \mapsto \mathbb{R}$ in some neighborhood $\mathcal{S}$ of O.

$$\partial C = \left\{(x, y, \gamma(x, y)) : (x, y) \in \mathcal{S} \subset \mathbb{R}^2\right\}$$

Furthermore,

$$\begin{aligned} \gamma(x, y) &= -vt + f(x, y) \\ \gamma(0, 0) &= -vt, \text{ hence } f(0, 0) = 0 \\ \nabla\gamma(0, 0) &= \nabla f(0, 0) = 0. \end{aligned}$$

The expression for M at O now can be written as follows

$$\begin{aligned} M(O) &= \int_{\mathbb{R}^3} \chi_C(x)\, \rho_{t^{1/4}}(x)\, dx = \\ &= \int_C \frac{\rho\left(\left(x^2+y^2+z^2\right)/t^{1/2}\right)}{t^{3/4}} dxdydz = \\ &= \frac{1}{2} + \int_{\mathbb{R}^2} \mathcal{I}(t, x, y)\, dxdy + O\left(e^{-t^{-1/2}}\right) \end{aligned}$$

where

$$\mathcal{I}(t, x, y) = \int_0^{g(t,x,y)} \rho\left(\left(x^2+y^2+z^2\right)\right) dz$$

with

$$g(t, x, y) = \frac{\gamma\left(t^{1/4}x, t^{1/4}y\right)}{t^{1/4}}.$$

We expand this integral into a power series in t at the point $t_0 = 0$. First we observe that $g(0, x, y) = 0$ and calculate some derivatives of $g(t, x, y)$ with respect to t at $t = 0$:

$$\begin{aligned} \frac{\partial g}{\partial t}(0, x, y) &= \frac{1}{2}y^2 f_{22}(0, 0) + x\, y\, f_{12}(0, 0) + \frac{1}{2}x^2 f_{11}(0, 0) \\ \frac{\partial^2 g}{\partial t^2}(0, x, y) &= \frac{1}{3}y^3 f_{222}(0, 0) + x\, y^2 f_{122}(0, 0) \\ &+ x^2\, y\, f_{112}(0, 0) + \frac{1}{3}x^3 f_{111}(0, 0) \\ \frac{\partial^3 g}{\partial t^3}(0, x, y) &= -6\, v + \frac{1}{4}y^4 f_{2222}(0, 0) + x\, y^3 f_{1222}(0, 0) + \frac{3}{2}\, x^2\, y^2 f_{1122}(0, 0) \\ &+ x^3\, y\, f_{1112}(0, 0) + \frac{1}{4}x^4 f_{1111}(0, 0). \end{aligned}$$

Then we substitute these expressions into the expansion

$$\mathcal{I}(t,x,y) =$$
$$\rho(x^2+y^2)\frac{\partial g}{\partial t}(0,x,y)\,t^{1/4} + \frac{1}{2}\rho(x^2+y^2)\frac{\partial^2 g}{\partial t^2}(0,x,y)\,(0,x,y)\,t^{1/2} +$$
$$+\frac{1}{6}\left(2\,\rho'(x^2+y^2)\frac{\partial g}{\partial t}(0,x,y)^3 + \rho(x^2+y^2)\frac{\partial^3 g}{\partial t^3}(0,x,y)\right)t^{3/4} + O(t)$$

integrate over x and y and get

$$\begin{aligned} M(O) &= \frac{1}{2} + \frac{t^{1/4}\pi N_3}{2}(f_{11}+f_{22}) + \frac{t^{3/4}\pi}{64}[-128N_1 v + \\ &- N_5\left[(f_{22}+f_{11})\left(5\,{f_{22}}^2 + 12\,{f_{12}}^2 - 2\,f_{22}\,f_{11} + 5\,{f_{11}}^2\right) - \right. \\ &- \left. 2\ (f_{2222} + 2\,f_{1122} + f_{1111})\right]] + O\left(t^{5/4}\right), \end{aligned}$$

where all derivatives of f are calculated at the origin. Recalling (3),(8) and (7) we arrive at

$$\begin{aligned} M(O) &= \frac{1}{2} + t^{1/4}\pi N_3 H + \\ &+ \frac{t^{3/4}\pi}{16}\left[-32N_1 v + N_5\left(\Delta H + 2H\left(H^2 - K\right)\right)\right] + O\left(t^{5/4}\right). \end{aligned}$$

□

Corollary 1. *Consider $\rho_{at^{1/4}}$ with $a>0$ and denote $M_a = \chi_C \star \rho_{at^{1/4}}$ then*

$$\begin{aligned} &\frac{a\,(2aM_1 - 2M_a + 1 - a)}{\pi\,(1-a^2)} = \\ &= -t^{3/4}\left(4N_1 v + a^2 N_5/8\left(\Delta H + 2H\left(H^2 - K\right)\right)\right) + O\left(t^{5/4}\right). \end{aligned}$$

Now if C is given, we calculate M_1 and M_a at each point and set $C_1 = \{\mathbf{x}\in\mathbb{R}^3 : 2aM_1 - 2M_a + 1 - a \geq 0\}$. According to the above asymptotics, $\partial C_1 = \{\mathbf{p} + vt\mathbf{N} : \mathbf{p}\in\partial C\}$, where

$$v = -\frac{a^2 N_5}{32N_1}\left(\Delta H + 2H\left(H^2 - K\right)\right) + O\left(t^{1/2}\right). \tag{11}$$

This motivates introducing an operator T acting on the family of smooth compact sets $\mathbb{K}\subset\mathbb{P}(\mathbb{R}^3)$

$$\begin{aligned} T(t):\mathbb{K} &\mapsto \mathbb{P}\left(\mathbb{R}^3\right) \\ T(t)\,C &= \left\{\mathbf{x}\in\mathbb{R}^3 : 2aM_1(t,\mathbf{x}) - 2M_a(t,\mathbf{x}) + 1 - a \geq 0\right\} \end{aligned} \tag{12}$$

Proposition 1. *Let $C \in \mathbb{K}$. Then $C_1 = T(t)\,C$ has smooth boundary for small enough values of t.*

Proof. Since the ∂C_1 is the zero level set of the thresholding function $F(t,\mathbf{x}) = 2aM_1(t,\mathbf{x}) - 2M_a(t,\mathbf{x}) + 1 - a$, it is enough to show that $\nabla F(t,\mathbf{x}) \neq 0$ on it. To see this, we take small t and expand the value of each component of ∇M_a into the power series in t. Since we are interested in values of ∇M_a on ∂C_1 we use the same system of coordinates as in the proof of Theorem 1.

$$\begin{aligned}
\nabla M_a(O) &= \int_{\mathbb{R}^3} \chi_C(x)\,\nabla \rho_{at^{1/4}}(x)\,dx = \\
&= \int_C \frac{2(x,y,z)\rho'\left(\left(x^2+y^2+z^2\right)/(a^2t^{1/2})\right)}{(at^{1/4})^5} dxdydz = \\
&= \int_{\mathbb{R}^2}\int_0^{-\infty} \frac{2(x,y,z)\rho'\left(\left(x^2+y^2+z^2\right)/(a^2t^{1/2})\right)}{(at^{1/4})^5} dzdxdy \\
&+ \int_{\mathbb{R}^2} \mathcal{I}(t,x,y)\,dxdy + O\left(e^{-t^{-1/2}}\right) = \\
&= \left(0,0,-\frac{2\pi M_1}{at^{1/4}}\right) + \int_{\mathbb{R}^2} \mathcal{I}(t,x,y)\,dxdy + O\left(e^{-t^{-1/2}}\right)
\end{aligned}$$

where

$$\begin{aligned}
\mathcal{I}(t,x,y) &= \frac{1}{at^{1/4}} \int_0^{g(t,x,y)} \left(0,0,\frac{\partial}{\partial z}\rho\left(x^2+y^2+z^2\right)\right) dz = \\
&= \frac{1}{at^{1/4}} \left(0,0,-\rho\left(x^2+y^2\right) + \rho\left(x^2+y^2+g^2(t,x,y)\right)\right)
\end{aligned}$$

with

$$g(t,x,y) = \frac{\gamma\left(t^{1/4}x, t^{1/4}y\right)}{t^{1/4}}.$$

Since $g(0,x,y) = 0$, we have

$$\nabla M_a(t,O) = \left(0,0,-\frac{2\pi N_1}{at^{1/4}} + O\left(t^{1/4}\right)\right)$$

and

$$\begin{aligned}
\nabla F(t,O) &= 2\left(a\nabla M_1(t,O) - \nabla M_a(t,O)\right) = \\
&= 4\pi\left(0,0,\frac{(1-a^2)\,N_1}{at^{1/4}} + O\left(t^{1/4}\right)\right) \neq 0.
\end{aligned}$$

□

The above proposition shows that for small enough t

$$T(t) : \mathbb{K} \mapsto \mathbb{K}.$$

Next we consider some finite t, then for some large $m \in \mathbb{N}$

$$T^m\left(\frac{t}{m}\right) : \mathbb{K} \mapsto \mathbb{K},$$

and investigate the following convergence

$$\partial\left(T^m\left(\frac{t}{m}\right)C\right) \to W(t)(\partial C) \text{ as } m \to \infty,$$

where by $W(t)\Sigma$ we denote the Willmore flow of Σ.

Theorem 2. *Suppose $f_0 : \mathbb{S}^2 \to \mathbb{R}^3$ is a smooth embedding of a sphere into $\mathbb{R}^3$ such that $\int_{\mathbb{S}^2} H^2(f)\,dA < 8\pi$. Denote the Willmore flow of f_0 by $f(t,u_1,u_2)$. By $\hat{f}_k(t/mt,u_1,u_2)$ denote a mapping of $\mathbb{S}^2$ onto $\partial\left(T^k\left(\frac{t}{m}\right)C\right)$, where $f_0(\mathbb{S}^2) = \partial C$. Then $\hat{f}_m(t/m,u_1,u_2) \to f(t,u_1,u_2)$ as $m \to \infty$ locally in $t \in [0,T]$ uniformly in u_1,u_2.*

Proof. Take $t \in (0,T]$. We omit arguments u_i and denote $f_i = f\left(i\frac{t}{n},u_1,u_2\right)$, then

$$f_1 = f_0 + \int_0^{t/m} N(t)\,w(t)\,dt = f_0 + \frac{t}{m}N_0w_0 + O\left((t/m)^2\right), \tag{13}$$

where $N(t)$ is the normal vector of $f(t)$ and

$$w(t) = -\Delta H(t) - 2H(t)\left(H^2(t) - K(t)\right)$$

the velocity of $f(t)$. The equality (13) is due to the fact that $f(t)$ is smooth by the assumption on $\int H_0^2 dA$ (see [13]). According to (11)

$$w_0 = \hat{v}_0 + O\left((t/m)^{1/2}\right),$$

where $\hat{w}_0$ satisfies $\hat{f}_1 = f_0 + N_0\hat{v}_0$. So

$$f_1 = \hat{f}_1 + O\left((t/m)^{3/2}\right). \tag{14}$$

Differentiation of the latter equality gives

$$N_1 = \hat{N}_1 + O\left((t/m)^{3/2}\right)$$

and

$$w_1 = \hat{w}_1 + O\left((t/m)^{3/2}\right) = hatv_1 + O\left((t/m)^{1/2}\right),$$

where the last equality is again due to (11). Now we can repeat the argument for f_1 considering f_2 to get

$$\begin{aligned} f_2 = f_1 + \int_{t/m}^{2t/m} N(t)\, w(t)\, dt &= f_1 + \frac{t}{m} N_1 w_1 + O\left((t/m)^2\right) \\ &= \hat{f}_2 + O\left((t/m)^{3/2}\right). \end{aligned}$$

This leads to

$$f_m - \hat{f}_m = \frac{t}{m} \sum_{i=0}^{m-1} \left(N_i w_i - \hat{N}_i \hat{w}_i\right) + O\left(\left(t^2/m\right)\right) = O\left((1/m)^{1/2}\right),$$

and the convergence follows. □

4 Numerical implementation and examples

Convolution-thresholding. Suppose the initial surface Σ_0 is the boundary of a smooth compact set $C = C_0 \subset \mathbb{R}^3$. Denote the Willmore flow of the Σ_0 by $\Sigma(t)$. Using the above asymptotics we construct surfaces ∂C_i for time moments $t_i = i\Delta t$, $i = 1, 2, ...$ as follows.

1. Convolution i.e. construction of functions

$$M_{a_k}(x) = \chi_{C_i} \star \rho_{a_k \Delta t^{1/4}}(x) \text{ for } k = 1, 2 \text{ with } a_1 = 1 \text{ and } a_2 < 1. \quad (15)$$

2. Thresholding i.e. localization of the next position of the surface

$$\partial C_{i+1} = \left\{x \in \mathbb{R}^3 : 2a_2 M_{a_1}(x) - 2M_{a_2}(x) + a_1 - a_2 = 0\right\}. \quad (16)$$

In our implementation we use a modification of so called Marching Cubes algorithm for extracting an iso-surface. A similar algorithm was proposed in [14] and first applied for the mean curvature flow calculations in [19].

Given an initial rectangular grid, refine all cubes that have a part of the surface in the interior. By refinement we mean just the binary dissection

that instead of one cube of volume v gives eight with volumes $v/8$. After this procedure is repeated several times, small cubes that have non-empty intersection with the surface are still present. Each such cube is then divided into six tetrahedrons and the surface is approximated linearly inside each tetrahedron. Thus the algorithm creates an adaptive spatial discretization of C

$$C = \cup_j \mathbf{C}_j \cup_k \mathbf{T}_k, \tag{17}$$

where $\mathbf{C}_j$ are cubes, $\mathbf{T}_k$ are tetrahedrons and the unions are disjoint.

Fourier method. We use Fourier series to calculate the convolutions M_{a_k}. Numerical aspects of similar computations in the case of the mean curvature evolution have been presented in [19] and [8].

In order to compute Fourier coefficients of χ_C where C is decomposed by the Marching Cubes procedure and is given by (17) we need to calculate integrals of trigonometric functions over cubes $\mathbf{C}_j$ and tetrahedrons $\mathbf{T}_k$. These integrals over $\mathbf{C}_j$ can be calculated exactly. The integrals over tetrahedrons can be well approximated by Gauss integration since the size of the integration domain is small. In both cases the computation of the Fourier coefficients $\{c_{jkl}\}_{i,j,k=0}^{N}$ of χ_C is reduced to the calculation of the following sums

$$c_{jkl} = \sum_{m=1}^{N_p} g_m \exp\left(-i\left(jx_m + ky_m + lz_m\right)\right), \tag{18}$$

where points $\{x_m, y_m, z_m\}_{m=1}^{N_p}$ are unequally spaced and g_m are some weights. A fast algorithm to approximately calculate such sums was proposed by Beylkin and can be found in [1]. The numerical cost of this algorithm is $O\left(\beta^3 N_p + N^3 \log\left(N\right)\right)$, where β is a constant depending on a desired accuracy in the calculation of the Fourier coefficients (in case $\beta = 23$ the accuracy is comparable with the machine truncation error).

Non-smooth initial data. The framework of the convolution thresholding method allows to consider not only initially smooth surfaces but also singular ones (see Figure 3). As a test example we consider a self-similar Willmore flow described in [7]. Take a sharp cone with the angle α as an initial surface. We can compare the calculated evolution of this surface with the one obtained in [7]. The shape comparison is shown on Figure 1, where the cross-section of the evolving cone is taken after 10 time steps. This shape is compared

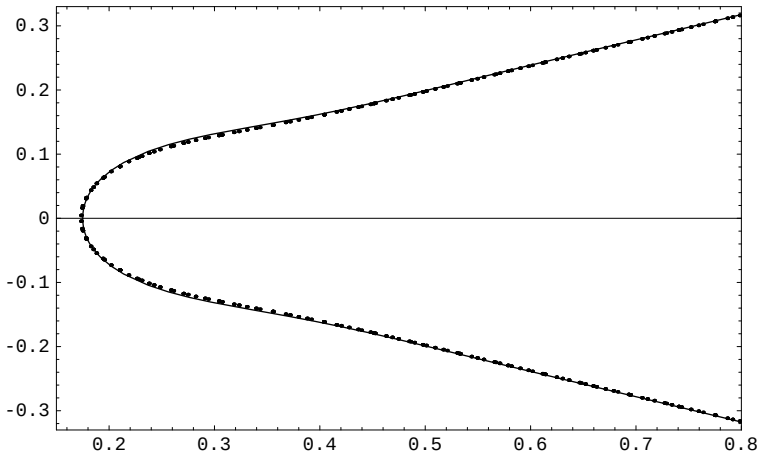

Figure 1: Calculated cross-section of the cone after a time interval $T = 1.6 \cdot 10^{-6}$ of the Willmore evolution (dots). Time step is $1.6 \cdot 10^{-7}$. The continuous line is the corresponding solution of the system of ODEs found in [7].

to the curve, obtained by solving numerically the corresponding system of ODEs (see [7]). In particular, the result in [7] states that coordinate of the vertex of the cone $r_v(t)$ will change in time according to the law

$$r_v(t) = C_\alpha t^{1/4},$$

where C_α is some constant depending only on α. We calculate the evolution of the cone and present the comparison result for the vertex coordinate on the Figure 2.

The Willmore flow of an initially non-smooth surfaces is depicted on the Fig. 3, 4.

Different functionals. Gradient flows for more complicated functionals depending for instance on the area of the surface and the volume of C can be also treated within the same scope of ideas. Suppose that the functional has the following form

$$\mathbb{F}(\mathbf{f}) = \int_\Sigma H^2 + 1 dS + \int_C dx,$$

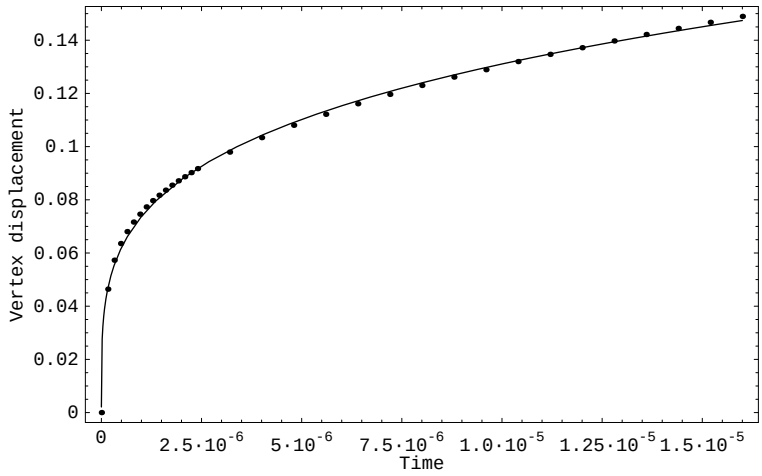

Figure 2: The coordinate of the vertex of the cone: time step is $1.6 \cdot 10^{-7}$, step numbers 0...15 and $5i$, $i = 4, 5, 6, ...20$. The continuous line is a graph of the function $2.33x^{1/4}$.

then evolution of a surface that minimizes it can be characterized by the normal velocity

$$\begin{aligned} v &= v_1 + v_2, \\ v_1 &= L_1 \left(\Delta H + 2H \left(H^2 - K \right) \right) \\ v_2 &= -L_2 H - L_3, \end{aligned}$$

where L_1, L_2 and L_3 are some constants. The surface evolution in this case can be captured by the following time splitting. To complete a single time step Δt with the velocity v we perform the following two steps. First propagate the surface with the velocity v_1 during the time $\Delta t/2$ with the method described above. Then propagate with the velocity v_2 during the time $\Delta t/2$ using the method described in [8].

Furthermore, by choosing appropriate values of L_3 at each time step one can achieve a constrained evolution of a surface that tends to minimize

$$\bar{\mathbb{F}}\left(\mathbf{f}\right) = \int_{\Sigma} H^2 + 1 dS.$$

For example, the conservation of the volume of C can be granted by the choice

$$L_3 = \int_{\Sigma_{i-1}} L_1 \left(\Delta H + 2H \left(H^2 - K \right) \right) - L_2 H dS$$

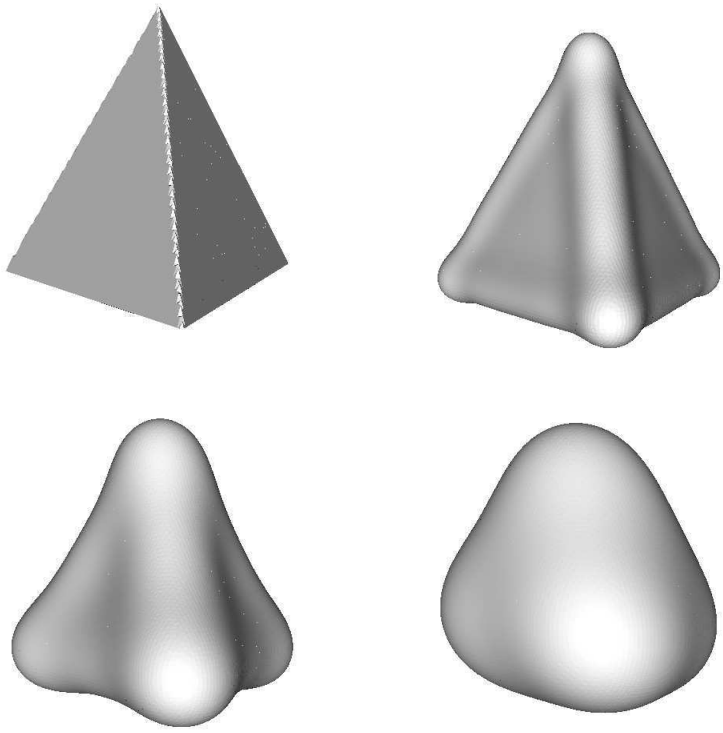

Figure 3: The evolution of a pyramid: time step is 10^{-8}, step numbers 0, 10, 110 and 610.

at a step number i. This particular surface evolution serves as a model describing a special kind of bilayer biological membranes.

References

[1] G. Beylkin, *On the fast Fourier transform of functions with singularities*, Appl. Comput. Harmon. Anal., 2 (1995), pp. 363–381.

[2] P. B. Canham, *The minimum energy of bending as a possible explanation of the biconcave shape of the human red blood cell*, J. Theor. Biol., 1 (1970), pp. 61–81.

[3] D. L. Chopp and J. A. Sethian, *Motion by intrinsic Laplacian of curvature*, Interfaces Free Bound., 1 (1999), pp. 107–123.

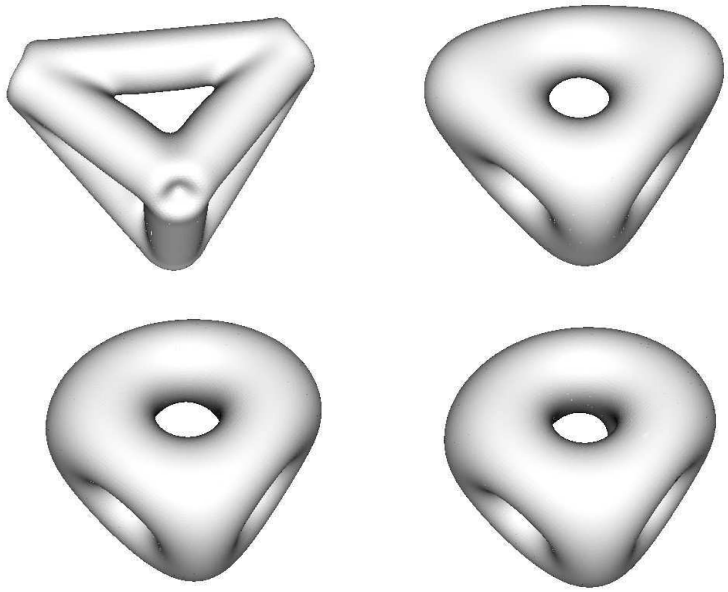

Figure 4: The evolution of a non-convex surface: time step is 10^{-8}, step numbers 0, 80, 480 and 1080.

[4] U. Clarenz, U. Diewald, G. Dziuk, M. Rumpf, and R. Rusu, *A finite element method for surface restoration with smooth boundary conditions*, CAGD, (2004). to appear.

[5] H. J. Deuling and W. Helfrich, *Red blood cell shapes as explained on the basis of curvature elasticity*, Biophysical Journal, 16 (1976), pp. 861–868.

[6] M. Droske and M. Rumpf, *A level set formulation for willmore flow*, Interfaces and Free Boundaries, (2004). accepted.

[7] R. Grzibovskis, *Willmore flow and self-similar evolution of surfaces*, Chalmers Univ. of Tech., Preprint 29, (2004).

[8] R. Grzibovskis and A. Heintz, *A convolution-thresholding approximation of generalised curvature flows*, Chalmers Univ. of Tech., Preprint 39, (2002).

[9] H. Ishii, *A generalization of the Bence, Merriman and Osher algorithm for motion by mean curvature*, in Curvature flows and related topics (Levico, 1994), Gakkōtosho, Tokyo, 1995, pp. 111–127.

[10] H. Ishii, G. E. Pires, and P. E. Souganidis, *Threshold dynamics type approximation schemes for propagating fronts*, J. Math. Soc. Japan, 51 (1999), pp. 267–308.

[11] E. Kuwert and R. Schätzle, *The Willmore flow with small initial energy*, J. Differential Geom., 57 (2001), pp. 409–441.

[12] ——, *Gradient flow for the Willmore functional*, Comm. Anal. Geom., 10 (2002), pp. 307–339.

[13] ——, *Removability of isolated singularities of Willmore surfaces*, Ann. of Math., (to appear).

[14] W. Lorensen and H. Cline, *Marching cubes: A high resolution 3d surface construction algorithm*, ACM Computer Graphics (Proceedings of SIGGRAPH' 87), 21 (1987), pp. 163–170.

[15] U. F. Mayer and G. Simonett, *Self-intersections for the Willmore flow*, Proceedings of the Seventh International Conference on Evolution Equations: Applications to Physics,Industry, Life Sciences and Economics, (2000), p. 9.

[16] ——, *A numerical scheme for axisymmetric solutions of curvature-driven free boundary problems, with applications to the Willmore flow*, Interfaces Free Bound., 4 (2002), pp. 89–109.

[17] R. Moser, *Weak solutions of the Willmore flow*, Max Planck Institute for Mathematics in the Sciences, Preprint Nr. 97, (2001).

[18] S. Ruuth, *Efficient algorithms for diffusion-generated motion by mean curvature*, Ph.D. thesis at the Univ. of Brithsh Columbia, (1996).

[19] S. J. Ruuth and B. Merriman, *Convolution-thresholding methods for interface motion*, J. Comput. Phys., 169 (2001), pp. 678–707.

[20] G. Simonett, *The Willmore flow near spheres*, Differential Integral Equations, 14 (2001), pp. 1005–1014.

[21] T. Tasdizen, R. Whitaker, P. Burchard, and S. Osher, *Geometric surface smoothing via anisotropic diffusion of normals*, Proceedings of the conference on Visualization, 1 (2002), pp. 125–132.

[22] T. J. Willmore, *Riemannian Geometry*, Clarendon Press, Oxford, 1993.

Paper [G1]

On self-similar Willmore and curvature evolutions of surfaces

Ricards Grzibovskis

Abstract

This study is devoted to the description of self-similar (homothetic) solutions of the Willmore and mean curvature flows of two dimensional surfaces in $\mathbb{R}^3$. We approach both evolutions in the same direct manner. This approach gives two classes of the evolution: the evolving surface develops a singularity in some finite time or the evolution originates from a singular initial surface. We also obtain the equation that describes the shape of these evolving surfaces. After introducing various symmetries, we come to systems of ordinary differential equations (ODEs) and describe some shapes of such surfaces in details.

1 Introduction

Self-similar evolution. Consider an evolving surface Σ and its immersion $\mathbf{s} : \Sigma \to \mathbb{R}^3$ into $\mathbb{R}^3$. We let this surface to evolve homotheticaly, i.e. at a time moment t the immersion of this surface into $\mathbb{R}^3$ will be

$$\mathbf{s}(t) = T(t)\,\mathbf{x} \tag{1}$$

where $T(t)$ is some smooth scalar function describing scaling in time and $\mathbf{x} : \Sigma \to \mathbb{R}^3$ describes the preserved shape of the surface. In this case the velocity of the surface along its normal is

$$V(\mathbf{s}) = \dot{T}(t)\,\mathbf{x} \cdot \mathbb{N}(\mathbf{s}), \tag{2}$$

where $\dot{T}(t) = \frac{d}{dt}T(t)$ and $(\cdot)$ denotes the inner product in $\mathbb{R}^3$.

In what follows we will consider two particular geometric evolutions: the Willmore flow and the mean curvature flow. Each of these evolutions can be characterized by the velocity of the evolving surface along its normal direction $V(\mathbf{s})$. By comparing the expression for this velocity with 2 in both cases we obtain the equations of motion.

In another words we propose a method how to choose the scaling function $T(t)$ and the shape of the surface $\mathbf{x}$ so that $\mathbf{s}(t)$ would be the curvature flow or the Willmore flow of $\mathbf{x}$.

Remark 1. *During any homothetic evolution the points on the surface in general has both normal and tangential components of the velocity. Tangential velocity does not change the shape of the surface provided there is no boundary. We restrict our consideration here to surfaces without boundaries.*

Willmore flow. A Willmore flow of a smooth surface Σ is defined as an L^2 gradient flow for the Willmore functional

$$\mathcal{W}(\Sigma) = \int_{\Sigma} H^2 dS, \tag{3}$$

where H denotes the mean curvature of Σ and dS is the induced area measure. Taking the variation of (3) another characterization of this evolution is obtained (see [15]). Consider a perturbation ϕ of the surface along its normal, then

$$\delta\mathcal{W} = \int_{\Sigma} \phi \left(\Delta H + 2H\left(H^2 - K\right)\right) dA,$$

where K is the Gaussian curvature of Σ and Δ is the Laplace-Beltrami operator . Thus, one can define the Willmore flow of Σ as an evolution of the surface when each point of it moves with the velocity along the normal

$$V = -\left(\Delta H + 2H\left(H^2 - K\right)\right) \equiv W \tag{4}$$

along its normal. If an immersion $\mathbf{s}$ of Σ into $\mathbb{R}^3$ is given then we write

$$V(\mathbf{s}) = W(\mathbf{s}) = -\left(\Delta H(\mathbf{s}) + 2H(\mathbf{s})\left(H^2(\mathbf{s}) - K(\mathbf{s})\right)\right) \tag{5}$$

to indicate the dependence on the point of Σ.

Remark 2. *It is easy to see, that the Willmore functional (3) is invariant under surface scaling. This implies that its value on any homothetic solution* $\mathbf{s}(t)$ *would have to be infinite. As an example, consider a cylinder that would expand homotheticaly under the Willmore evolution.*

The mathematical properties of the Willmore flow attracted much attention during the last years. Simonett have studied the Willmore flow near spheres in [14]. An example of occurrence of a self-intersection during the evolution is constructed in [12]. Small initial energy was considered by Kuwert and Schatzle in [9]. In [10] and [11] they have obtained a lower bound on the existence time of the flow. A definition of the weak solutions can be found in [13]. The author defines a continuation of the flow after eventual singularities occur and establishes the existence of the weak solution.

Curvature flow. The curvature flow (more precisely, the mean curvature flow) of a surface Σ can be viewed as the L^2 gradient flow corresponding to the area functional

$$\mathbb{A} = \int_{\Sigma} dS.$$

The normal velocity of the surface at each point corresponding to this evolution is the mean curvature

$$V = H.$$

Here again if an immersion $\mathbf{s}$ of Σ into $\mathbb{R}^3$ is given then we write

$$V(\mathbf{s}) = H(\mathbf{s}). \tag{6}$$

This type of surface evolution has been a popular topic of research for many years now [3], [6], [4], [8], [5], [2]. In particular, the homothetic mean curvature evolutions were considered in [1], [7].

Outline. We seek for the homothetic evolutions, therefore

$$\dot{T}(t)\,\mathbf{x}\cdot\mathbb{N}(\mathbf{s}) = V(\mathbf{s}), \tag{7}$$

where $V(\mathbf{s})$ is given by (5) in case of the Willmore flow and by (6) in case of the mean curvature flow. Assuming that the immersion $\mathbf{x}$ can be parameterized by three smooth functions of two variables

$$\mathbf{x}(u,v) = \{x(u,v), y(u,v), z(u,v)\},$$

we substitute $\mathbf{s}$ into (7) we get corresponding equations for curvature and Willmore flows (see section 2):

$$\dot{T}(t)\,\mathbf{x}\cdot\mathbb{N}(\mathbf{x}) = \frac{H(\mathbf{x})}{T(t)} \tag{8}$$

$$\dot{T}(t)\,\mathbf{x}\cdot\mathbb{N}(\mathbf{x}) = -\frac{W(\mathbf{x})}{T^3(t)}. \tag{9}$$

Both these equations allow a separation of time and space variables which yields to the equation for the time function $T(t)$ and the equation for the shape $\mathbf{x}(u_1, u_2)$

$$\begin{cases} \dot{T}(t) T(t) &= A \\ A\mathbf{x} \cdot \mathbb{N}(\mathbf{x}) &= H(\mathbf{x}) \end{cases} \tag{10}$$

for the mean curvature flow and

$$\begin{cases} \dot{T}(t) T^3(t) &= A \\ A\mathbf{x} \cdot \mathbb{N}(\mathbf{x}) &= -W(\mathbf{x}) \end{cases} \tag{11}$$

for the Willmore flow, where the constant A is arbitrary. Moreover, the equation for the time function can be solved explicitly in both cases yielding

$$T(t) = (1 + mAt)^{1/m},$$

where $m = 2$ in the case of mean curvature flow and $m = 4$ in the case of Willmore flow and we imposed a natural condition $T(0) = 1$. Suppose we have taken a negative A, then the parameterization $\mathbf{s}(t)$ can develop a singularity at the time moment $t_* = |mA|^{-1}$. A typical example of such singularity in the case of mean curvature flow is a round sphere or a straight cylinder. In the case of Willmore flow, this choice of the constant A leads to the new result: a smooth embedded surface develops a singularity in finite time. Taking a positive value of A the time multiplier vanishes at a time moment $t_* = -|mA|^{-1}$. In this case the corresponding evolution has a singular initial data. We present examples where this singular initial data is a sharp cone or a graph of the function $f(x, y) = \alpha |x|$ for some $\alpha \in \mathbb{R}$.

The equations for the shape function $\mathbf{x}$ in (10) and (11) are treated in cases of rotational and translational symmetries. By doing so, we reduce the corresponding PDE to a system of ODEs. It is easy to show that the solution to the latter system exists and is smooth. This proves, in particular, the existence of a smooth immersion that develops a singularity in finite time during the Willmore evolution. We also present some numerical experiments that suggest the Willmore evolution of some non-smooth surfaces.

Abresch and Langer [1] have studied homothetic solutions in the case of the mean curvature evolution of closed curves in $\mathbb{R}^2$. The curves, that they have found were used by Huisken in [7] to classify singularities that may occur during the mean curvature evolution of a two dimensional surface in $\mathbb{R}^3$. Likewise, homothetic solutions that we find in this work can be used to study singularities of the mean curvature evolution and the Willmore flow.

The solutions with positive A in certain cases suggest a continuation of the evolution after the singularity occured. Since the shapes of the surfaces are obtained here solving a system of ODEs, they can also be used to verify more complicated general approximation methods of the corresponding evolutions.

2 Transformation of geometric properties under scaling

Let us express the normal vector $\mathbb{N}(\mathbf{s})$, the mean curvature $H(\mathbf{s})$, the Gauss curvature $K(\mathbf{s})$, the Laplace-Beltrami of the mean curvature $\Delta H(\mathbf{s})$ and the time derivative $\dot{\mathbf{s}}$ by means of the corresponding operators acting on $\mathbf{x}$, function $T(t)$ and its derivative $\dot{T}(t)$. Denote $\mathbf{x}_i = \partial\mathbf{x}/\partial u_i$ and $\mathbf{s}_i = \partial\mathbf{s}/\partial u_i$ for $i = 1..2$. Directly from the definition of $\mathbf{s}(u_1, u_2, t)$ and $\mathbb{N}(\mathbf{s})$ follows that

$$\dot{\mathbf{s}}(u_1, u_2, t) = \frac{\partial\mathbf{s}(u_1, u_2, t)}{\partial t} = \dot{T}(t)\,\mathbf{x}(u_1, u_2)$$
$$\mathbb{N}(\mathbf{s}) = \frac{\mathbf{s}_1 \times \mathbf{s}_2}{|\mathbf{s}_1 \times \mathbf{s}_2|} = \frac{T^2(t)(\mathbf{x}_1 \times \mathbf{x}_2)}{|T^2(t)(\mathbf{x}_1 \times \mathbf{x}_2)|} = \mathbb{N}(\mathbf{x}).$$

The coefficients of the first fundamental form are

$$g_{ij}(\mathbf{s}) = \langle \mathbf{s}_i, \mathbf{s}_j \rangle = T^2(t)\langle \mathbf{x}_i, \mathbf{x}_j \rangle = T^2(t)\, g_{ij}(\mathbf{x})$$

and the second fundamental form have coefficients

$$h_{ij}(\mathbf{s}) = -\langle \mathbb{N}_i, \mathbf{s}_j \rangle = -T(t)\langle \mathbb{N}_i, \mathbf{x}_j \rangle = T(t)\, h_{ij}(\mathbf{x}),$$

where $\mathbb{N}_i = \partial\mathbb{N}/\partial u_i$. Therefore the mean curvature is

$$H(\mathbf{s}) = \frac{1}{2}\sum_i g^{ii}(\mathbf{s})\, h_{ii}(\mathbf{s}) = \frac{1}{2T(t)}\sum_i g^{ii}(\mathbf{x})\, h_{ii}(\mathbf{x}) = \frac{H(\mathbf{x})}{T(t)}, \qquad (12)$$

where g^{ij} denotes the elements of the matrix inverse to g. We proceed to find the relation between $K(\mathbf{s})$ and $K(\mathbf{x})$ in the same manner

$$K(\mathbf{s}) = \det\left(g^{ij}(\mathbf{s})\, h_{ij}(\mathbf{s})\right) = \det\left(\frac{1}{T(t)} g^{ij}(\mathbf{x})\, h_{ij}(\mathbf{x})\right) = \frac{K(\mathbf{x})}{T^2(t)},$$

In order to calculate ΔH we use the Christoffel symbols

$$\Gamma^k_{ij} = \frac{1}{2}\sum_h g^{hk}\left(\partial g_{ih}/\partial u_j + \partial g_{jh}/\partial u_i - \partial g_{ij}/\partial u_h\right),$$

which turned out to be the same for both $\mathbf{s}$ and $\mathbf{x}$:

$$\begin{aligned}\Gamma_{ij}^{k}(\mathbf{s}) &= \frac{1}{2}\sum_{h} g^{hk}(\mathbf{s})\left(\frac{\partial g_{ih}}{\partial u_j}(\mathbf{s})+\frac{\partial g_{jh}}{\partial u_i}(\mathbf{s})-\frac{\partial g_{ij}}{\partial u_h}(\mathbf{s})\right)= \\ &= \frac{1}{2}\sum_{h}\frac{g^{hk}(\mathbf{x})}{T^2(t)}\left(T^2(t)\frac{\partial g_{ih}}{\partial u_j}(\mathbf{x})+T^2(t)\frac{\partial g_{jh}}{\partial u_i}(\mathbf{x})-T^2(t)\frac{\partial g_{ij}}{\partial u_h}(\mathbf{x})\right)= \\ &= \Gamma_{ij}^{k}(\mathbf{x})\end{aligned}$$

The covariant derivatives of H are

$$\begin{aligned}\nabla_i H &= H_i = \frac{\partial H}{\partial u_i} \\ \nabla_i\nabla_j H &= H_{ij} - \sum_k \Gamma_{ji}^{k} H_k\end{aligned}$$

thus

$$\nabla_i\nabla_j H(\mathbf{s}) = \frac{\nabla_i\nabla_j H(\mathbf{x})}{T(t)}$$

Since the Laplace-Beltrami of H can be written as

$$\Delta H = \sum_{i,j} g^{ij}\nabla_i\nabla_j H, \tag{13}$$

we get

$$\Delta H(\mathbf{s}) = \frac{\Delta H(\mathbf{x})}{T^3(t)}$$

and

$$W(\mathbf{s}) = \frac{\Delta H(\mathbf{x})}{T^3(t)} + 2\frac{H(\mathbf{x})}{T(t)}\left(\frac{H^2(\mathbf{x})}{T^2(t)}-\frac{K(\mathbf{x})}{T^2(t)}\right) = \frac{W(\mathbf{x})}{T^3(t)}. \tag{14}$$

3 Mean curvature flow

In the case of mean curvature evolution the velocity along the normal is equal to the mean curvature $V(\mathbf{s}) = H(\mathbf{s})$. We substitute (12) into the equation of motion (7) to get

$$\begin{aligned}\dot{T}(t)\,\mathbf{x}\cdot\mathbb{N}(\mathbf{x}) &= \frac{H(\mathbf{x})}{T(t)} \\ \dot{T}(t)\,T(t) &= \frac{H(\mathbf{x})}{\mathbf{x}\cdot\mathbb{N}(\mathbf{x})} = A = const\end{aligned}$$

This gives the following two equations

$$\dot{T}(t)\,T(t) = A \tag{15}$$

$$H(\mathbf{x}) = A\mathbf{x}\cdot\mathbb{N}(\mathbf{x}). \tag{16}$$

The first of them can be integrated exactly. Together with the initial condition $\mathbb{T}(0) = 1$ it gives the solution

$$T(t) = \sqrt{2}\,(1/2 + At)^{1/2}. \tag{17}$$

This formula suggests considering the following three cases:

1. Case $A = 0$. The time function $T(t) = 1$ is constant and we have no evolution. The equation for the shape (16) becomes $H(\mathbf{x}) = 0$ and the solutions are the critical points of the area functional. There is no surface evolution in this case.

2. Case $A > 0$. The surface evolution exists and is smooth for $t \in \left(-\frac{1}{2A}, \infty\right]$ provided that the solution of the shape equation (16) exists and is smooth. However, one might suspect that this evolution has a singular initial data at $t = -\frac{1}{2A}$.

3. Case $A < 0$. The evolution exists and is smooth for $t \in \left(-\infty, \frac{1}{-2A}\right]$ provided that the solution of the shape equation (16) exists and is smooth. However, one might expect that this evolution encounters a singularity at a time moment $t = -\frac{1}{2A}$.

Remark 3. *Let S denote the area of the surface. Then during the curvature flow*

$$\frac{d}{dt}S = -\int_{\Sigma} H^2(\mathbf{s})\,dS(\mathbf{s}). \tag{18}$$

Substituting () into the above we get

$$\frac{d}{dt}S = -\int_{\Sigma} H^2(\mathbf{x})\,dS(\mathbf{x}) = const. \tag{19}$$

Thus, during the homothetic curvature flow, the surface decreases linearly if it is bounded. This means that the infinite evolution time in the case $A > 0$ imply that the area of the evolving surface in this case would have to be infinite.

The equation (16) for the shape of the surface is qualitatively different form the equation (15). We next study the equation (16) with some symmetries that allow a detailed qualitative analysis.

3.1 Translational symmetry

In the case when the surface under consideration is invariant with respect translations along Z-axis the parameterization of

$$\mathbf{x}(u,v) = \{x(u,v), y(u,v), z(u,v)\}$$

can be chosen as follows:

$$x(u,v) = x(u) = x_0 + \int_0^u \cos(\theta(s))\, ds \tag{20}$$

$$y(u,v) = y(u) = y_0 + \int_0^u \sin(\theta(s))\, ds \tag{21}$$

$$z(u,v) = z(v) = v. \tag{22}$$

Here u is the arclength of the curve $\{x(u), y(u)\}$ and $\theta(u)$ is the angle between x-axis and the vector tangent to this curve at the point $(x(u), y(u))$. In this setting the mean curvature of the surface is

$$H(\mathbf{x}) = \frac{\theta'(u)}{2},$$

and the shape equation (16) together with (20) and (21) give the system of three first order ordinary differential equations for unknown functions $\theta(u)$, $x(u)$ and $y(u)$

$$\begin{cases} \theta'(u) = 2A\left[y(u)\cos(\theta(u)) - x(u)\sin(\theta(u))\right] \\ x'(u) = \cos(\theta(u)) \\ y'(u) = \sin(\theta(u)). \end{cases} \tag{23}$$

The existence and uniqueness of the global in u solution to the corresponding Cauchy problem follows from the fact that the right hand sides are Lipschitz with the Lipschitz constant equal to 1. Thus, for each x_0, y_0 and θ_0 the system defines some curve. This curve in turn forms the cylindrical surface that evolves homotheticaly by mean curvature. In what follows we try to classify the above curves.

Proposition 1. *Solutions to the Cauchy problem for the system (23) have the following properties:*

1. *If $A > 0$ the solution curve in the XY-plane is unbounded. It is a straight line containing the origin if the tangent line passes through the origin at some point. Otherwise, it tends to a straight line that passes*

through the origin as $u \mapsto +\infty$. It also tends to a different straight line containing the origin as $u \mapsto -\infty$. The curve comes not closer then r_1 to the origin, where r_1 is the solution of

$$\log r_1 + C_1(x_0, y_0, \theta_0, A) = -Ar_1^2. \tag{24}$$

2. *If $A < 0$ the solution curve in the XY-plane is contained in a closed ring. The inner and the outer radii of this ring are two only solutions of the equation (24).*

Proof. We introduce a function $r(u) = \left(x^2(u) + y^2(u)\right)^{1/2}$. After calculating the derivatives of this function and using (23) we get

$$\begin{aligned} \frac{1}{2}\frac{d}{du}r^2(u) &= x(u)\cos(\theta(u)) + y(u)\sin(\theta(u)) \\ \frac{1}{2}\frac{d^2}{du^2}r^2(u) &= 1 + 2A\left[y(u)\cos(\theta(u)) - x(u)\sin(\theta(u))\right]^2 \end{aligned}$$

The latter expression is greater then 1 provided that $A > 0$. Moreover in this case we conclude

$$\begin{aligned} \frac{d^2}{du^2}r^2(u) &\geq 2 \\ \frac{d}{du}r^2(u) &\geq 2u + \left[x_0\cos(\theta(0)) + y_0\sin(\theta(0))\right] \\ r^2(u) &\geq u^2 + u\left[x_0\cos(\theta(0)) + y_0\sin(\theta(0))\right] + r^2(0). \end{aligned} \tag{25}$$

Thus we deduce that for positive A the solution has to go to infinity at least as fast as the arclength. It is also easy to see what happens with the mean curvature $\theta'(u)$ as $u \mapsto \infty$ ($r \mapsto \infty$). We differentiate the equation (23) with respect to u to obtain

$$\begin{aligned} \theta''(u) &= -2A\theta'(u)\left[y(u)\sin(\theta(u)) + x(u)\cos(\theta(u))\right] \\ \frac{\theta''(u)}{\theta'(u)} &= -Ar^2(u)' \\ \log(\theta'(u)) - \log(\theta'(0)) &= -A\left[r^2(u) - r^2(0)\right] \\ \theta'(u) &= \theta'(0)\exp\left(-A\left[r^2(u) - r^2(0)\right]\right). \end{aligned} \tag{26}$$

Now we can use the estimate (25) on the growth of $r(u)$ to conclude the following: if $A > 0$ the curve is unbounded and far away from the origin has exponentially small curvature (is essentially a straight line). Moreover, the comparison of (26) and (23) for large r gives that this line includes the origin.

Moreover from (26) we deduce that the curvature of the curve has the same sign along it. The next step is to use this expression to obtain bounds for r, namely the equation (24). We have

$$2A\left[y\cos\theta - x\sin\theta\right] = 2A\left[y_0\cos\theta_0 - x_0\sin\theta_0\right]e^{-A\left(r^2-r_0^2\right)}. \tag{27}$$

Observing that $\left[y\cos\theta - x\sin\theta\right] = r\cos\beta$ for some β we get

$$\begin{aligned}
\frac{r\cos\beta}{r_0\cos\beta_0} &= e^{-A\left(r^2-r_0^2\right)} \\
\frac{r}{\left|r_0\cos\beta_0\right|} &\geq e^{-A\left(r^2-r_0^2\right)} \\
\log r - \log\left|r_0\cos\beta_0\right| &\geq -A\left(r^2-r_0^2\right) \\
\log r - \left(\log\left|r_0\cos\beta_0\right| + Ar_0^2\right) &\geq -Ar^2. \qquad (28)
\end{aligned}$$

The latter inequality implies (24). □

It is also convenient to rewrite the system (23) using polar coordinates $x(u) = r(u)\cos(\phi(u))$ and $y(u) = r(u)\sin(\phi(u))$:

$$\left\{\begin{array}{rcl}
\tau'(u) &=& -\frac{\sin(\tau(u))}{r(u)}\left(1 + 2Ar^2(u)\right) \\
r'(u) &=& \cos\left(\tau(u)\right) \\
\phi'(u) &=& -\frac{\sin(\tau(u))}{r(u)},
\end{array}\right. \tag{29}$$

where $\tau(u) = \phi(u) - \theta(u)$.

Corollary 1. *As a consequence of the above proposition we obtain the relation between the initial data and the constant A that is necessary and sufficient to have the obvious homothetic solution, namely a circle. We observe, that in this case $\tau(u) = \tau(0) = \pm\pi/2$, thus $\tau'(u) = 0$ and we use (29) to obtain the radius of the circle $r(u) = r(0) = (-2A)^{-1/2}$.*

We can also conclude, that the circle is not the only periodical and bounded curve that one can obtain solving (23).

Proposition 2. *For a fixed negative value of A one can choose the initial data r_0, ϕ_0 and θ_0 so that the projection of the trajectory of the solution to (23) onto the xy-plane will be periodic.*

Proof. (Since this result was already obtained in [1], we omit some technical details of this alternative elementary proof.) One can easily check, that

$$r(u)\sin(\tau(u))\,e^{Ar^2(u)} = r(0)\sin(\tau(0))\,e^{Ar^2(0)} \equiv C_0 = const. \tag{30}$$

Let us fix $\phi(0) = \pi/2$, $\theta(0) = 0$. We also choose $r_0 < (-2A)^{-1/2}$. Now r_0 is the smallest of two roots of (30). Equations (29) imply that if u grows $r(u)$ also grows until it reaches the largest of roots of (30), namely r_1. Meanwhile ϕ decreases to a value ϕ_1. In order for the curve to be periodic, $\phi_0 - \phi_1$ has to be a rational part of π:

$$\delta\phi = \phi_0 - \phi_1 = \frac{m}{n}\pi \tag{31}$$

for some $m, n \in \mathbb{Z}$. We express this difference in terms of an integral

$$\begin{aligned} \delta\phi &= \int_0^{u_1} \frac{\sin(\tau(u))}{r(u)} du \\ &= \int_{r_0}^{r_1} \frac{\sin(\tau(u))}{r\sqrt{1-\sin^2(\tau(u))}} dr, \end{aligned}$$

where $\sin(\tau(u))$ is given by (30)

$$\sin(\tau(u)) = \frac{r_0 e^{Ar_0^2} e^{-Ar^2}}{r}.$$

Next, we check that singularities at $r = r_0$ and $r = r_1$ are integrable. We expand the integrand into power series with respect to r at the point $r = r_0$ to get

$$\frac{C_0 e^{-Ar^2}}{r\sqrt{r^2 - C_0^2 e^{-2Ar^2}}} = \left(r_0^2 (2/r_0 + 4Ar_0)(r - r_0)\right)^{-1/2} + O\left(\sqrt{r - r_0}\right),$$

which is integrable at $r = r_0$. Singularity at $r = r_1$ can be treated in the same manner.

It remains to observe, that $\delta\phi$ depends continously on r_0 because r_1 and the integrand depend continously on it. (Further investigation shows that $\delta\phi \to \pi/4$ when $r_0 \to 0$ and $\delta\phi \to \pi\sqrt{2}/4$ when $r_0 \to (-2A)^{-1/2}$.)

□

This class of closed self-similar solutions was obtained in [1] and used in [7] to classify singularities that occur during the mean curvature flow of the two-dimensional surface in $\mathbb{R}^3$. Some periodical representatives of the solutions for the negative values of A are depicted on Figures 1. These curves were obtained by integrating the system (23) numerically. As follows from (17), these curves shrink into a point at the origin.

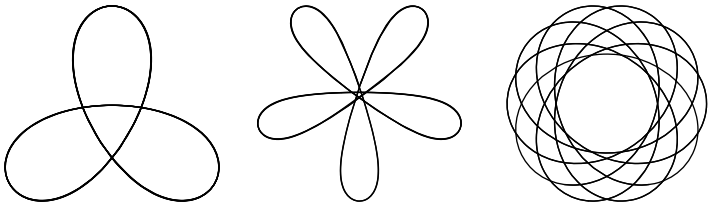

Figure 1: Shapes of collapsing homothetic solution of the curvature flow (translational symmetry).

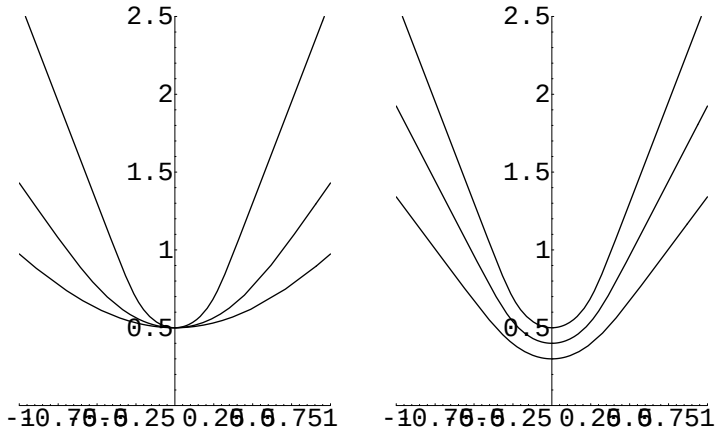

Figure 2: The shape of a homothetic solution of the curvature flow with an infinite area (translational symmetry). On the left picture A varies. On the right picture the value of A is fixed but the initial data varies.

Typical solutions to the system (23) with $A > 0$ are shown on Figure 2. The evolution in time of one such curve is depicted on Figure 3. If we look for the position of the surface for negative values of t we find, that this evolution might be considered as the curvature flow of the initially non-smooth data.

3.2 Axial symmetry

In the case of the axial symmetry around Z-axis the parameterization of

$$\mathbf{x}(u,v) = \{x(u,v), y(u,v), z(u,v)\}$$

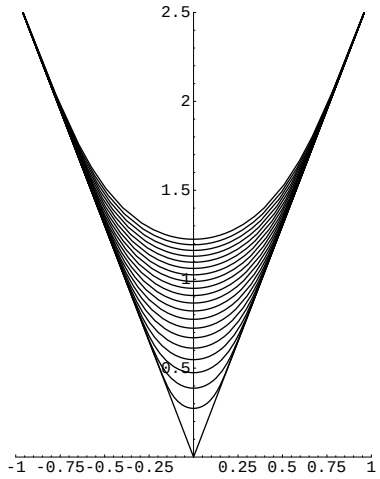

Figure 3: The homothetic curvature flow of a singular initial data.

can be chosen as:

$$x(u,v) = \xi(u)\cos(v) \tag{32}$$
$$y(u,v) = \xi(u)\sin(v) \tag{33}$$
$$z(u) = \eta(u), \tag{34}$$

where

$$\xi(u) = \xi_0 + \int_0^u \cos(\theta(s))\,ds$$
$$\eta(u) = \eta_0 + \int_0^u \sin(\theta(s))\,ds$$

Here u is the arclength of the curve $\{\xi(u), \eta(u)\}$ and $\theta(u)$ is the angle between ξ-axis and the vector tangent to this curve at the point $(\xi(u), \eta(u))$. The curve rotates around z-axis and forms the surface Σ. The mean curvature of this surface is

$$H(\mathbf{x}) = \frac{\theta'(u)}{2} + \frac{\sin(\theta(u))}{2\xi(u)},$$

and the shape equation (16) together with (32) and (33) give the system of three first order ordinary differential equations for unknown functions $\theta(u)$, $\xi(u)$ and $\eta(u)$

$$\begin{cases} \theta'(u) = 2A\left[\eta(u)\cos(\theta(u)) - \xi(u)\sin(\theta(u))\right] - \frac{\sin(\theta(u))}{\xi(u)} \\ \xi'(u) = \cos(\theta(u)) \\ \eta'(u) = \sin(\theta(u)). \end{cases} \tag{35}$$

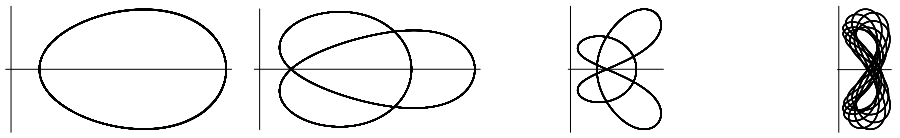

Figure 4: The shape of collapsing homothetic solution of the curvature flow (axial symmetry).

In what follows we describe results that we have obtained by integrating (35) numerically.

Case $A < 0$**.** Similarly to the case of translational symmetry, one can obtain periodical trajectories in the $\xi\eta$-plane. Several representatives of such curves are depicted on Figure 4. Some of these trajectories have their analogy among the periodic solutions of (23). For example, the first curve on the Figure 4 corresponds to a circle, the second one corresponds to the first curve depicted on Figure 1. One can also find some curves that come out of the system (23) and seems to have no corresponding solution in the case of translational symmetry. As an example, consider the last curve on Figure 4. Each of the above periodic curves forms a surface of revolution. By construction, the mean curvature evolution of these surfaces is homothetic and since $A < 0$, () implies that these surfaces will shrink homotheticaly to a point at the origin.

Case $A > 0$**.** The curve in the $\xi\eta$-plane is unbounded. We have $r \to \infty$ both for $u \to \infty$ and $u \to -\infty$. When r is large, the curve behaves as a straight line passing through the origin. Thus, in general we obtain two different straight lines. One when $u \to \infty$ and another when $u \to -\infty$. The corresponding surface of revolution is a result of the mean curvature evolution starting from a double cone (see Figure 5). Choosing the initial data closer to the η-axis the asymptotical straight lines come closer (see Figure 6). They coincide if we take $\xi_0 = 0$, $\theta(0) = 0$ and $\theta'(0) = 2A\eta(0)$.

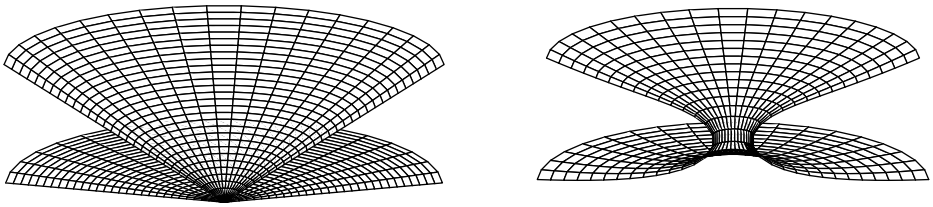

Figure 5: The shape at time $t = 5$ of the self-similar curvature flow (fight) starting from the double cone (left) at time $t = 0$. Only the parts of the surfaces with $y > 0$ are shown.

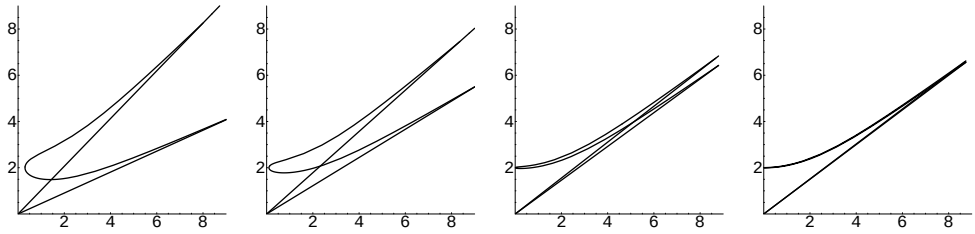

Figure 6: Projections of solutions to (35) onto the $\xi\eta$-plane and their asymptotes. $A = 0.1$, $\eta_0 = 2$, $\theta_0 = \pi/2$ and values of ξ_0 are equal to 0.3, 0.1, 0.01, 0.001.

4 Willmore flow

We substitute (14) into the equation of motion (7) to get

$$\begin{aligned} \dot{T}(t)\,\mathbf{x}\cdot\mathbb{N}(\mathbf{x}) &= -\frac{W(\mathbf{x})}{T^3(t)} \\ \dot{T}(t)\,T^3(t) &= -\frac{W(\mathbf{x})}{\mathbf{x}\cdot\mathbb{N}(\mathbf{x})} = A = const \end{aligned}$$

This gives the following two equations

$$\dot{T}(t)\,T^3(t) = A \tag{36}$$

$$-W(\mathbf{x}) = A\mathbf{x}\cdot\mathbb{N}(\mathbf{x}). \tag{37}$$

The first of them can be integrated exactly. Together with the initial condition $T(0)=1$ it gives the solution

$$T(t) = \sqrt{2}\,(1/4 + At)^{1/4}.$$

Similarly with the curvature flow we obtain a solution that develops a singularity for a negative value of A and a solution that is a result of the evolution of some singular shape for a positive A.

4.1 Translational symmetry

In the case of transitional symmetry, we choose a parameterization of our surface as in subsection 3.1 to obtain the following system of ordinary differential equations

$$\begin{cases} 2\theta'''(u) + (\theta'(u))^3 &= -4A\left[y(u)\cos(\theta(u)) - x(u)\sin(\theta(u))\right] \\ x'(u) &= \cos(\theta(u)) \\ y'(u) &= \sin(\theta(u)). \end{cases} \tag{38}$$

The order of this system is five, therefore it produces a much larger variety of curves in the xy-plane then the system (23) does. In what follows we consider the cases $A>0$ and $A<0$ separately and extract some illustrative examples in each of the cases.

Case $A > 0$. If we consider only the curves that are symmetrical with respect to the y-axis, two interesting classes of curves appear: periodical and

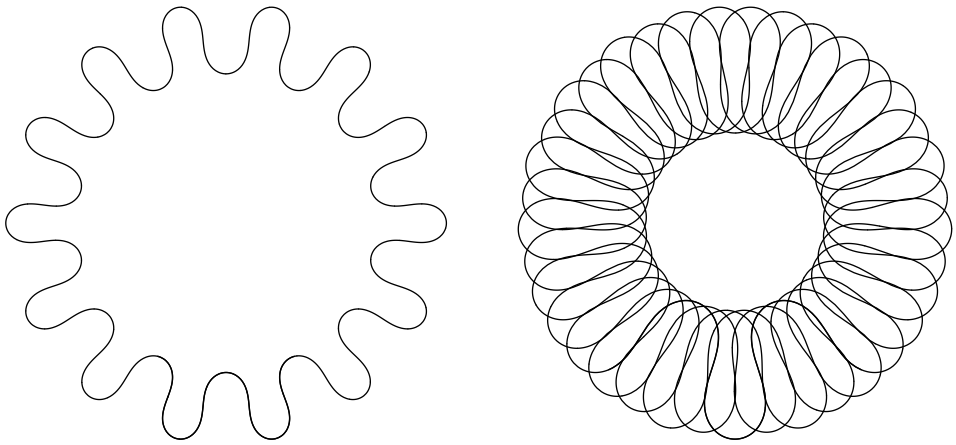

Figure 7: Cross-sections of some cylindrical surfaces that expand homothetically during the Willmore evolution.

asymptotically flat. One obvious periodical curve is a circle. Two non-trivial periodical curves appear on the Figure 7. The asymptotically flat curves are depicted on the Figure 8. They represent the cross-section of the initially singular surfaces $\Sigma = \{(x, y, z) : z = \alpha |x|\}$ for some $\alpha \in \mathbb{R}$.

Case $A < 0$**.** Calculations show, that in this case $r \to \infty$ as $u \to \pm\infty$. If we restrict ourselves to symmetrical shapes as in the previous case, we get some oscilating curves that form a singularity during the evolution. Some of these curves are shown on the Figure 9. By varying the parameter A and the curvature at the starting point we can find many different curves that give the same singular surface during the evolution.

4.2 Axial symmetry

In the case of axial symmetry, we choose a parameterization of our surface as in subsection 3.2 to obtain the following system of ordinary differential

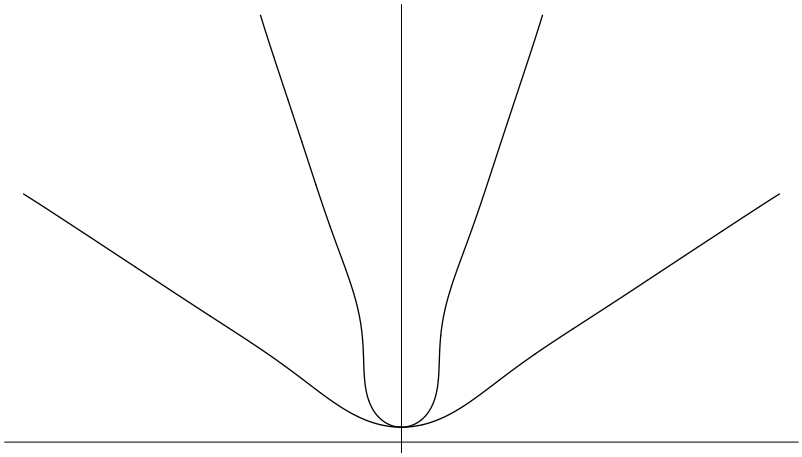

Figure 8: Cross-sections of some cylindrical surfaces that expand homothetically during the Willmore evolution.

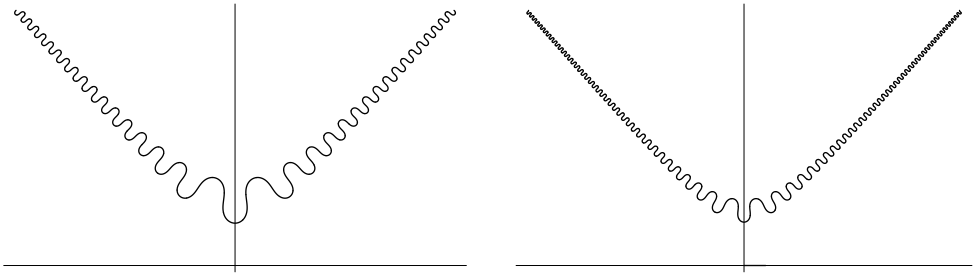

Figure 9: Cross-sections of two cylindrical surfaces that form a singularity during The Willmore evolution. The surfaces are different, but the resulting singular one is the same.

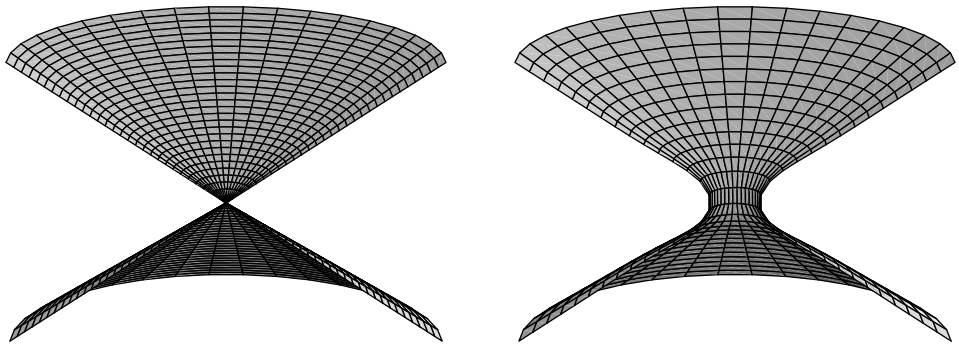

Figure 10: Willmore evolution of a double cone.

equations

$$\begin{cases} 2\theta''' + (\theta')^3 + \frac{1}{4\xi^3}\left(5\sin(\theta) + \sin(3\theta)\right) - \frac{\theta'}{2\xi^2}\left(1 + 3\cos(2\theta)\right) + \\ + \frac{1}{\xi}\left(4\theta''\cos(\theta) - 3(\theta')^2\sin(\theta)\right) = -4A\left[\eta\cos(\theta) - \xi\sin(\theta)\right] \\ \xi' = \cos(\theta) \\ \eta' = \sin(\theta), \end{cases} \tag{39}$$

where θ, ξ and η are functions of u.

Inspired by the results of the section 3.2 we look for the shape of the surface resulting from the Willmore evolution of the double cone. One obtains the cross-section of such surface solving the boundary value problem for the system (39) with some positive value of A. The boundary conditions can be chosen as

$$\begin{aligned} \xi(0) = \xi_0 > 0 \qquad & \eta(0) = 0 \\ \theta(0) = \pi/2 \qquad & \theta''(0) = 0 \\ \theta'(L) = 0, & \end{aligned}$$

where L has to be large enough. The numerical solution of such boundary value problem gives the shape depicted on the Figure 10.

There is also another class of surfaces that can be obtained by integrating the system (39) with $A > 0$. This class consists of bounded embedded surfaces of revolution. Cross-sections of two representatives of this family of surfaces are shown on the Figure 11.

In the case of negative A we also obtain bounded surfaces. These surfaces collapse into the origin. Some examples of such surfaces are depicted on the Figure 12.

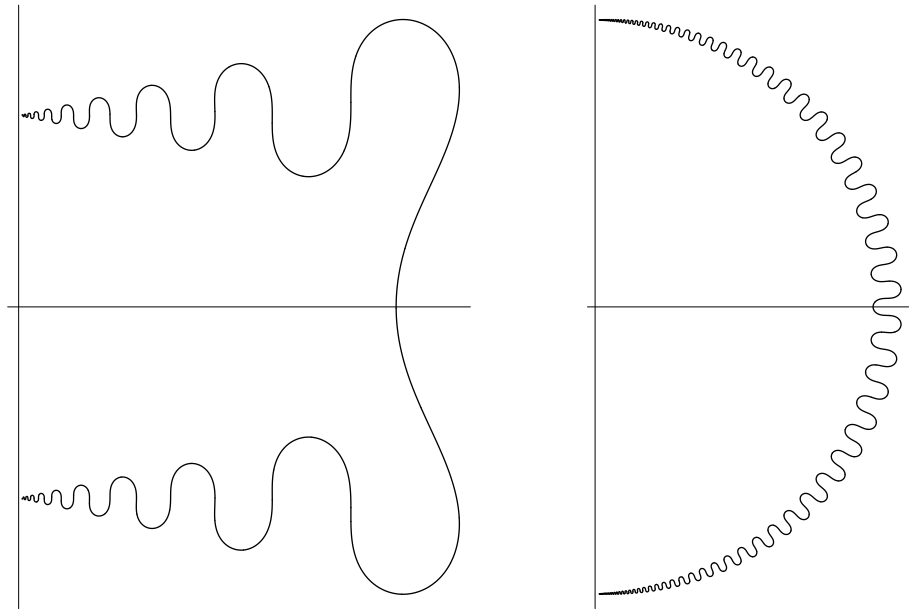

Figure 11: Half of the cross-section of some surfaces that expand homothetically during the Willmore evolution.

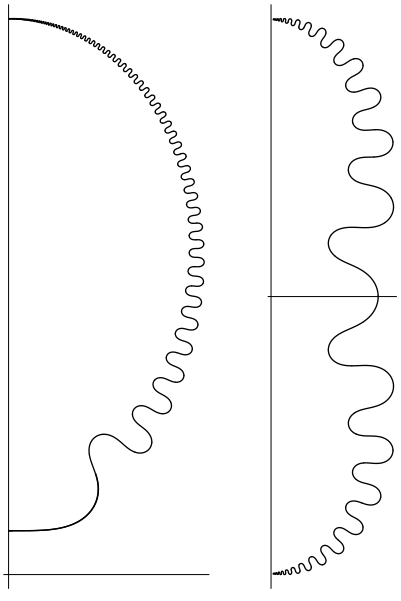

Figure 12: Half of the cross-section of some surfaces that collapse homothetically during the Willmore evolution.

Acknowledgement

We would like to thank Alexei Heintz for a number of long and fruitful discussions on the topic of this paper. We also express our gratitude to Girgori Rozenblioum for providing some useful references.

References

[1] U. Abresch and J. Langer, *The normalized curve shortening flow and homothetic solutions*, J. Differential Geom., 23 (1986), pp. 175–196.

[2] G. Bellettini and M. Paolini, *Comparison theorems for various notions of curvature-driven motion*, Atti Accad. Naz. Lincei Cl. Sci. Fis. Mat. Natur. Rend. Lincei (9) Mat. Appl., 6 (1995), pp. 45–54.

[3] K. A. Brakke, *The motion of a surface by its mean curvature*, Princeton University Press, Princeton, N.J., 1978.

[4] Y. G. Chen, Y. Giga, and S. Goto, *Uniqueness and existence of viscosity solutions of generalized mean curvature flow equations*, J. Differential Geom., 33 (1991), pp. 749–786.

[5] E. De Giorgi, *Conjectures on limits of some quasilinear parabolic equations and flow by mean curvature*, in Partial differential equations and related subjects (Trento, 1990), Longman Sci. Tech., Harlow, 1992, pp. 85–95.

[6] L. C. Evans and J. Spruck, *Motion of level sets by mean curvature. I*, J. Differential Geom., 33 (1991), pp. 635–681.

[7] G. Huisken, *Local and global behaviour of hypersurfaces moving by mean curvature*, in Differential geometry: partial differential equations on manifolds (Los Angeles, CA, 1990), vol. 54 of Proc. Sympos. Pure Math., Amer. Math. Soc., Providence, RI, 1993, pp. 175–191.

[8] H. Ishii and P. Souganidis, *Generalized motion of noncompact hypersurfaces with velocity having arbitrary growth on the curvature tensor*, Tohoku Math. J. (2), 47 (1995), pp. 227–250.

[9] E. Kuwert and R. Schätzle, *The Willmore flow with small initial energy*, J. Differential Geom., 57 (2001), pp. 409–441.

[10] ——, *Gradient flow for the Willmore functional*, Comm. Anal. Geom., 10 (2002), pp. 307–339.

[11] ——, *Removability of isolated singularities of Willmore surfaces*, Ann. of Math., (to appear).

[12] U. F. Mayer and G. Simonett, *Self-intersections for the Willmore flow*, Proceedings of the Seventh International Conference on Evolution Equations: Applications to Physics,Industry, Life Sciences and Economics, (2000), p. 9.

[13] R. Moser, *Weak solutions of the Willmore flow*, Max Planck Institute for Mathematics in the Sciences, Preprint Nr. 97, (2001).

[14] G. Simonett, *The Willmore flow near spheres*, Differential Integral Equations, 14 (2001), pp. 1005–1014.

[15] T. J. Willmore, *Riemannian Geometry*, Clarendon Press, Oxford, 1993.

Paper [HKG]

FAST NUMERICAL METHOD FOR THE BOLTZMANN EQUATION ON NON-UNIFORM GRIDS

ALEXEI HEINTZ, PIOTR KOWALCZYK, AND RICARDS GRZIBOVSKIS

Abstract. We introduce a new fast numerical method for computing discontinuous solutions to the Boltzmann equation and illustrate it by numerical examples. A combination of adaptive grids for approximation of the distribution function and an approximate fast Fourier transform on non-uniform grids for computing smooth terms in the Boltzmann collision integral is used.

1. Introduction

This paper is devoted to a new deterministic scheme for numerical solution of the classical *Boltzmann equation* [10] for a dilute gas of particles.

$$\frac{\partial f}{\partial t} + \mathbf{v} \cdot \nabla_x f = Q(f, f), \tag{1.1}$$

where $f := f(t, \mathbf{x}, \mathbf{v})$ and $f : \mathbb{R}_+ \times \Omega \times \mathbb{R}^3 \to \mathbb{R}_+$. The collision operator Q is defined as follows

$$Q(f, f)(\mathbf{v}) := \int_{\mathbb{R}^3} \int_{S^2} B(|\mathbf{v} - \mathbf{w}|, \theta) \left[f(\mathbf{v}') f(\mathbf{w}') - f(\mathbf{v}) f(\mathbf{w}) \right] d\omega \, d\mathbf{w}, \tag{1.2}$$

where $\mathbf{v}$, $\mathbf{w}$ are the velocities of the particles before the collision and $\mathbf{v}'$, $\mathbf{w}'$ – the velocities of the particles after collision – are given by

$$\mathbf{v}' := \frac{1}{2} \left(\mathbf{v} + \mathbf{w} + |\mathbf{v} - \mathbf{w}| \omega \right), \qquad \mathbf{w}' := \frac{1}{2} \left(\mathbf{v} + \mathbf{w} - |\mathbf{v} - \mathbf{w}| \omega \right).$$

Moreover θ is the angle between the relative velocity $\mathbf{u} = \mathbf{v} - \mathbf{w}$ before and $\mathbf{u}' = \mathbf{v}' - \mathbf{w}'$ after collision.

The function $B(|\mathbf{v} - \mathbf{w}|, \theta)$ is of the form

$$B(|\mathbf{u}|, \theta) = B_0 \left(|\mathbf{u}|, \frac{|(\mathbf{u}, \omega)|}{|\mathbf{u}|} \right), \; u \in \mathbb{R}^3, \omega \in S^{(2)}, \; S^{(2)} = \{ \mathbf{q} \in R^3 : |\mathbf{q}| = 1 \}.$$

It contains the information about the binary interactions of particles and reflects the physical properties of the model.

The condition $B(|\mathbf{u}|, \cdot) \in L^1(S^{(2)})$, $\mathbf{u} \in \mathbb{R}^3$ is usually assumed to obtain separately convergent integrals for the positive "gain" and the negative "loss" parts in (1.2). For example if the particle interactions are modeled by inverse

Key words and phrases. Boltzmann equation, non-uniform grids.

power forces with angular cut-off that means that grazing collisions do not take place, then

$$B_0(r, x) = r^\gamma b(x), \tag{1.3}$$

where $\gamma \in (-3, 1]$, and $b \in L^1([0, 1])$. In the case of "hard sphere" molecules, $B_0(r, x) = rx$.

In the case of popular Variable Hard Sphere model (VHS) the collision kernel B has the following form

$$B(|\mathbf{v} - \mathbf{w}|, \theta) = C_\alpha |\mathbf{v} - \mathbf{w}|^\alpha. \tag{1.4}$$

with $-3 < \alpha \leq 1$. For $\alpha = 0$ with $C_0 = \frac{1}{4\pi}$ we get the so called Maxwellian gas and for $\alpha = 1$ with $C_1 = 1$ we get the gas of hard spheres.

To solve the non-stationary Boltzmann equation numerically a splitting method in time is commonly applied.

At each time step in one solves first the *homogeneous Boltzmann equation*

$$\frac{\partial f}{\partial t} = Q(f, f) \quad \text{for all } \mathbf{x} \in \Omega \tag{1.5}$$

and then the *transport equation*

$$\frac{\partial f}{\partial t} + \mathbf{v} \cdot \nabla_x f = 0 \quad \text{for all } \mathbf{v} \in \mathbb{R}^3. \tag{1.6}$$

The main problem for the efficient numerical computations of the Boltzmann equation is a proper approximation of the collision operator $Q(f, f)$. We concentrate here mainly on the approximation of the collision operator in velocity space and hence demonstrate the method on examples with space homogeneous solutions. The application of the same approach for space dependent problems will be demonstrated in a subsequent paper.

In the next sections we will omit the dependence of f on the t and $\mathbf{x}$ variables for brevity where it is not confusing.

The numerical solution of the Boltzmann equation is difficult due to the nonlinearity of the collision integral, the large number of independent variables and the complicated integration over a five-dimensional cone in the six-dimensional space of pre and post collisional velocities. This analytical structure of $Q(f, f)$ implies that a straightforward computation of the collision integral by a standard quadrature has the computational cost N^3 for N points representing state of a gas in the velocity space. We point out that this is the cost of computations just in one point x in the physical space for a space non-homogeneous problem.

Particular symmetries of the collision operator imply conservation laws that in turn imply important connections between the Boltzmann equation and equations of classical gas dynamics.

Consequently the major part of practical applied computations concerning the Boltzmann equation is based on different variants of the probabilistic

Monte Carlo methods. Monte Carlo methods are advantageous for many high dimensional problems in physics, giving realistic and meaningful results with low computational cost proportional to the number N of particles (points) representing the system. On the other hand getting high precision results by Monte Carlo methods requires a higher computational time and for the number N_{tr} of stochastic trajectories they demonstrate low convergence order $\sqrt{N_{tr}}$. We refer to the direct simulation method (DSMC) by Bird [5] and to variants of Monte Carlo method for the Boltzmann equation by Nanbu [17] and Babovsky [3].

Development of deterministic methods for the Boltzmann equation is usually motivated, see [22], [18] by the desire of higher precision results, and by the existence of situations (low Knudsen numbers, slow convection flows) when probabilistic methods are not effective enough. Also not at the last place in the motivation of studies in this direction one finds the mathematical challenge of the problem itself.

We begin with a short discussion of the earlier results in the area of deterministic methods for the Boltzmann equation. Historically so called discrete velocity models (DVM) with uniform cubic grid of velocities were the first example of a numerical approach designed specially for the Boltzmann equation, starting from D. Goldstein, B. Sturtevant and J.E. Broadwell [12]. Later several different ideas led to other types of models all satisfying exact conservation laws in discrete form [23]. [9], [20].

Also rigorous consistency and convergence results for such models were proved [19], [16], [20].

Let n denote the number of points along one coordinate direction in the uniform velocity grid. All above mentioned DVM methods have high n^7 computational cost and have also a disadvantage that the integration over the sphere S^2 of the possible outputs of collisions in $Q(f, f)$ is approximated with low precision of order $1/\sqrt{n}$ [19]. In the case of the alternative so called Carleman formulation for $Q(f, f)$ this integration is substituted by the integration over some arbitrarily oriented planes with the same approximation problems [20]. It happens because only a small number of points from the uniform cubic grid meets spheres and arbitrarily oriented planes and these points are distributed not uniformly.

The Kyoto group in kinetic theory developed a family of finite difference methods for the Boltzmann equation, linearized Boltzmann equation, and the BGK equation and investigated numerically many mostly stationary problems [18],[14]. These computations demonstrate precise results but they are very time and memory consuming.

For computation of macroscopic flows with low Knudsen numbers so called lattice Boltzmann computational models with small (6 to 30 velocity points) are successfully applied, see [24] for references in this area. These simple

models have structure that reminds the Boltzmann equation but without the goal to approximate solutions to the last one. Also several larger simplified models of the collision operator $Q(f, f)$ were suggested recently, see for example [1] that do not approximate of the Boltzmann equation precisely but demonstrate somehow reasonable behavior of macro-parameters.

The simpler structure of the Boltzmann collision operator in the case of Maxwell pseudo molecules, by applying Fourier transform lets to reduce the collision operator to an expression with smaller dimension of the integration [7]. Using this reduction and the Fast Fourier Transform (FFT) led authors in [11] and [6] to a fast deterministic method restricted to Maxwell pseudo molecules and having low computational cost N^4 but still low accuracy $1/\sqrt{N}$. Here N is the number of Fourier modes along one coordinate direction. Another method designed for the model of hard spheres and also using FFT was suggested in [8] and has computational cost $N^6 \log N$ and a higher accuracy of order $1/N^2$.

A spectral method based on the restriction of the Boltzmann equation to a finite domain and on the representation of the solution by Fourier series was suggested in [21], and developed further in [22]. This method has an advantage of high spectral accuracy for smooth solutions to the Boltzmann equation and complexity N^6.

Any effort to develop a deterministic scheme for boundary value problems for the Boltzmann equation, includes as a necessary step computation of the collision operator $Q(f, f)$ for distribution functions typical for flows with boundaries. A typical distribution function for a gas close to the boundary has a discontinuity along a plane.

One observes easily that in a collisionless flow around a body the distribution function has a discontinuity in velocity space along a cone like surface that is built of the contour of the body seen from the point of observation. Computations done by the Kyoto group show that typical distribution functions for flows around a body have actually a similar discontinuity for a wide spectrum of Knudsen numbers [25].

It means that solutions to a boundary value problem are typically not smooth and Fourier based spectral approximations for them loose accuracy. The Gibbs phenomenon makes an alternative way of approximation necessary for such solutions.

To overcome this difficulty is the main goal of the present paper. One of the main ideas of the project comes from the classical result that the gain term $Q^+(f, f)$ in the collision operator has certain smoothing properties [15], [26] and therefore is smooth even for discontinuous f. One can illustrate this fact by the graph of $Q^+(f, f)$ in the x-z plane for a discontinuous function, see Figure 1. Collision frequency $q^-(f)$ is also a smooth function because it is a convolution of f with a regular function.

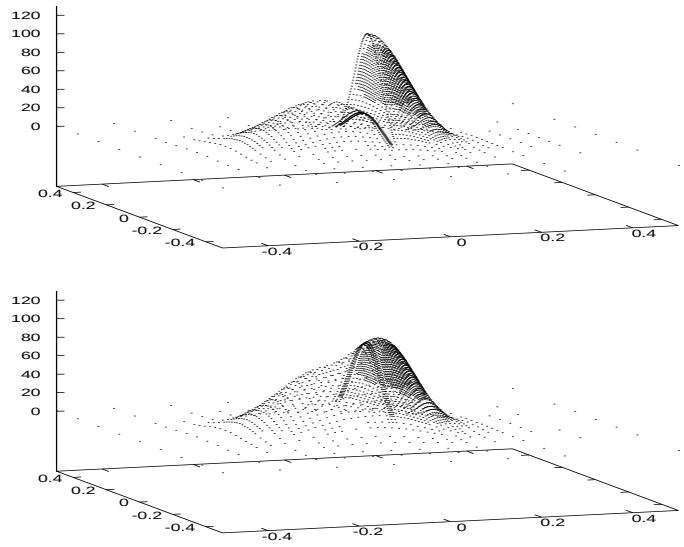

FIGURE 1. A distribution function f with discontinuity and the corresponding gain term $Q^+(f, f)$

We introduce here an approximation scheme that can effectively handle solutions to the Boltzmann equations discontinuous in velocity space. It is based on a new method for approximation of the Boltzmann collision operator and its solutions using non-uniform grids in velocity space. The following techniques make input to its computational efficiency:

i) Fourier based spectral representation of the gain part of collision operator as a bilinear pseudodifferential operator excluding effectively integration over spheres from numerical computations;

ii) effective resolution of discontinuities of solutions using an adaptive grid;

iii) high precision spectral representation for smooth terms in the Boltzmann equation;

iv) application of an approximate Fast Fourier transform on non-uniform grid for fast computation of the gain term and collision frequency on the adaptive grid;

v) an approximate algebraic decomposition of the symbol of the bilinear pseudodifferential expression for the gain term.

Techniques i) and iii) were used before, ii), iv), v) are new for the Boltzmann equation. The idea to combine a spectral representation for smooth terms in the Boltzmann equation with approximation on and adaptive grid for the discontinuous distribution function f is new. The combination of

adaptive grids with non-uniform Fast Fourier transform was previously used for approximation of geometric flows in [13].

2. Transformation of the collision integral

The collision operator (1.2) for potentials with angular cut off [10] can be decomposed into the *gain* and the *loss* parts

$$Q(f,f)(\mathbf{v}) = Q^+(f,f)(\mathbf{v}) - Q^-(f,f)(\mathbf{v}), \tag{2.1}$$

where

$$Q^+(f,f)(\mathbf{v}) = \int_{\mathbb{R}^3}\int_{S^2} B(|\mathbf{u}|,\theta) f(\mathbf{v}-\frac{1}{2}(\mathbf{u}-|\mathbf{u}|\omega)) f(\mathbf{v}-\frac{1}{2}(\mathbf{u}+|\mathbf{u}|\omega)\, d\omega\, d\mathbf{u} \tag{2.2}$$

and

$$Q^-(f,f)(\mathbf{v}) = f(\mathbf{v}) q^-(f)(\mathbf{v}) \tag{2.3}$$

with q^- denoting the *collision frequency* term

$$q^-(f)(\mathbf{v}) = \int_{\mathbb{R}^3} f(\mathbf{v}-\mathbf{u}) \int_{S^2} B(|\mathbf{u}|,\theta)\, d\omega\, d\mathbf{u}.$$

We have changed the variables $\mathbf{u} = \mathbf{v} - \mathbf{w}$ in the collision integral in (1.2) to get the above formulations.

We will use the following form of the Fourier transform

$$F_v(\mathbf{m})[f] := \hat{f}_m = \int_{\mathbb{R}^3} f(\mathbf{v}) e^{2\pi\imath(\mathbf{v},\mathbf{m})}\, d\mathbf{v} \tag{2.4}$$

and inverse Fourier transform

$$F_m^{-1}(\mathbf{v})[\hat{f}] := f(\mathbf{v}) = \int_{\mathbb{R}^3} \hat{f}_m e^{-2\pi\imath(\mathbf{m},\mathbf{v})}\, d\mathbf{m}. \tag{2.5}$$

Now we can reformulate the gain and collision frequency terms using the Fourier transform:

$$Q^+(f,f)(\mathbf{v}) = F_l^{-1}(\mathbf{v}) F_m^{-1}(\mathbf{v}) \left[\hat{f}_l \hat{f}_m \hat{B}(\mathbf{l},\mathbf{m})\right], \tag{2.6}$$

$$q^-(f)(\mathbf{v}) = F_m^{-1}(\mathbf{v}) \left[\hat{f}_m \hat{B}(\mathbf{m},\mathbf{m})\right], \tag{2.7}$$

where

$$\hat{B}(\mathbf{l},\mathbf{m}) = \int_{\mathbb{R}^3}\int_{S^2} B(|\mathbf{u}|,\theta) e^{2\pi\imath(\frac{\mathbf{l}+\mathbf{m}}{2},\mathbf{u})} e^{2\pi\imath|\mathbf{u}|(\frac{\mathbf{m}-\mathbf{l}}{2},\omega)}\, d\omega d\mathbf{u}. \tag{2.8}$$

The gain term is a kind of bilinear pseudodifferential operator with symbol $\hat{B}(\mathbf{l},\mathbf{m})$. The kernel $\hat{B}(\mathbf{l},\mathbf{m})$ is a distribution, hence for using it in practical

computations we have to regularize it. We will choose in a proper way the constant $R > 0$ and write the regularized kernel as

$$\hat{B}_R(\mathbf{l},\mathbf{m}) = \int_{\mathcal{B}(0,R)} \int_{S^2} B(|\mathbf{u}|,\theta) e^{2\pi\imath(\frac{\mathbf{l}+\mathbf{m}}{2},\mathbf{u})} e^{2\pi\imath|\mathbf{u}|(\frac{\mathbf{m}-\mathbf{l}}{2},\omega)}\, d\omega d\mathbf{u}. \tag{2.9}$$

We denote by $Q_R^+(f,f)$ and $q_R^-(f)$ the gain and collision frequency terms with regularized kernel $\hat{B}_R$.

The kernel $\hat{B}_R$ can be computed analytically for some special cases of VHS model (see [22]). In particular, for hard sphere gas it is given by

$$\hat{B}_R(\mathbf{l},\mathbf{m}) = \\ 8\frac{p^2\left[\pi Rq\sin(\pi Rq)+\cos(\pi Rq)\right] - q^2\left[\pi Rp\sin(\pi Rp)+\cos(\pi Rp)\right] - 4\xi\eta}{\pi^2\xi\eta p^2 q^2},$$

whereas for Maxwellian gas we have the following formula

$$\hat{B}_R(\mathbf{l},\mathbf{m}) = 2\frac{p\sin(\pi Rq) - q\sin(\pi Rp)}{\pi^2\xi\eta pq},$$

where $p = \xi + \eta$, $q = \xi - \eta$ and $\xi = |\mathbf{l}+\mathbf{m}|$, $\eta = |\mathbf{l}-\mathbf{m}|$.

3. Discretization of the collision integral

3.1. **Discretization of velocity space.** We will illustrate our approach to the numerical solution of the Boltzmann equation by space homogeneous problems with discontinuous initial data. A standard semi-implicit finite difference scheme in time will be applied pointwise with respect to velocity variable.

The distribution function $f(t,\mathbf{v})$ is usually negligible small outside some ball, so for the numerical treatment of the Boltzmann equation we assume that

$$\text{supp } f \subset \Omega_v := [-L,L]^3,$$

where we take $L = \frac{1}{2}$ for the technical reason which will be given later.

One of the main problems with efficient deterministic computation of the Boltzmann equation is a fixed usually uniform discretization of the velocity domain. Hence a huge number of discretization points is required to get the desired accuracy.

We overcome this problem by introducing a nonuniform velocity grid $\mathcal{G}_v \subset \Omega_v$ with N_v denoting the number of points in $\mathcal{G}_v$. The grid $\mathcal{G}_v \subset \Omega_v$ of discrete points will be chosen in such a way that the jump of the function values between neighboring points is lower than some prescribed threshold. Thus the grid will have much more discrete points in regions where the function changes rapidly than in the regions where the function is almost constant. In

order to treat the discontinuous functions we impose an additional condition that the neighboring points should not be closer than some given number.

The numerical method that we introduce in this paper gives a possibility after some preprocessing to compute approximate values of the gain term $Q^+(f,f)$ and the collision frequency $q^-(f)$ at arbitrary points in velocity space for a very low cost. It makes that $Q_R^+(f,f)$ and $q_R^-(f)$ can be computed effectively on a non-uniform grid different from one where the function f is defined.

This property lets to a natural idea to built at each time step a nonuniform grid in Ω_v that is changed adaptively to follow the the changes of the distribution function f (see Section 4).

At each time step we will first compute the values of the solution at vertexes of cells that build some initial coarse grid. Then using some reasonable criteria we will decide which cells in this coarse grid must be divided into smaller ones. The simplest criteria is a threshold for the variation of the solution within the cell.

After dividing chosen cells we compute values of the solution in new vertexes of the new cells and then continue the subdivision in the same way. Thus we generate much more grid points in parts of Ω_v where the function f changes rapidly than in those where the function is almost constant. In order to treat discontinuous functions we impose an additional condition that the neighboring points should not be closer than some given number.

During this process of subdivision we create an adaptive grid in parallel with computation of the values of the solution at each time step. Details of this adaptive procedure like distribution of grid points and the shape of the cells can be managed in various ways. They are in our method completely independent from the main challenge that is the effective computation of the gain term $Q_R^+(f,f)$ on an arbitrary non-uniform grid.

Particular adaptive grids that we use in examples at the end of the paper are grids consisting of an hierarchy of cubes, subdivided into eight smaller ones in a binary way in regions with high variation of f.

3.2. **Discretization of Fourier transform.** Now we focus on the numerical approximation of the Fourier transform integrals (2.4) and (2.5) for f defined on a non-regular grid.

We have restricted the function f to a bounded domain Ω_v. See [22] for discussion of the validity of such a restriction. For the sake of simplicity we will describe here the evaluation of the integral

$$\hat{f}_m = \int_{\Omega_v} f(\mathbf{v}) e^{2\pi\imath(\mathbf{v},\mathbf{m})}\, d\mathbf{v},$$

for f approximated by a function $\bar{f}$ piecewise constant on cells defined by the discretization of the velocity space. The approach we use below does not depend on this issue.

Using an approximation $\bar{f}$ for f we get the following discrete in velocity variable approximation for Fourier transform of f (we keep the same notation for the Fourier transform and its discretization)

$$\hat{f}_m = \sum_K \bar{f}_K \int_K e^{2\pi\imath(\mathbf{v},\mathbf{m})}\, d\mathbf{v} = \sum_K C_m \bar{f}_K \sum_{\mathbf{v}_K} e^{2\pi\imath(\mathbf{v}_K,\mathbf{m})},$$

where K denotes a cubic cell of the discretization of Ω_v, $\bar{f}_K$ is a constant approximating f on K and C_m is a constant depending only on $\mathbf{m}$. The above formulation has a disadvantage that some points are counted multiple times depending on how many cells have the given point in common. To avoid this multiple counting we build the *unique-node* grid of velocity points to get the following formulation

$$\hat{f}_m = C_m \sum_j \bar{f}_j\, e^{2\pi\imath(\mathbf{v}_j,\mathbf{m})}, \tag{3.1}$$

where $\bar{f}_j$ is a value of function f in a point $\mathbf{v}_j$. Another higher order approximation for f on cells using values $\bar{f}_j$ in vertexes of the cells would lead to a similar formula.

The standard Fast Fourier Transform (FFT) algorithm commonly used to compute numerically trigonometric sums cannot be used here for sums like one in (3.1), since the points $\mathbf{v}_j$ in the velocity space Ω_v are not equidistant. To manage this problem we use the *Unequally Spaced Fast Fourier Transform* (USFFT) algorithm developed by G. Beylkin [4]. This procedure is convenient to formulate if we scale the problem so that points $\mathbf{v}_j$ lay within the cube $[-\frac{1}{2},\frac{1}{2}]^3$. Hence we assume later that the problem is scaled so that the support of the function f lies in such a cube.

Below we give for completeness of the presentation an outline of the algorithm. Values of Fourier transform $\hat{f}_m$ by formula (3.1) will be computed on a uniform grid in R^3 in Fourier domain: $\{\mathbf{m} = (m_1, m_2, m_3) : m_1, m_2, m_3 = -M, \ldots, M-1\}$ for $M = 2^{-n-2}$ with $n < 0$. We will use for brevity the shortened notation $\mathbf{m} = -M, \ldots, M-1$ for multi-indices denoting points of such grids. Hence we need to compute the sum (3.1) for $\mathbf{m} = -M, \ldots, M-1$.

Let $N = 4M$. The first step is computing the coefficients

$$g_k = \sum_j \bar{f}_j \beta^{(p)}_{k_1,n}(v_{j,1}) \beta^{(p)}_{k_2,n}(v_{j,2}) \beta^{(p)}_{k_3,n}(v_{j,3}), \quad \mathbf{k} = 0, \ldots, N-1,$$

where $\mathbf{v}_j = (v_{j,1}, v_{j,2}, v_{j,3})$ and $\beta^{(p)}_{r,n}(x) = 2^{-\frac{n}{2}} \beta^{(p)}(2^{-n}x - r)$ with $\beta^{(p)}$ being the central B-spline of order p. The computational cost of this step is $\mathrm{O}(p^3 N_v)$.

Then we evaluate a trigonometric sum

$$F_l = \sum_{\mathbf{k}=0}^{N-1} g_k e^{2\pi\imath(\mathbf{k},\mathbf{l})/N}, \quad \mathbf{l} = -N/2, \ldots, N/2-1$$

using standard FFT algorithm with the cost $\mathrm{O}(N^3 \log N)$.

The last step is a scaling of Fourier transform F_l according to the formula

$$\hat{f}_m = \frac{1}{N^{\frac{3}{2}}\sqrt{a^{(p)}(m_1/N)a^{(p)}(m_2/N)a^{(p)}(m_3/N)}} F_m, \quad \mathbf{m} = -M, \ldots, M-1.$$

This step requires only $\mathrm{O}(N^3)$ multiplications, hence the total cost of the USFFT algorithm can be estimated as $\mathrm{O}(p^3 N_v)+\mathrm{O}(N^3 \log N)$. The precision of these computations depends on the order p of the the central B-splines $\beta^{(p)}$ and on the oversampling that is relation between 2 in this case.

A similar procedure is used to calculate the inverse Fourier transform (2.5) which, discretized in Fourier domain, is given by

$$f(\mathbf{v}) = \sum_{\mathbf{m}=-M}^{M-1} \hat{f}_m e^{-2\pi\imath(\mathbf{m},\mathbf{v})}, \quad \mathbf{v} \in \Omega_v. \tag{3.2}$$

Namely, we start with extending the Fourier coefficients

$$g_k = \begin{cases} \hat{f}_{k+M} & \text{if } -M \le \mathbf{k} \le M-1, \\ 0 & \text{otherwise,} \end{cases} \qquad \mathbf{k} = -N/2, \ldots, N/2-1.$$

Then we scale g_k according to the formula

$$\tilde{g}_k = \frac{g_k}{\hat{b}_{k_1}\hat{b}_{k_2}\hat{b}_{k_3}},$$

where $\hat{b}_{k_j} = \sum_{l=-\frac{p-1}{2}}^{\frac{p-1}{2}} \beta^{(p)}(l) e^{2\pi\imath l k_j/N}$. Next we apply the FFT algorithm to compute the sum

$$f_l = \sum_{\mathbf{k}=-N/2}^{N/2-1} \tilde{g}_k e^{2\pi\imath(\mathbf{l},\mathbf{k})/N}, \quad \mathbf{l} = -N/2, \ldots, N/2-1.$$

Finally, we evaluate f at any point $\mathbf{v} \in \Omega_v$ using the formula

$$f(\mathbf{v}) = \sum_{\mathbf{l}=-N/2}^{N/2-1} f_l \beta^{(p)}(\frac{N}{2}v_1 - l_1)\beta^{(p)}(\frac{N}{2}v_2 - l_2)\beta^{(p)}(\frac{N}{2}v_3 - l_3).$$

The cost of the first two steps of the algorithm is $\mathrm{O}(N^3 \log N)$. The cost of the last step depends on the number of required computations of f in the velocity domain and for N_v points it is $\mathrm{O}(p^3 N_v)$. Hence the total cost of calculation of the inverse Fourier transform is the same as before.

3.3. **Decomposition of the gain term $Q^+(f,f)$.** Discretization of the collision operator is splitted into two parts according to (2.1). We start with the gain term $Q^+(f,f)$ (2.2), which is discretized as follows

$$Q^+(f,f)(\mathbf{v}) = \sum_{\mathbf{l},\mathbf{m}=-M}^{M-1} \hat{f}_l \hat{f}_m \hat{B}(\mathbf{l},\mathbf{m}) e^{-2\pi\imath(\mathbf{l}+\mathbf{m},\mathbf{v})}.$$

To reduce the computational cost of this formulation we want to decouple dependence on variables $\mathbf{l}$ and $\mathbf{m}$ in the kernel $\hat{B}(\mathbf{l},\mathbf{m})$. This makes the bilinear expression easy to calculate.

It is easy to check that the kernel $\hat{B}(\mathbf{l},\mathbf{m})$ is a symmetric matrix. It is a function of $|\mathbf{l}-\mathbf{m}|$, $|\mathbf{l}+\mathbf{m}|$ and $(\mathbf{l}-\mathbf{m})(\mathbf{l}+\mathbf{m})$ (and in the case of VHS model of $|\mathbf{l}-\mathbf{m}|$ and $|\mathbf{l}+\mathbf{m}|$ only) [22]. Hence we use the spectral decomposition to get

$$\hat{B}(\mathbf{l},\mathbf{m}) = \sum_{r=1}^{s} d_r U_r(\mathbf{l}) U_r(\mathbf{m}), \tag{3.3}$$

where $s = 8M^3$ is the number of eigenvalues and U_r is the eigenvector corresponding to the eigenvalue d_r. Obviously we can take in (3.3) only significant eigenvalues (with some prescribed threshold) to get a reasonable approximation of the kernel.

Now let s denote the number of significant eigenvalues of $\hat{B}(\mathbf{l},\mathbf{m})$, which is typically $\frac{1}{8}$ to $\frac{1}{4}$ part of the total number. Hence we get the following approximation to the gain term

$$Q^+(f,f)(\mathbf{v}) = \sum_{p=1}^{s} d_r \left[\sum_{\mathbf{m}=-M}^{M-1} \hat{f}_m U_r(\mathbf{m}) e^{-2\pi\imath(\mathbf{m},\mathbf{v})} \right]^2. \tag{3.4}$$

In our algorithm we need to compute the sum (3.4) in many arbitrary points $\mathbf{v}$ in the velocity domain Ω_v so that finally they will build an adaptive grid that suites well for the approximation of the solution f at the next time step. A straightforward calculation of the sum of squares in (3.4) would be too much time and memory consuming. To do it efficiently we compute first the sums $\sum_{\mathbf{m}=-M}^{M-1} \hat{f}_m U_r(\mathbf{m}) e^{-2\pi\imath(\mathbf{m},\mathbf{v})}$ on a regular grid in Ω_v using standard FFT algorithm and then compute (3.4) on the same regular grid. After that we compute the FFT of (3.4) back into the Fourier domain. Then the computation of $Q^+(f,f)(\mathbf{v})$ on an adaptive grid is done effectively by the USFFT algorithm described before.

The discretization of the loss term $Q^-(f,f)$ (2.3) consists of computation of the discrete collision frequency term (2.7)

$$q^-(f)(\mathbf{v}) = \sum_{\mathbf{m}=-M}^{M-1} \hat{f_m} \hat{B}(\mathbf{m},\mathbf{m}) e^{-2\pi\imath(\mathbf{m},\mathbf{v})},$$

which is a convolution operator and a pointwise multiplication of $q^-(f)(\mathbf{v})$ by $f(\mathbf{v})$. We compute $q^-(f)(\mathbf{v})$ again using USFFT algorithm with $\mathrm{O}(p^3 N_v) + \mathrm{O}(\sigma N^3 \log N)$ operations.

The total computational cost of the numerical approximation of the collision operator is $\mathrm{O}(p^3 N_v) + \mathrm{O}(\sigma N^6 \log N)$, where σ is a small number depending on the required accuracy in the approximation of the kernel $\hat{B}(\mathbf{l}, \mathbf{m})$.

We point out that the computational cost consists of two parts. The first one depends on the approximation of the discontinuous solution and increases linearly with the number N_v of points in the adaptive velocity grid. Another part depends on the approximation of the smooth terms in the equation. Here N is the number of Fourier modes along one coordinate direction necessary for approximating smooth terms in the Boltzmann equation that is moderate, It implies that the suggested deterministic method for computing the Boltzmann collision operator seems to be considerably more effective than previous ones.

4. Time discretization

The homogeneous Boltzmann equation is solved numerically using the standard semi-implicit Euler scheme

$$\frac{f^{n+1} - f^n}{\Delta t} = Q^+(f^n, f^n) - f^{n+1} q^-(f^n),$$

where $f^n = f(t_n)$ denotes the solution f at time t_n. Solving this equation for f^{n+1} we get

$$f^{n+1} = \frac{f^n + \Delta t\, Q^+(f^n, f^n)}{1 + \Delta t\, q^-(f^n)}. \tag{4.1}$$

A higher order finite difference scheme can be also easily adapted.

4.1. Conservation procedure.

Since the Boltzmann equation is based on a balance principle and since the hydrodynamic equations for the macroscopic quantities have the form of the conservation laws, one may expect that the proper numerical scheme should in some sense reflect these properties. However the proposed numerical scheme, as a spectral method do not representing higher moments of solutions exactly, conserves only mass – momentum and energy are not conserved.

A correction technique which enforces the conservativeness was proposed by Aristov and Tcheremisin (see [2]). The numerical solution f^{n+1} given by (4.1) is corrected by adding a term

$$f^{n+1} \sum_{i=0}^{4} \alpha_i \psi_i,$$

where $\psi_0(\mathbf{v}) = 1$, $\psi_i(\mathbf{v}) = v_i$ for $i = 1, 2, 3$, and $\psi_4(\mathbf{v}) = |\mathbf{v}|$. The numbers α_i are determined by requiring that the (discretized) conservation laws

$$\sum_{\mathbf{v}_j \in \mathcal{G}_v} \psi_l(\mathbf{v}_j) f^{n+1}(\mathbf{v}_j) \Big(1 + \sum_{i=0}^{4} \alpha_i \psi_i(\mathbf{v}_j)\Big) = \sum_{\mathbf{v}_j \in \mathcal{G}_v} \psi_l(\mathbf{v}_j) f^{n}(\mathbf{v}_j)$$

are satisfied for $l = 0, \ldots, 4$.

Hence we get the following formula for the solution

$$f^{n+1} = \frac{f^n + \Delta t\, Q^+(f^n, f^n)}{1 + \Delta t\, q^-(f^n)} \Big(1 + \sum_{i=0}^{4} \alpha_i \psi_i\Big). \tag{4.2}$$

4.2. **Adaptive grid.** At each time step a new grid (based on existing one) is built for the solution f^{n+1} according to the formula (4.2).

We build this grid using the values of f^n on the existing grid. In case the grid should be finer (we need more nodes in the new grid) we interpolate the values of f^n on the neighboring nodes. We use for this purpose a simple trilinear interpolation i.e. the interpolating function is linear in each direction. The values of $Q^+(f^n, f^n)$ and $q^-(f^n)$ are computed straightforwardly at the desired points using the inverse USFFT algorithm.

5. Numerical examples

We illustrate our new method on several examples with discontinuous initial data. Having in mind future applications of our approach to boundary value problems we chosen data with discontinuities typical for flows around bodies. Despite the simplicity of these examples they reflect certain computational problems one is faced with solving boundary value problems.

If we think about the flow around a body then simple physical reasons based on the collisionless picture of gas dynamics imply that the distribution function $f(t, x, v)$ at a space point x should include two type of inputs. These are the input from the particles coming from the body and having corresponding temperature and zero mean velocity. Another one is the input from the particles coming from infinity and having large mean velocity and another temperature. Depending on the position of the point x with respect the body and depending on the shape of the body one observes different cone like surfaces of discontinuity in the distribution function.

We present here numerical results for maxwell molecules. On the other hand our method is independent of this particular model.

Example 1.

The first example is the evolution starting from the initial distribution function $f_0(v)$ that is a maxwell distribution function with temperature 0.0115 and velocity 0 in the half space $x \leq 0$ and is another maxwell distribution with temperature 0.0115 and velocity -0.1 in the half space $x < 0$

. Therefore f_0 is discontinuous on the $y - z$ plane. This function imitates the distribution of the gas close to the surface of a body with the similar temperature.

Example 2. The second example imitates the distribution function in the gas flow around a sphere at a point x at some finite distance from the sphere. We chosen the initial distribution $f_0(\mathbf{v})$ similar to one that is observed in such a flow if collisions between molecules are absent. Namely the distribution function is initially equal to a maxwell distribution function with temperature 0.0115 and velocity 0 for points within a cone with center at the origin. This part of the distribution function imitates particles reflected from the body. Outside of this cone the initial distribution function is taken equal to another maxwell distribution with temperature 0.0065 and velocity -0.1. This part of the distribution functions imitates the flow coming from infinity. Therefore in this case the initial distribution has a discontinuity at the surface of a cone. We have chosen a cone having the axis laying in x-z plane with angle 135^0 with respect to x- axis. The cosine of the angle between the cone and its axis is 0.85.

Example 3.

The third example is given to illustrate the flexibility of the method to solutions with large difference of gradients. The initial data is similar to one in the first example but maxwell distributions in two half spaces have different temperatures 0.0115 and 0.065 and there are no particles within a gap in velocities with $-0.1 < v_x < 0$.

For each of these examples we present a sequence of graphs for values of the distribution function $f(t_i, \mathbf{v})$ for several time points $t_i = 0.02 * i$. in x-z plane and also the corresponding crossections of the three dimensional adaptive grid with x-z plane.

One can see in all these numerical results that the initial discontinuity in the distribution function decreases but preserves its position in complete accordance with known properties of the Boltzmann equation.

References

[1] L. S. Andallah and H. Babovsky, *A discrete Boltzmann equation based on hexagons*, Math. Models Methods Appl. Sci., 13 (2003), pp. 1537–1563.

[2] V. V. Aristov and F. G. Tcheremisin, *The conservative splitting method for the solution of a Boltzmann equation*, Zh. Vychisl. Mat. i Mat. Fiz., 20 (1980), pp. 191–207, 262.

[3] H. Babovsky, *On a simulation scheme for the Boltzmann equation*, Math. Methods Appl. Sci., 8 (1986), pp. 223–233.

[4] G. Beylkin, *On the fast Fourier transform of functions with singularities*, Appl. Comput. Harmon. Anal., 2 (1995), pp. 363–381.

[5] G. A. Bird, *Recent advances and current challenges for DSMC*, Comput. Math. Appl., 35 (1998), pp. 1–14. Simulation methods in kinetic theory.

[6] A. Bobylev and S. Rjasanow, *Difference scheme for the Boltzmann equation based on the fast Fourier transform*, European J. Mech. B Fluids, 16 (1997), pp. 293–306.
[7] A. V. Bobylev, *The method of the Fourier transform in the theory of the Boltzmann equation for Maxwell molecules*, Dokl. Akad. Nauk SSSR, 225 (1975), pp. 1041–1044.
[8] A. V. Bobylev and S. Rjasanow, *Fast deterministic method of solving the Boltzmann equation for hard spheres*, Eur. J. Mech. B Fluids, 18 (1999), pp. 869–887.
[9] C. Buet, *A discrete-velocity scheme for the Boltzmann operator of rarefied gas dynamics*, Transport Theory Statist. Phys., 25 (1996), pp. 33–60.
[10] C. Cercignani, *The Boltzmann equation and its applications*, vol. 67 of Applied Mathematical Sciences, Springer-Verlag, New York, 1988.
[11] E. Gabetta and L. Pareschi, *The Maxwell gas and its Fourier transform towards a numerical approximation*, in Waves and stability in continuous media (Bologna, 1993), vol. 23 of Ser. Adv. Math. Appl. Sci., World Sci. Publishing, River Edge, NJ, 1994, pp. 197–201.
[12] D. Goldstein, B. Sturtevant, and J. Broadwell, *Investigation of the motion of discrete-velicity gases*, in Proceedings of the 16-th Int. Symp. on RGD, in: Ser. Progress in Astronautics and Aeronautics. Vol. 118, ed. E.P. Muntz et al., pp. 100-117, 1989, vol. 118, 1989, pp. 100–117.
[13] R. Grzibovskis and A. Heintz, *On a a kinetic approach to generalised curvature flows and its applications.*, Preprint, Department of Mathematics. Chalmers, 39 (2002), pp. 1–36.
[14] S. Kosuge, K. Aoki, and S. Takata, *Shock-wave structure for a binary gas mixture: Finite-difference analysis of the boltzmann equation for hard-sphere molecules*, European J. Mech. B Fluids, 20 (2001), pp. 87–101.
[15] P.-L. Lions, *Compactness in Boltzmann's equation via Fourier integral operators and applications. I, II*, J. Math. Kyoto Univ., 34 (1994), pp. 391–427, 429–461.
[16] S. Mischler, *Convergence of discrete-velocity schemes for the Boltzmann equation*, Arch. Rational Mech. Anal., 140 (1997), pp. 53–77.
[17] K. Nanbu, *Stochastic solution method of the master equation and the model Boltzmann equation*, J. Phys. Soc. Japan, 52 (1983), pp. 2654–2658.
[18] T. Ohwada, *Structure of normal shock waves: direct numerical analysis of the Boltzmann equation for hard-sphere molecules*, Phys. Fluids A, 5 (1993), pp. 217–234.
[19] A. Palczewski, J. Schneider, and A. V. Bobylev, *A consistency result for a discrete-velocity model of the Boltzmann equation*, SIAM J. Numer. Anal., 34 (1997), pp. 1865–1883.
[20] V. A. Panferov and A. G. Heintz, *A new consistent discrete-velocity model for the Boltzmann equation*, Math. Methods Appl. Sci., 25 (2002), pp. 571–593.
[21] L. Pareschi and B. Perthame, *A Fourier spectral method for homogeneous Boltzmann equations*, in Proceedings of the Second International Workshop on Nonlinear Kinetic Theories and Mathematical Aspects of Hyperbolic Systems (Sanremo, 1994), vol. 25, 1996, pp. 369–382.
[22] L. Pareschi and G. Russo, *Numerical solution of the Boltzmann equation. I. Spectrally accurate approximation of the collision operator*, SIAM J. Numer. Anal., 37 (2000), pp. 1217–1245 (electronic).
[23] F. Rogier and J. Schneider, *A direct method for solving the Boltzmann equation*, Transport Theory Statist. Phys., 23 (1994), pp. 313–338.
[24] S. Succi, R. Benzi, and M. Vergassola, *Recent advances in the theory of the lattice Boltzmann equation*, in Discrete models of fluid dynamics (Figueira da Foz,

1990), vol. 2 of Ser. Adv. Math. Appl. Sci., World Sci. Publishing, River Edge, NJ, 1991, pp. 97–103.

[25] S. Takata, Y. Sone, and K. Aoki, *Numerical analysis of a uniform flow of a rarefied gas past a sphere on the basis of the Boltzmann equation for hard-sphere molecules*, Phys. Fluids A, 5 (1993), pp. 716–737.

[26] B. Wennberg, *The geometry of binary collisions and generalized Radon transforms*, Arch. Rational Mech. Anal., 139 (1997), pp. 291–302.

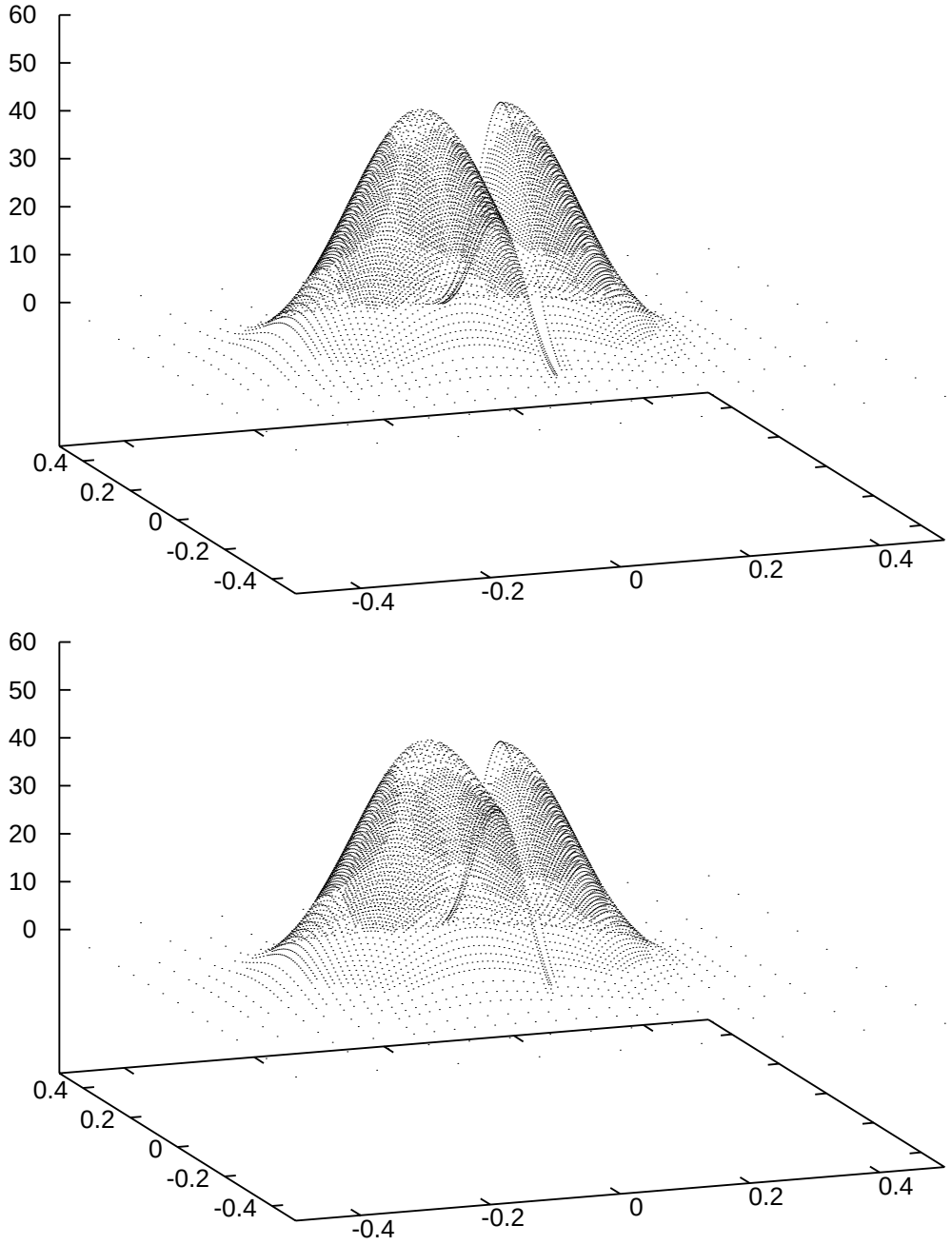

FIGURE 2. Example 1, solution steps 0 and 5

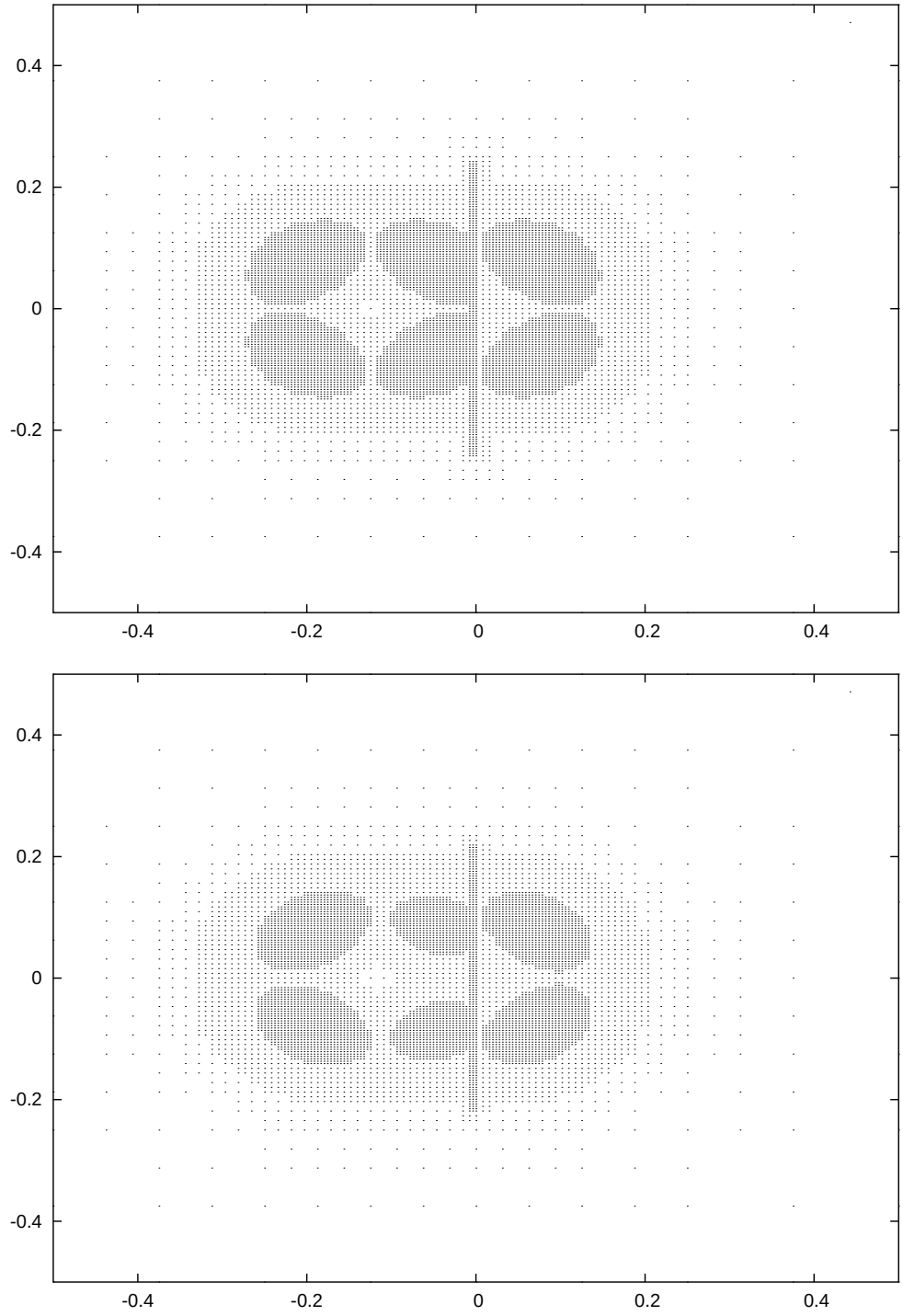

FIGURE 3. Example 1, grid steps 0 and 5

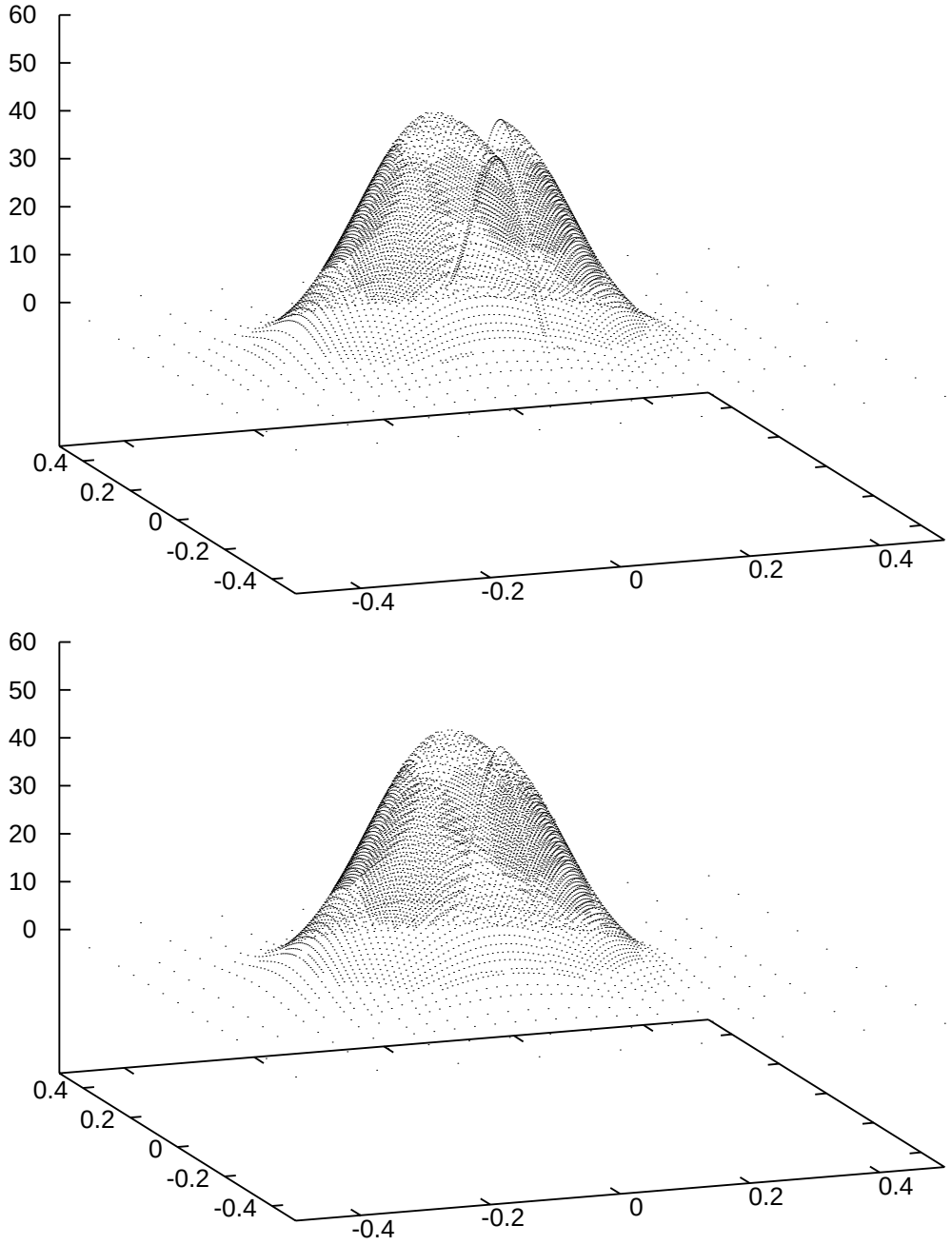

FIGURE 4. Example 1, solution steps 40 and 80

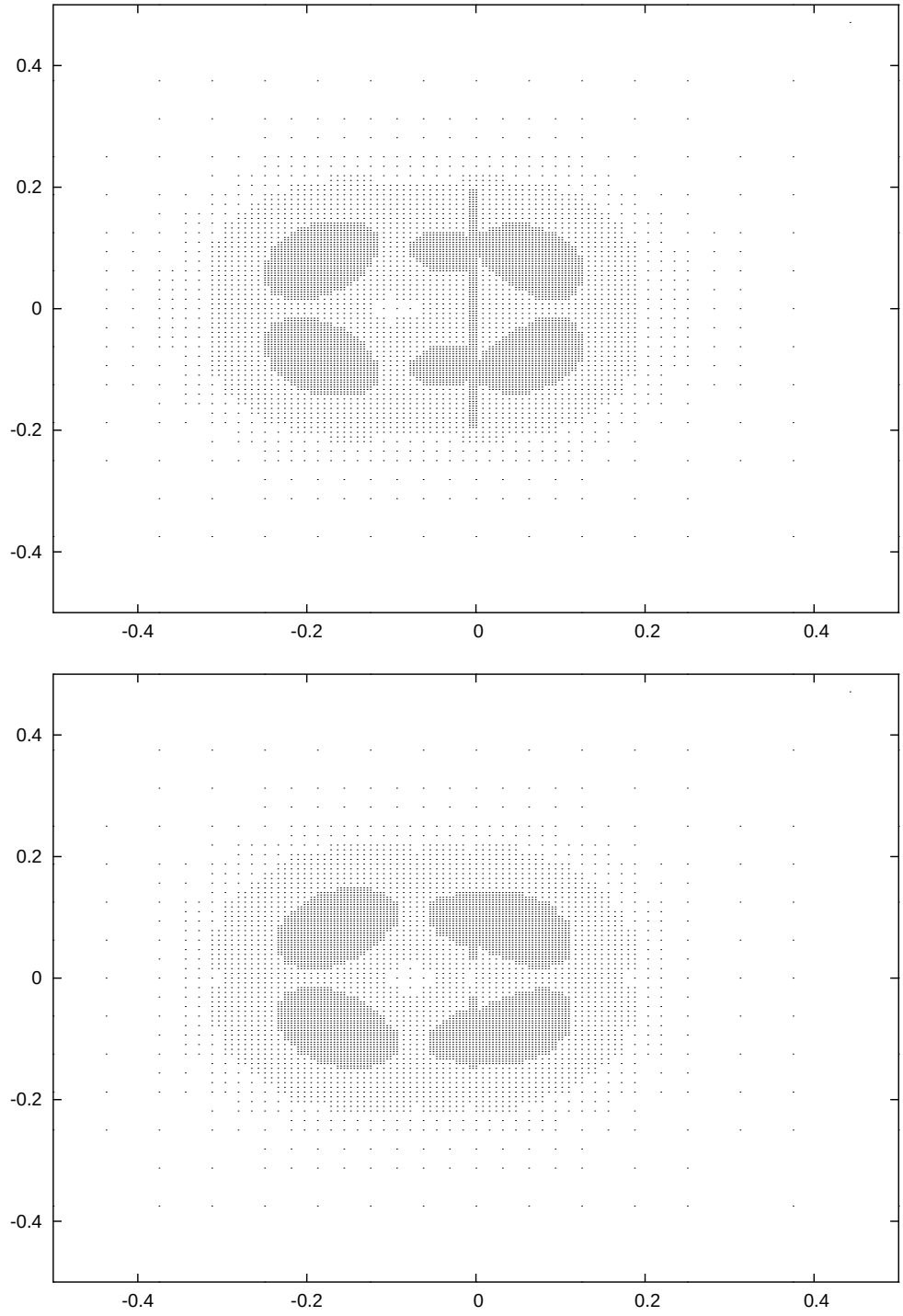

FIGURE 5. Example 1, grid steps 40 and 80

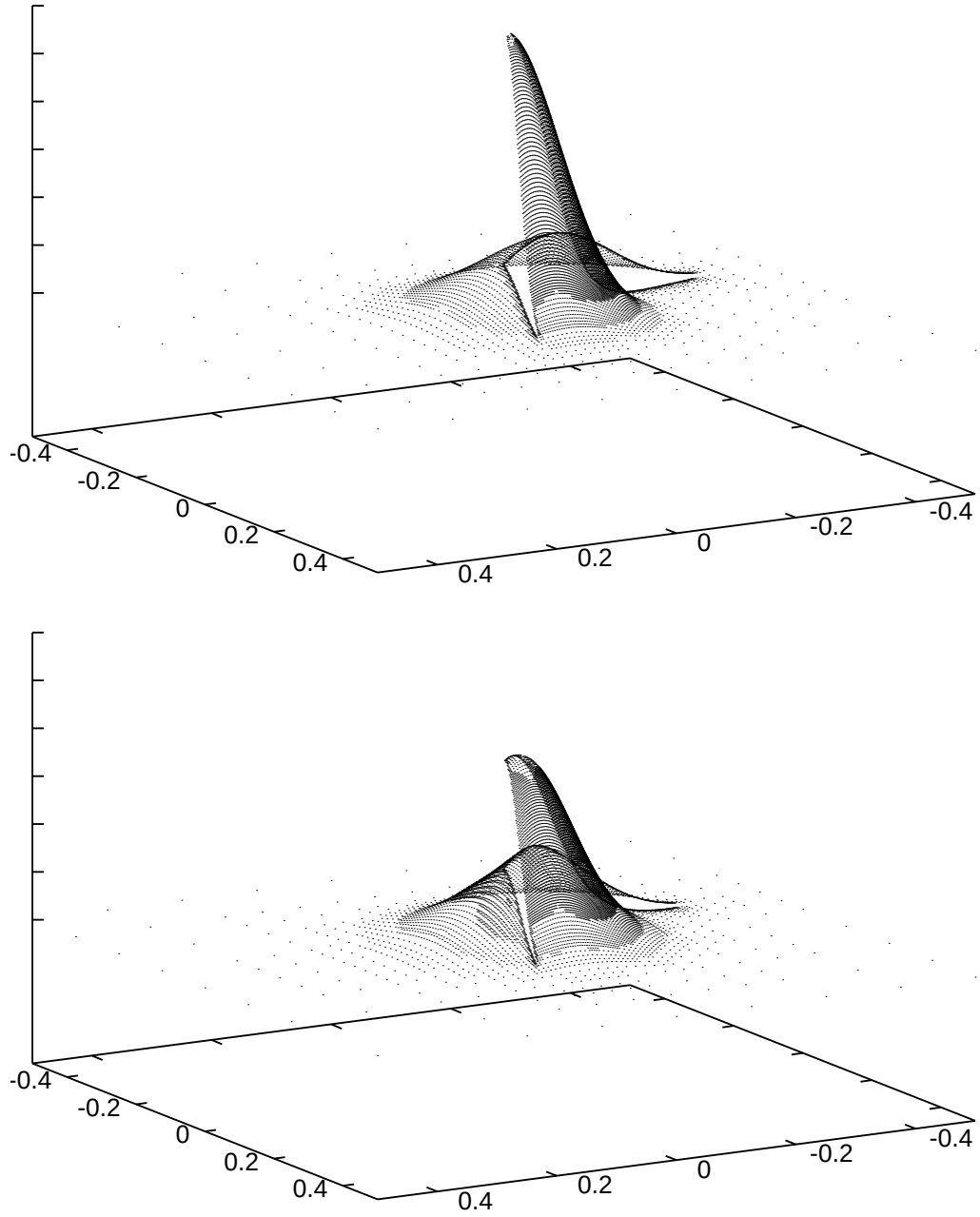

FIGURE 6. Example 2 solution steps 0 and 10

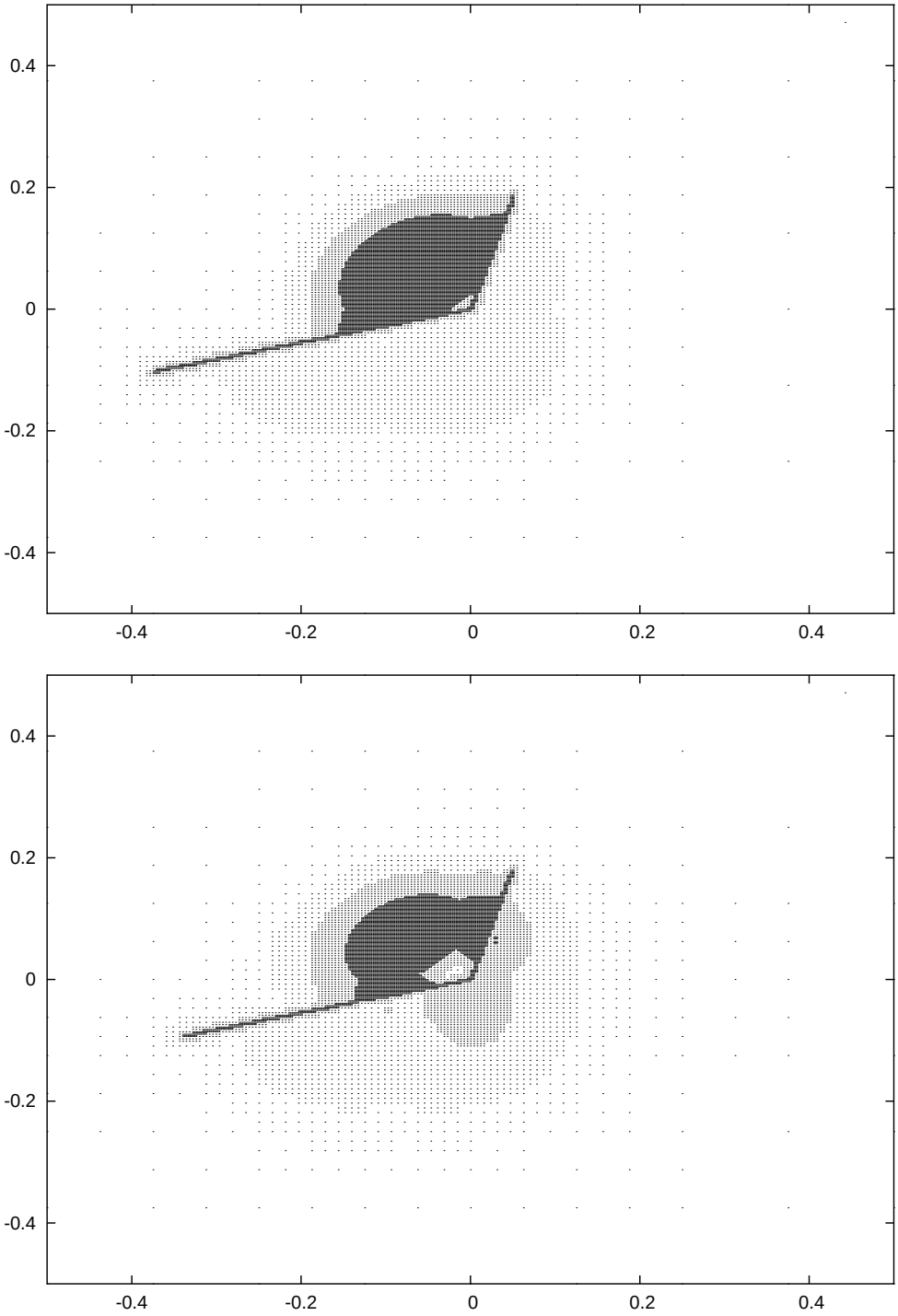

FIGURE 7. Example 2, grid steps 0 and 10

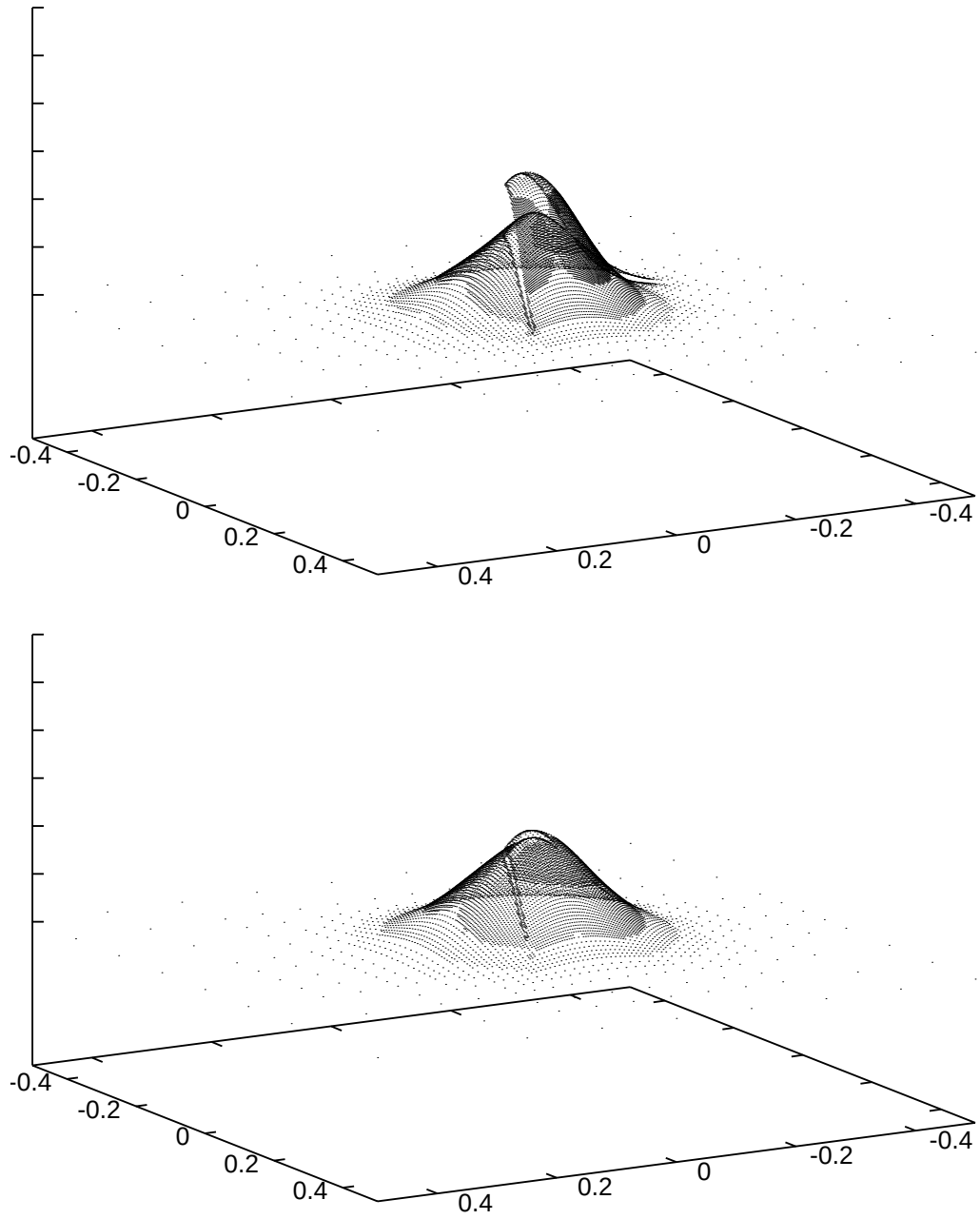

FIGURE 8. Example 2, solution steps 20 and 40

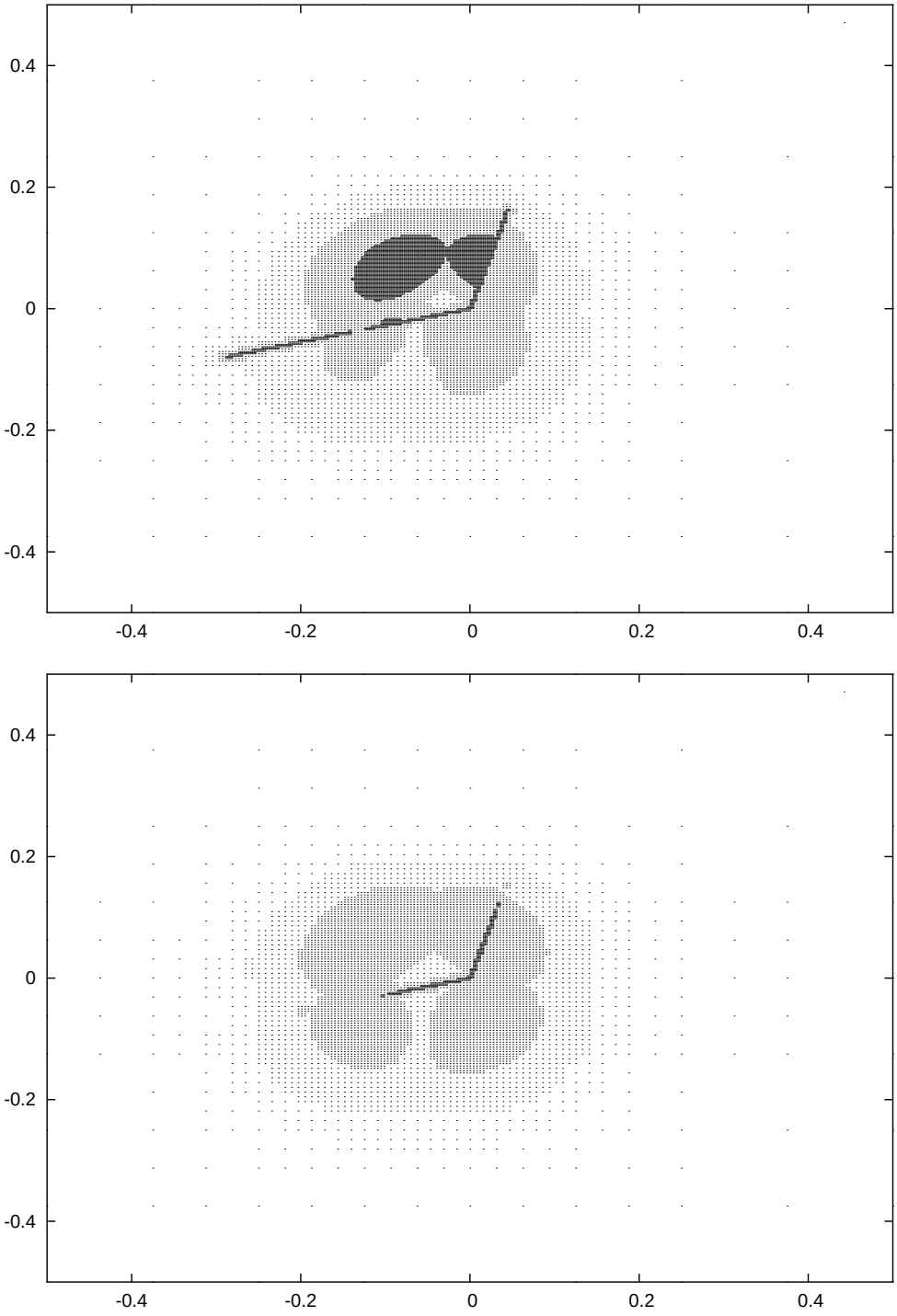

FIGURE 9. Example 2, grid steps 20 and 40

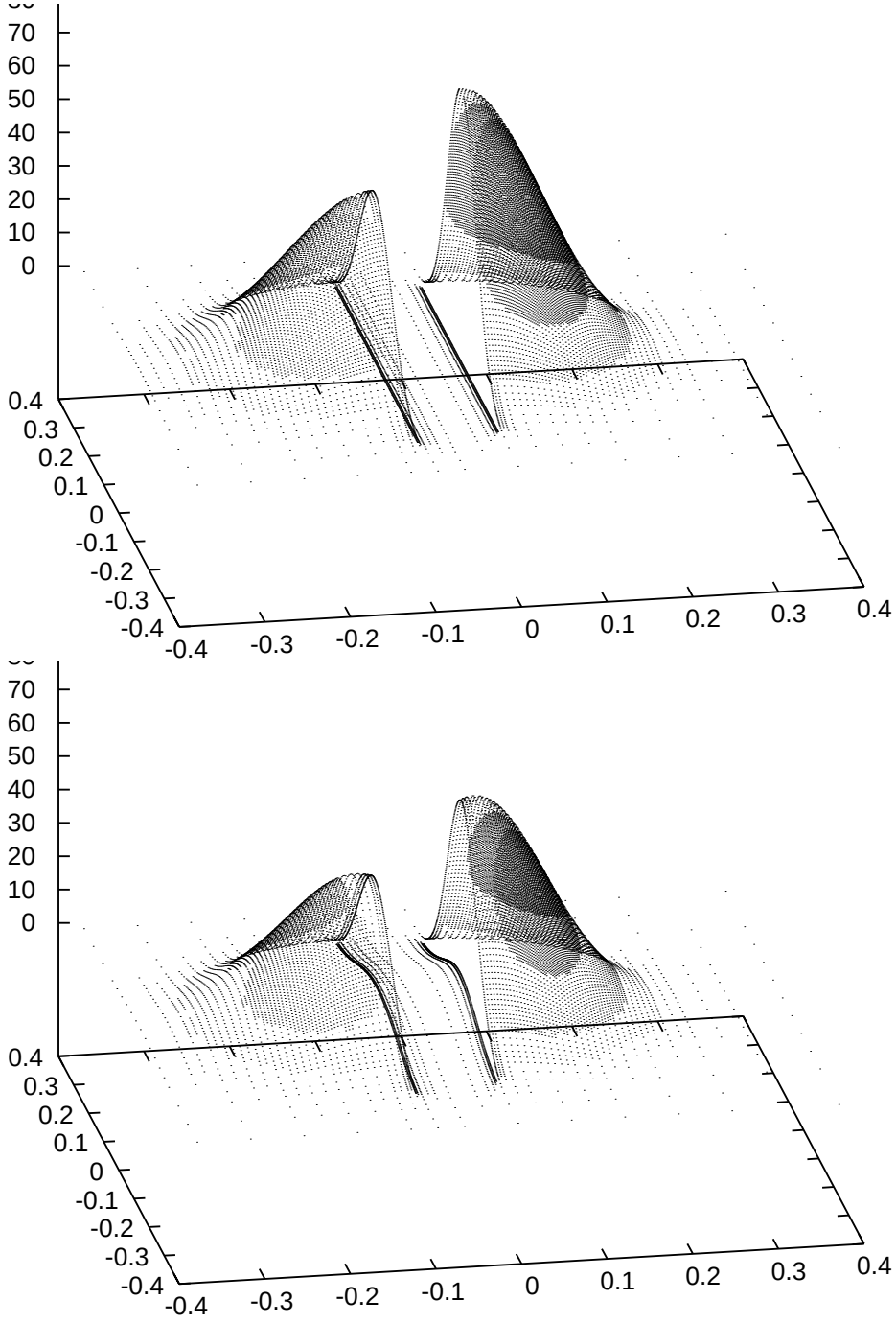

FIGURE 10. Example 3, solution steps 0 and 5

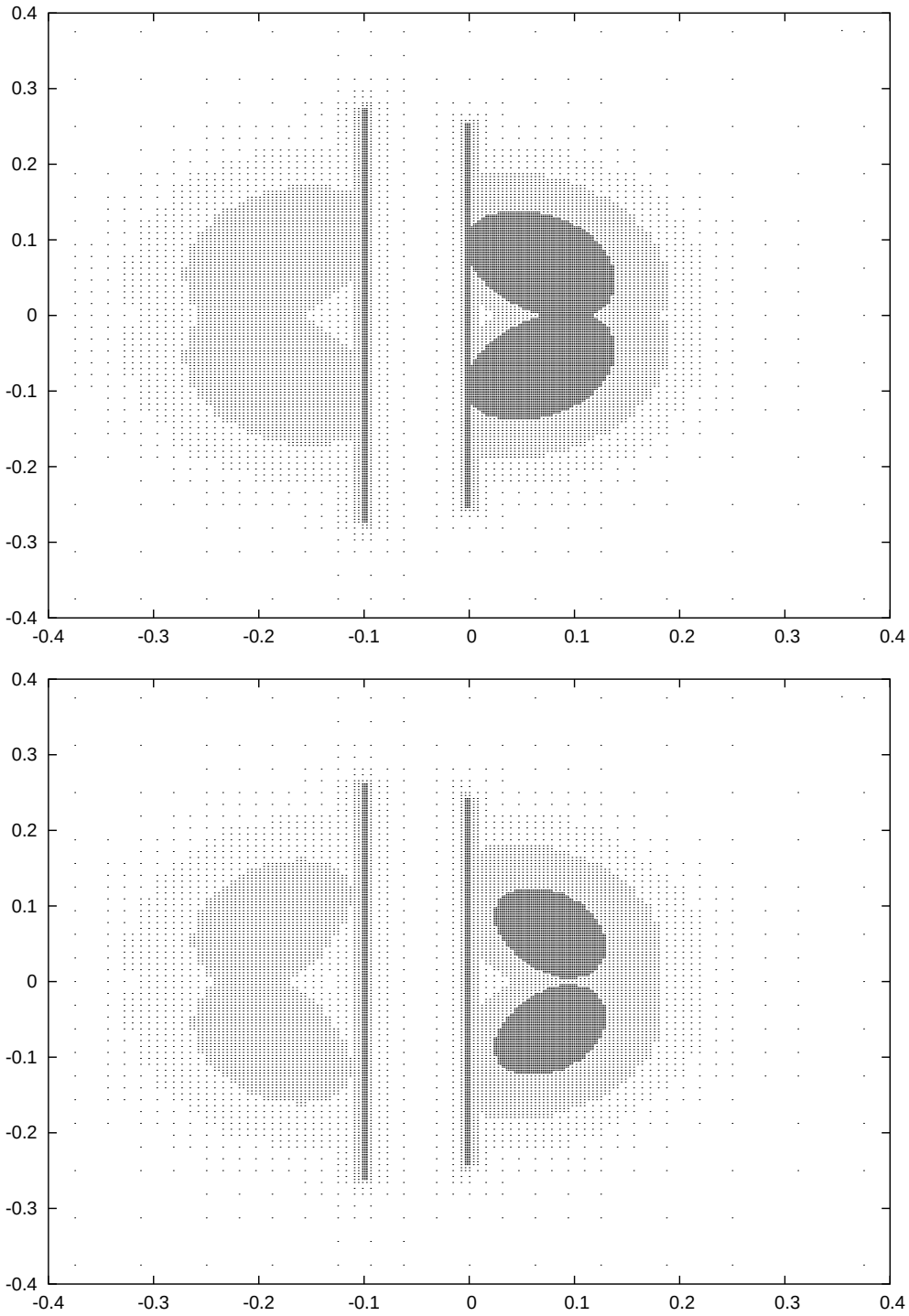

FIGURE 11. Example 3, grid steps 0 and 5

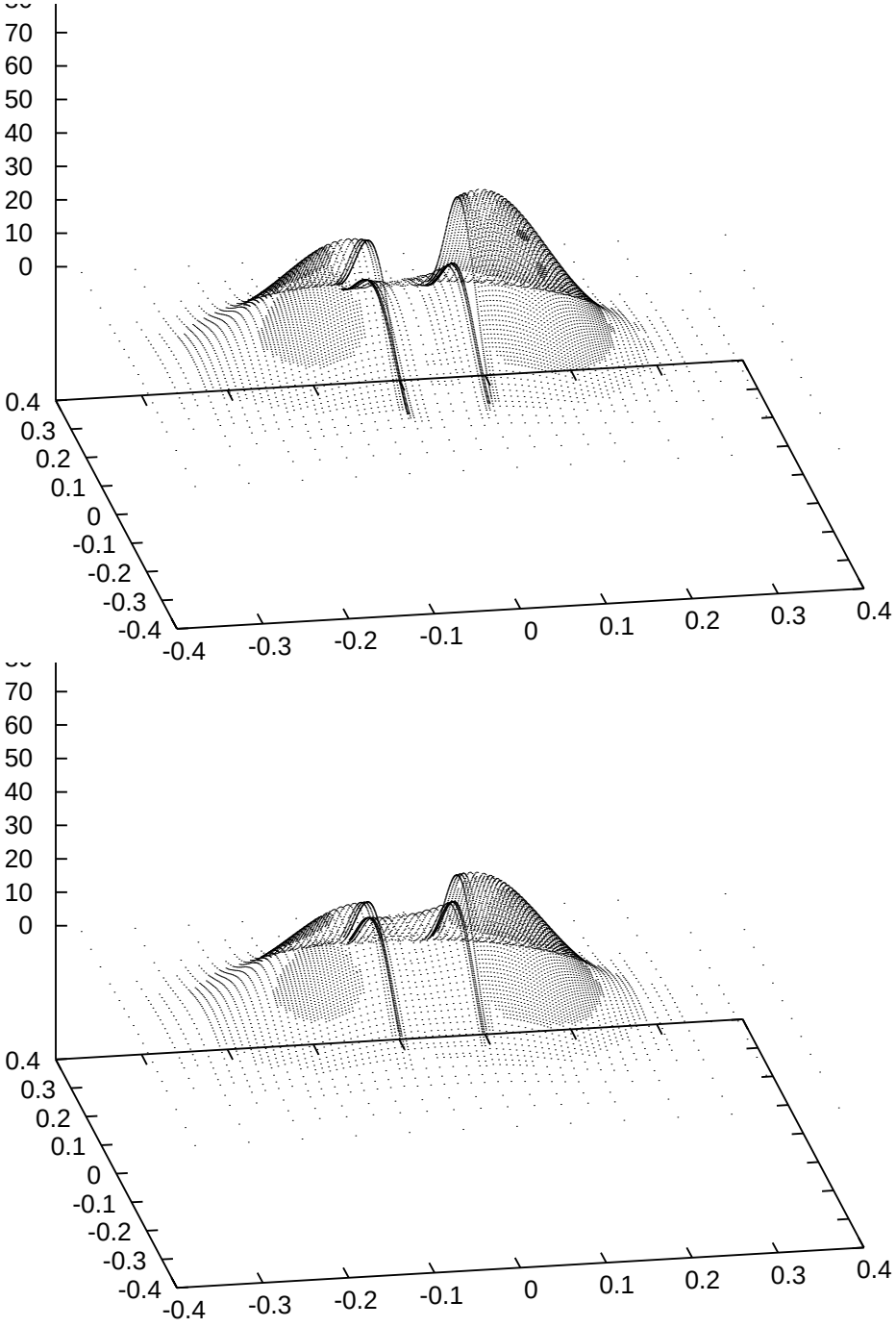

FIGURE 12. Example 3, solution steps 15 and 25

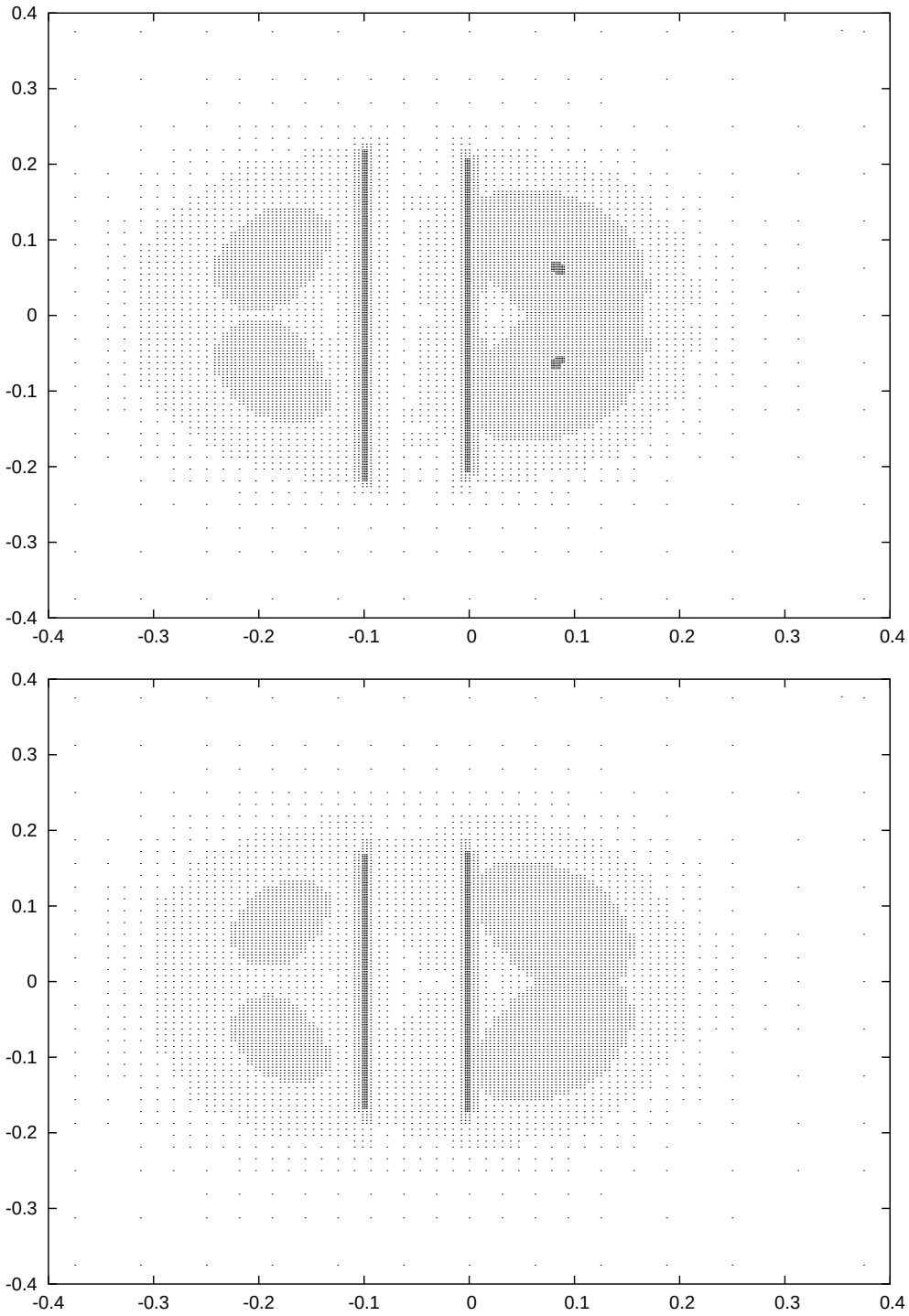

FIGURE 13. Example 3, grid steps 15 and 25

Department of Mathematics, Chalmers University of Technology and Göteborg University, SE–412 96, Göteborg, Sweden
E-mail address: heintz@math.chalmers.se

Department of Mathematics, Informatics and Mechanics, Warsaw University, Banacha 2, 02-097 Warszawa, Poland
E-mail address: pkowal@mimuw.edu.pl

Department of Mathematics, Chalmers University of Technology and Göteborg University, SE–412 96, Göteborg, Sweden
E-mail address: richards@math.chalmers.se